Searching for neutrinoless double-beta decay of germanium-76 in the presence of backgrounds

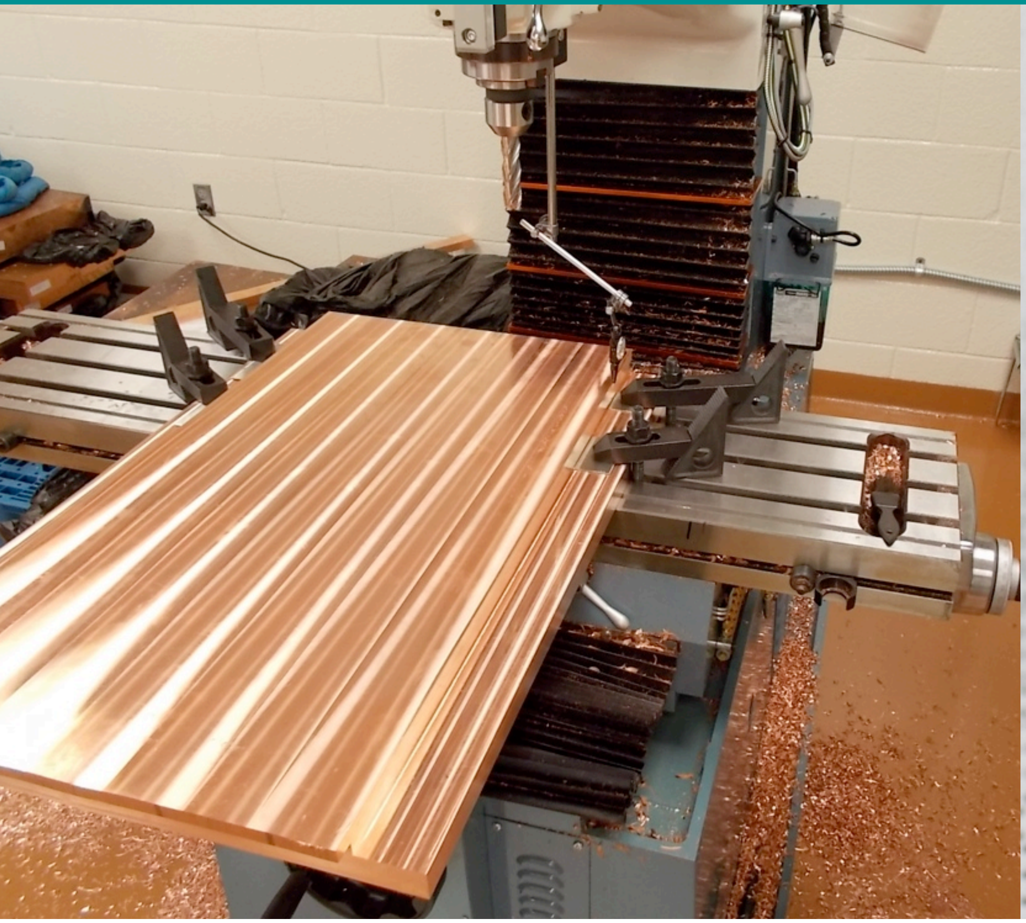
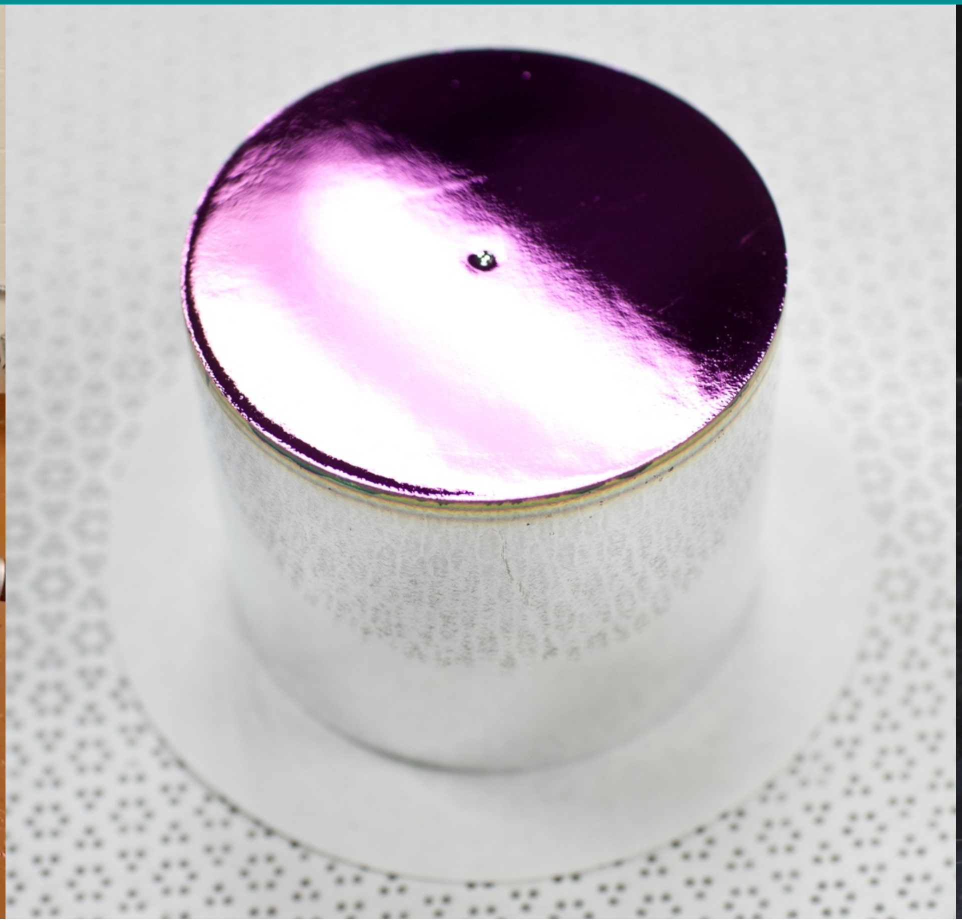
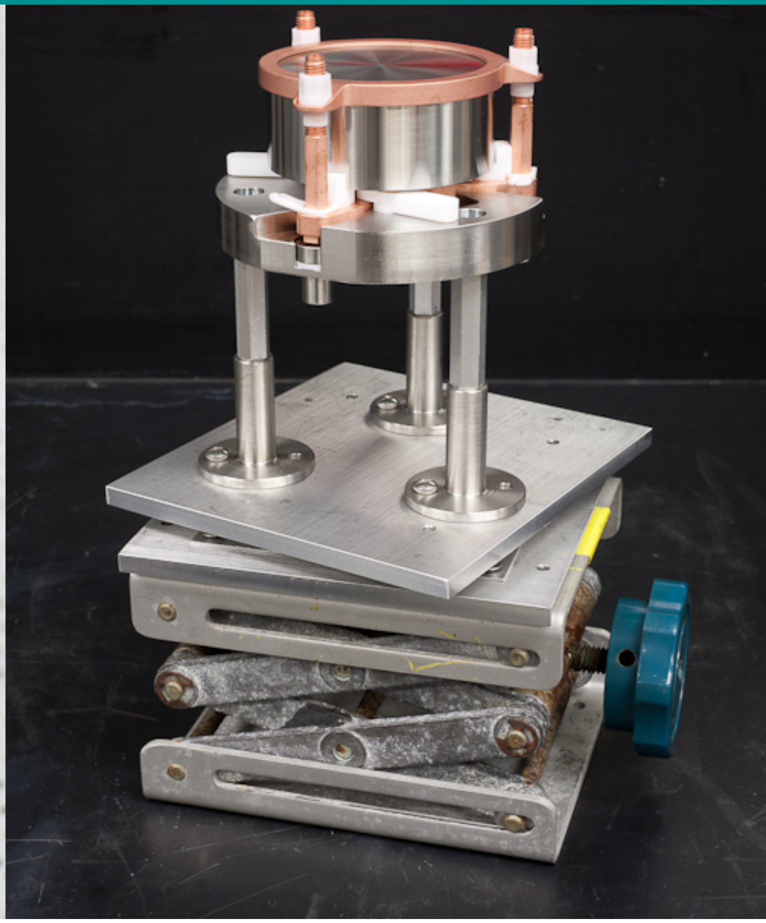

Alexis Schubert
MAJORANA Collaboration

CENPA
Center for Experimental Nuclear Physics and Astrophysics

UNIVERSITY of WASHINGTON

The MAJORANA Collaboration

Black Hills State University, Spearfish, SD
Kara Keeter, Brianna Mount, Greg Serfling, Jared Thompson

Duke University, Durham, North Carolina , and TUNL
Matthew Busch, James Esterline, Gary Swift, Werner Tornow

Institute for Theoretical and Experimental Physics, Moscow, Russia
Alexander Barabash, Sergey Konovalov, Vladimir Yumatov

Joint Institute for Nuclear Research, Dubna, Russia
Viktor Brudanin, Slava Egorov, K. Gusey, Oleg Kochetov, M. Shirchenko, V. Timkin, E. Yakushev

Lawrence Berkeley National Laboratory, Berkeley, California and the University of California - Berkeley
Nicolas Abgrall, Mark Amman, Paul Barton, Yuen-Dat Chan, Alex Hegai, James Loach, Paul Luke, Ryan Martin, Susanne Mertens, Alan Poon, Kai Vetter, Harold Yaver

Los Alamos National Laboratory, Los Alamos, New Mexico
Melissa Boswell, Steven Elliott,, Johnny Goett, Keith Rielage, Larry Rodriguez, Michael Ronquest, Harry Salazar, Wenqin Xu

North Carolina State University, Raleigh, North Carolina and TUNL
Dustin Combs, Lance Leviner, David G. Phillips II, Albert Young

Oak Ridge National Laboratory, Oak Ridge, Tennessee
Jim Beene, Fred Bertrand, Greg Capps, Alfredo Galindo-Uribarri, Kim Jeskie, David Radford, Robert Varner, Brandon White, Chang-Hong Yu

Osaka University, Osaka, Japan
Hiroyasu Ejiri, Ryuta Hazama, Masaharu Nomachi, Shima Tatsuji

Pacific Northwest National Laboratory, Richland, Washington
Estanislao Aguayo, Jim Fast, Eric Hoppe, Richard T. Kouzes, Brian LaFerriere, Jason Merriman, John Orrell, Nicole Overman, Doug Reid

South Dakota School of Mines and Technology, Rapid City, South Dakota
Adam Caldwell, Cabot-Ann Christofferson, Stanley Howard, Anne-Marie Suriano

Tennessee Tech University, Cookeville, Tennessee
Mary Kidd

University of Alberta, Edmonton, Alberta
Aksel Hallin

University of North Carolina, Chapel Hill, North Carolina and TUNL
Padraic Finnerty, Florian Fraenkle, Graham K. Giovanetti, Matthew P. Green, Reyco Henning, Mark Howe, Sean MacMullin, Kyle Snavely, Jacqueline Strain, Kris Vorren, John F. Wilkerson

University of South Carolina, Columbia, South Carolina
Frank Avignone, Leila Mizouni

University of South Dakota, Vermillion, South Dakota
Vince Guiseppe, Kirill Pushkin, Nathan Snyder

University of Tennessee, Knoxville, Tennessee
Yuri Efremenko, Sergey Vasiliev

University of Washington, Seattle, Washington
Tom Burritt, Jason Detwiler, Peter J. Doe, Greg Harper, Jonathan Leon, David Peterson, R. G. Hamish Robertson, Alexis Schubert, Tim Van Wechel

Outline

- Neutrinoless double-beta decay
- The MAJORANA DEMONSTRATOR
- Studies with an R&D detector

The MAJORANA Collaboration at Sanford Lab, SD

Neutrino questions

- What is the absolute mass scale of neutrinos?
- What is the neutrino mass hierarchy?
- Is the neutrino its own antiparticle (a Majorana particle)?
- Is lepton number a conserved quantity?

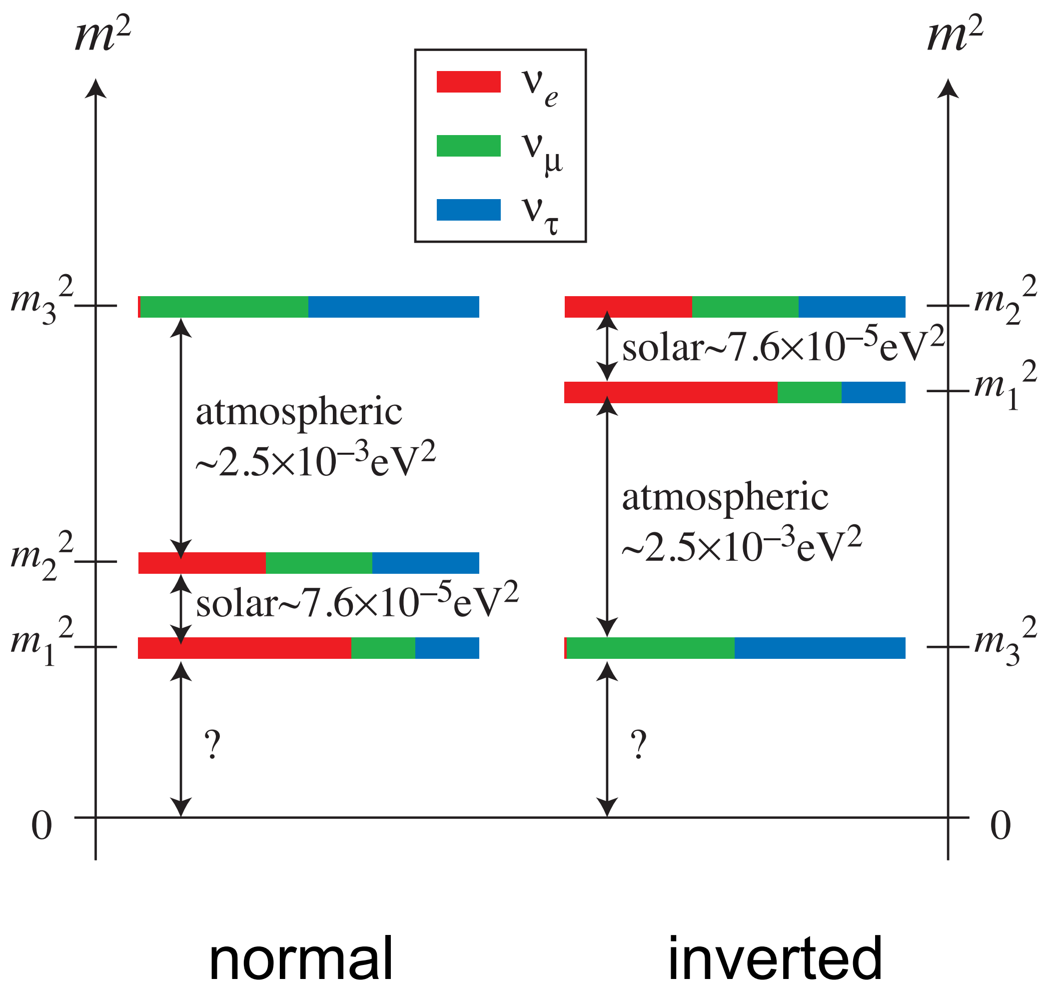

hitoshi.berkeley.edu/neutrino

Double-beta decay

- Process that occurs for some nuclei with even number of protons and neutrons
- Occurs with the emission of two neutrinos (2vββ)
- Observed in many nuclei
- $T_{1/2} \sim 10^{19}$ to 10^{21} years

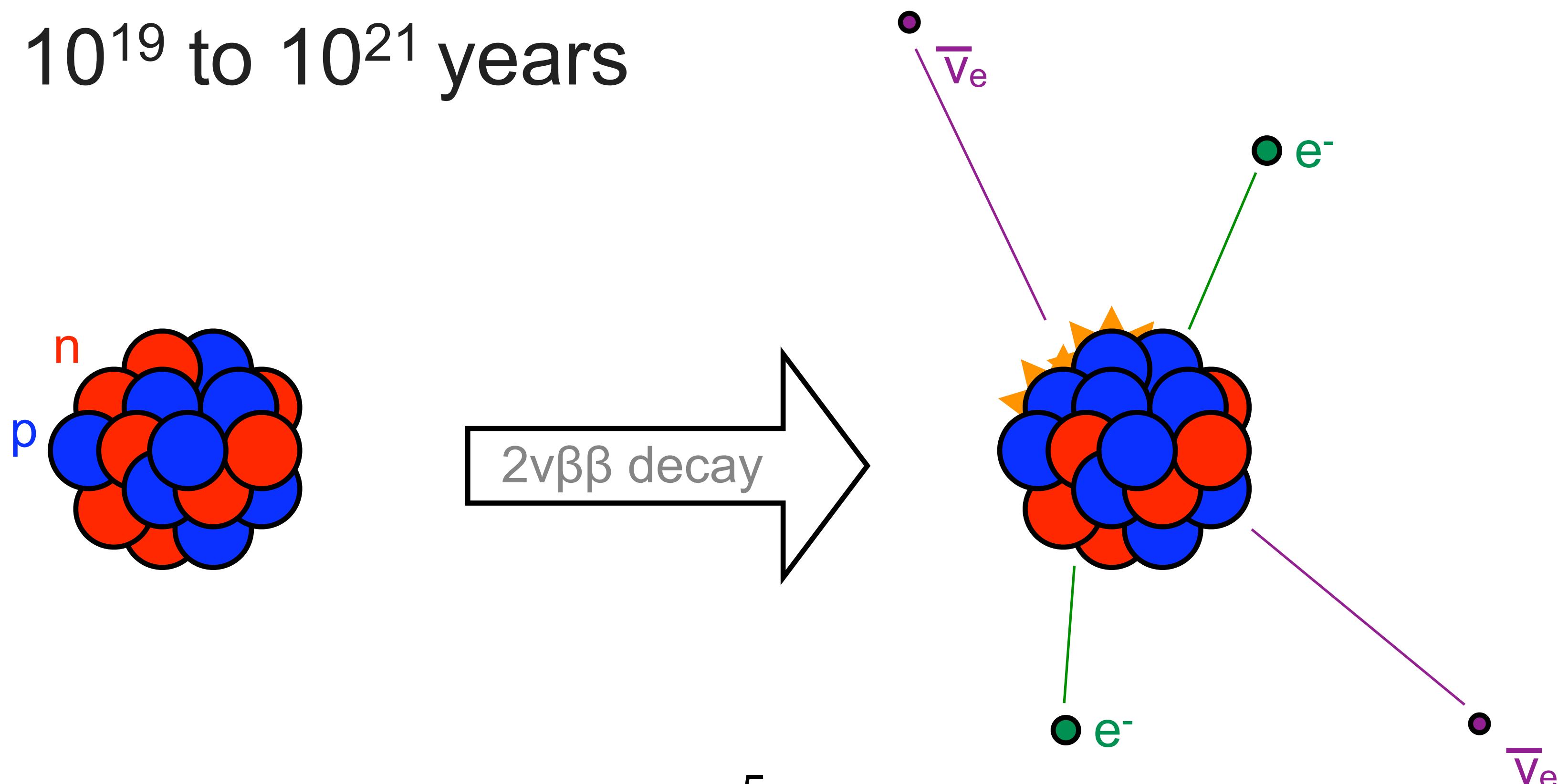

Neutrinoless double-beta decay (0νββ)

- Observation would indicate:
  - Neutrino is a Majorana particle
  - Lepton number is violated
- Information about mass may be available

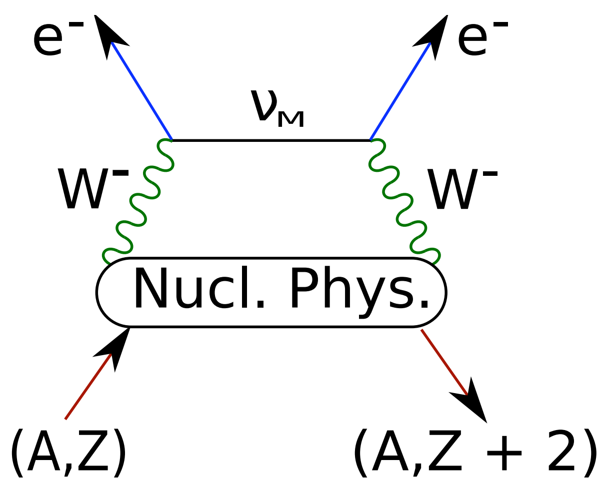

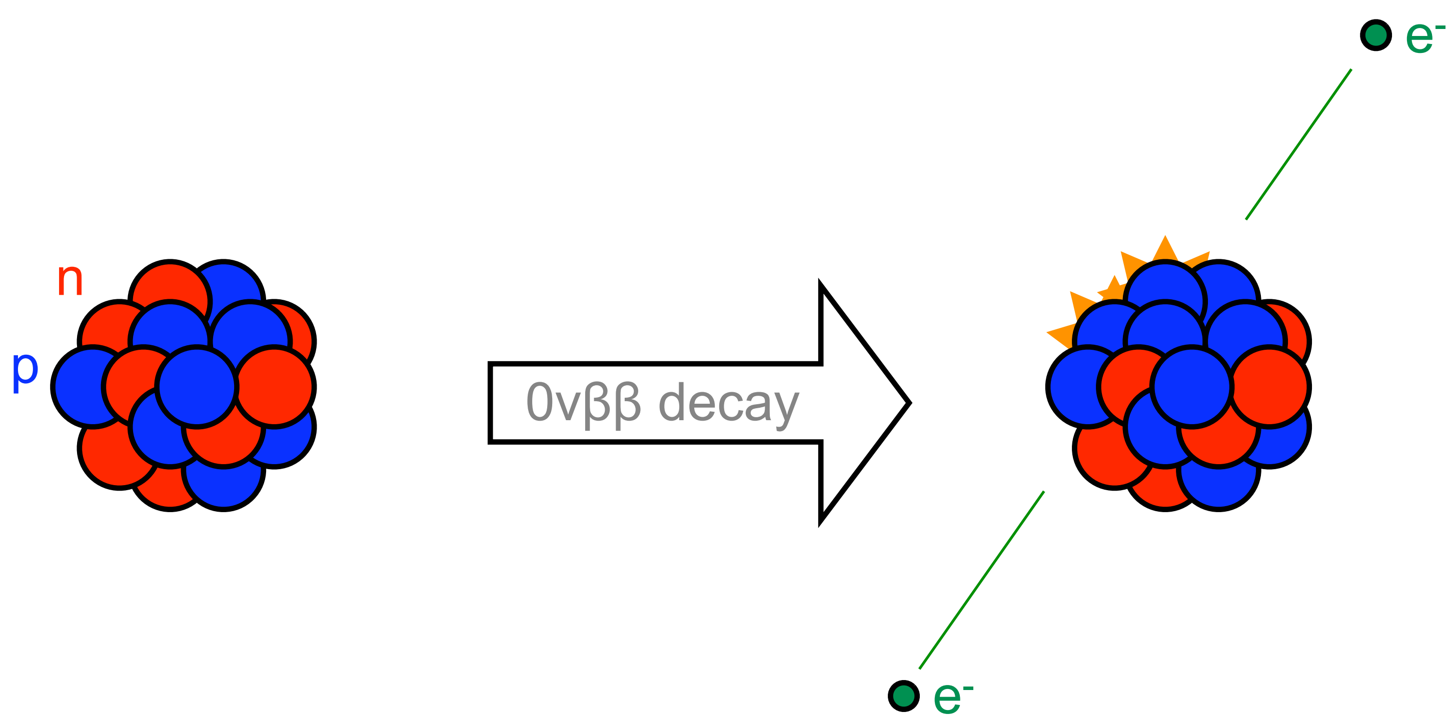

0νββ and neutrino mass

decay rate: $[T_{1/2}^{0\nu\beta\beta}]^{-1} = G^{0\nu\beta\beta}(E_0,Z)\ (M^{0\nu\beta\beta})^2\ \langle m_{0\nu\beta\beta}\rangle^2$

eff. mass: $m_{0\nu\beta\beta} = \left| |U_{e1}|^2 m_1 + |U_{e2}|^2 m_2 e^{i\Phi 2} + |U_{e3}|^2 m_3 e^{i\Phi 3} \right|$

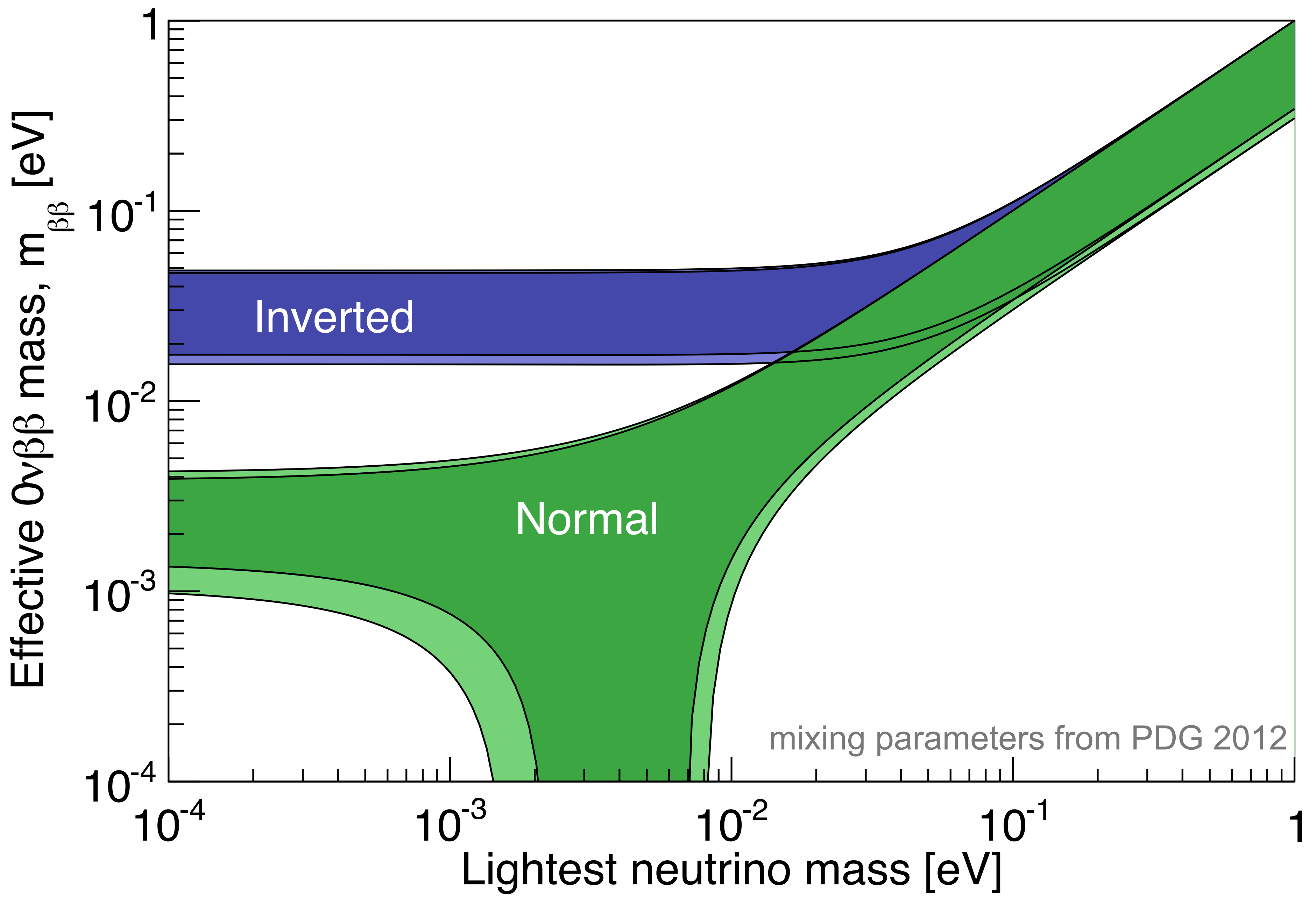

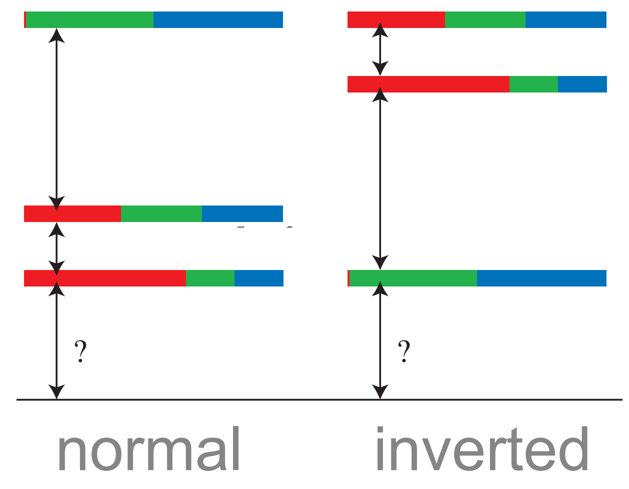

0νββ and neutrino mass

decay rate: $[T_{1/2}^{0\nu\beta\beta}]^{-1} = G^{0\nu\beta\beta}(E_0,Z)\ (M^{0\nu\beta\beta})^2 \ \langle m_{0\nu\beta\beta}\rangle^2$

eff. mass: $m_{0\nu\beta\beta} = \left| |U_{e1}|^2 m_1 + |U_{e2}|^2 m_2 e^{i\Phi 2} + |U_{e3}|^2 m_3 e^{i\Phi 3} \right|$

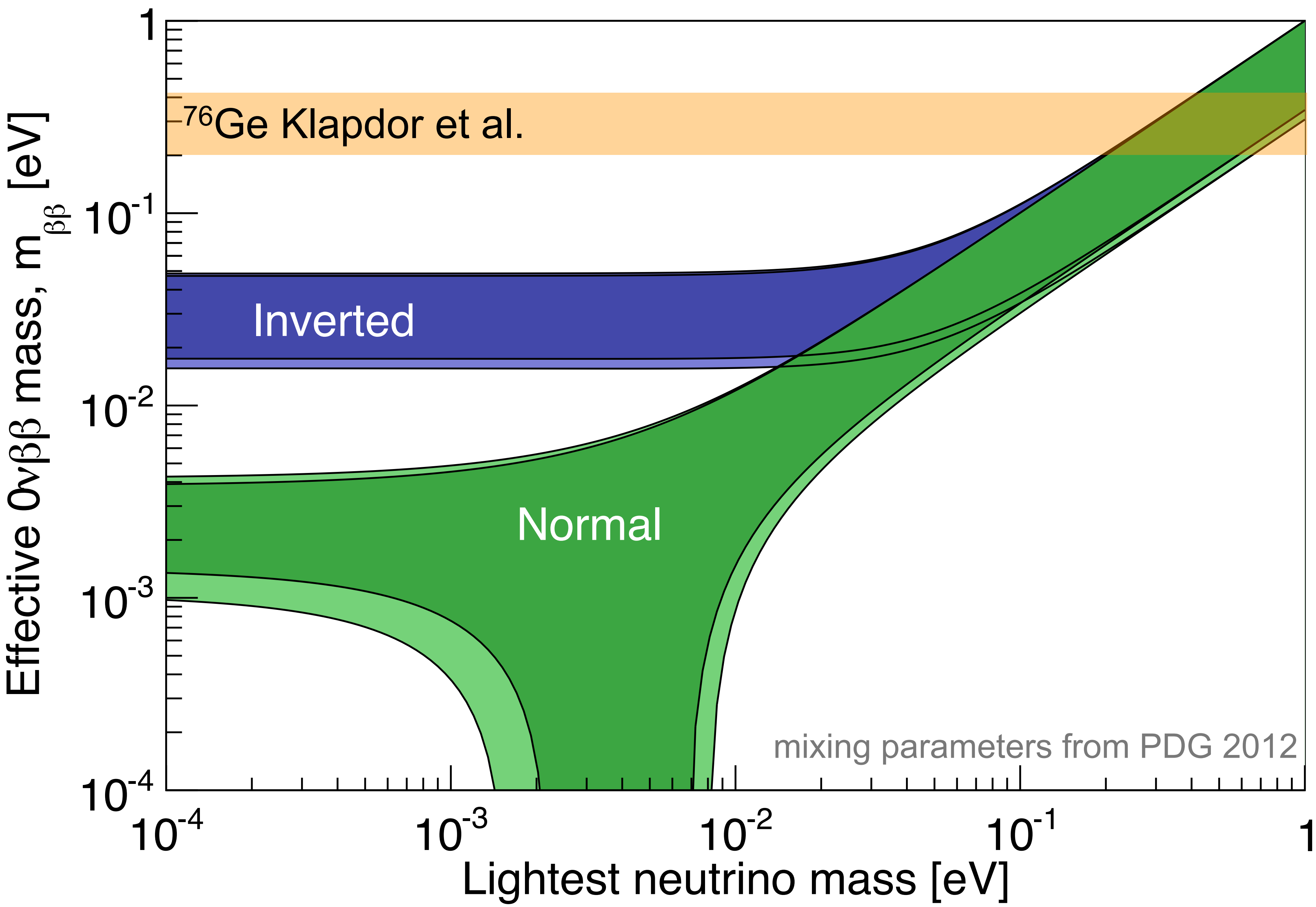

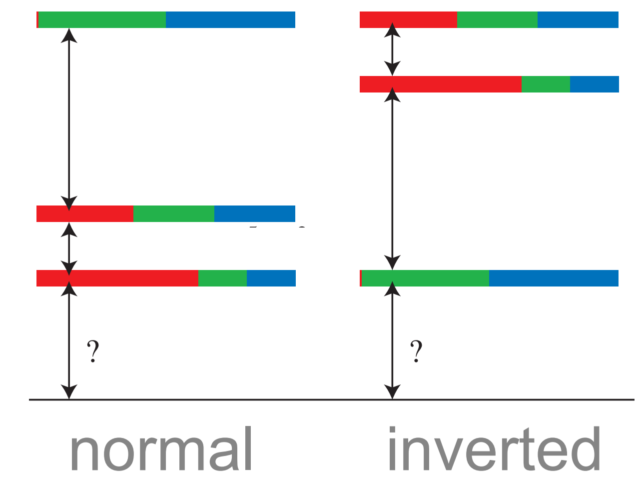

Klapdor: Mod. Phys. Lett. A21 (2006) 1547
HM: Eur Phys. Journal A12 (2001) 147
EXO-200: Phys. Rev. Lett. 109 (2012) 032505
KamLAND-Zen: Phys. Rev. C 86 (2012) 021601

$0\nu\beta\beta$ and neutrino mass

decay rate: $[T_{1/2}^{0\nu\beta\beta}]^{-1} = G^{0\nu\beta\beta}(E_0,Z)\ (M^{0\nu\beta\beta})^2\ \langle m_{0\nu\beta\beta}\rangle^2$

eff. mass: $m_{0\nu\beta\beta} = \left|\, |U_{e1}|^2 m_1 + |U_{e2}|^2 m_2 e^{i\Phi 2} + |U_{e3}|^2 m_3 e^{i\Phi 3} \,\right|$

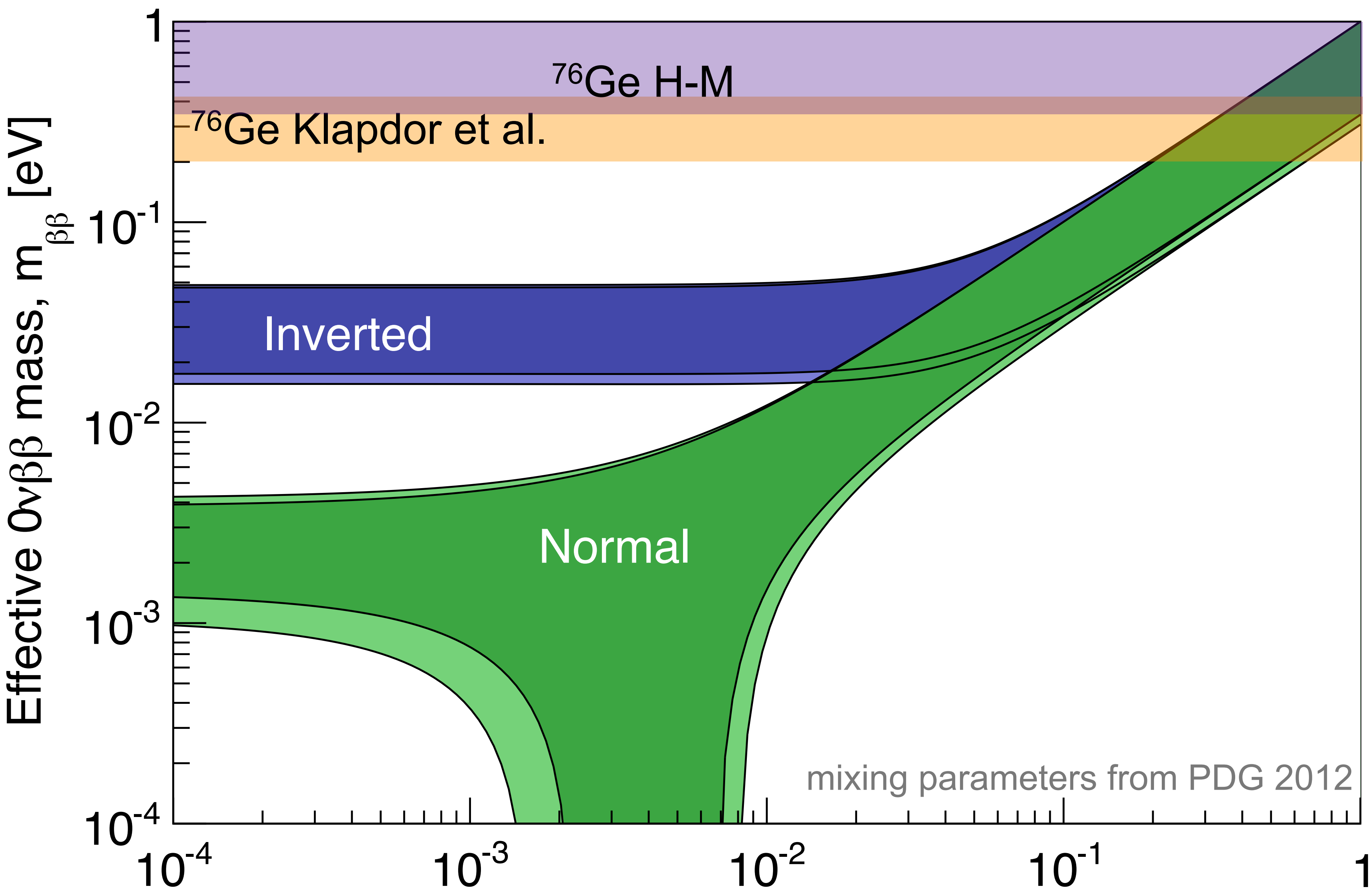

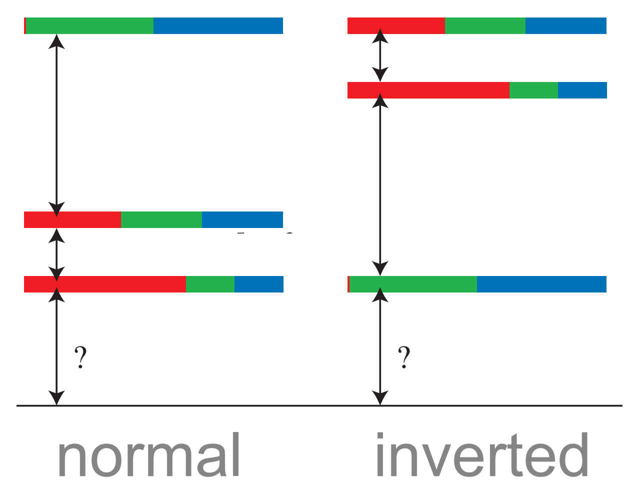

Klapdor: Mod. Phys. Lett. A21 (2006) 1547
HM: Eur Phys. Journal A12 (2001) 147
EXO-200: Phys. Rev. Lett. 109 (2012) 032505
KamLAND-Zen: Phys. Rev. C 86 (2012) 021601

0νββ and neutrino mass

decay rate: $[T_{1/2}^{0\nu\beta\beta}]^{-1} = G^{0\nu\beta\beta}(E_0,Z)\ (M^{0\nu\beta\beta})^2\ \langle m_{0\nu\beta\beta}\rangle^2$

eff. mass: $m_{0\nu\beta\beta} = \left|\, |U_{e1}|^2 m_1 + |U_{e2}|^2 m_2 e^{i\Phi 2} + |U_{e3}|^2 m_3 e^{i\Phi 3} \,\right|$

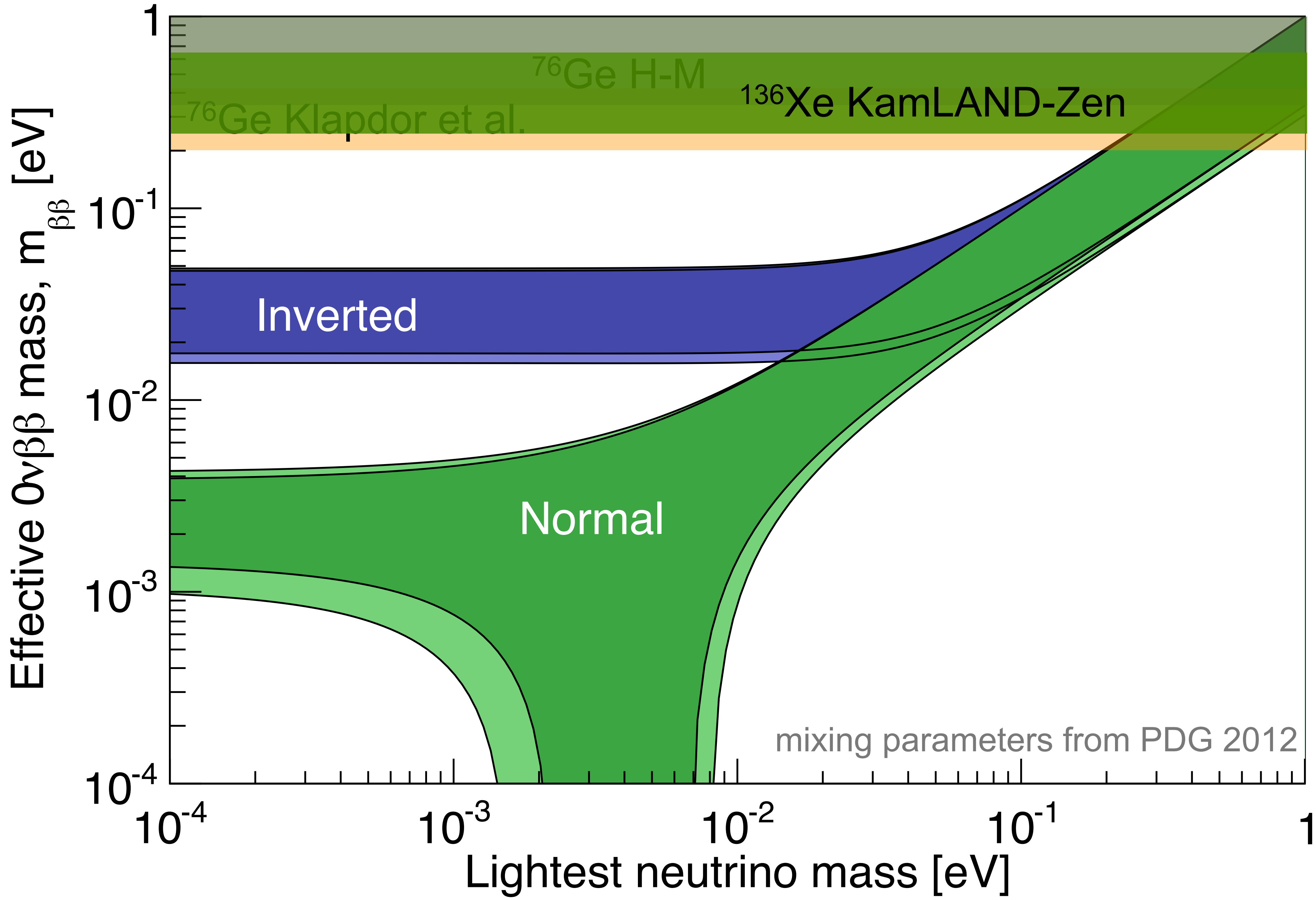

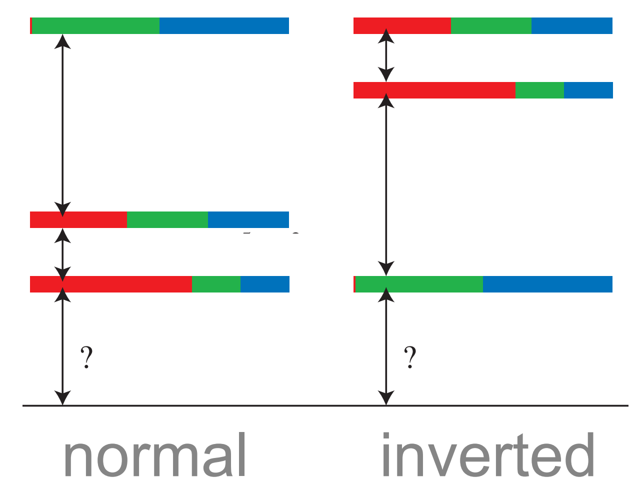

Klapdor: Mod. Phys. Lett. A21 (2006) 1547
HM: Eur Phys. Journal A12 (2001) 147
EXO-200: Phys. Rev. Lett. 109 (2012) 032505
KamLAND-Zen: Phys. Rev. C 86 (2012) 021601

0νββ and neutrino mass

decay rate: $[T_{1/2}^{0\nu\beta\beta}]^{-1} = G^{0\nu\beta\beta}(E_0,Z)\ (M^{0\nu\beta\beta})^2\ \langle m_{0\nu\beta\beta}\rangle^2$

eff. mass: $m_{0\nu\beta\beta} = \Big|\, |U_{e1}|^2 m_1 + |U_{e2}|^2 m_2 e^{i\Phi_2} + |U_{e3}|^2 m_3 e^{i\Phi_3} \,\Big|$

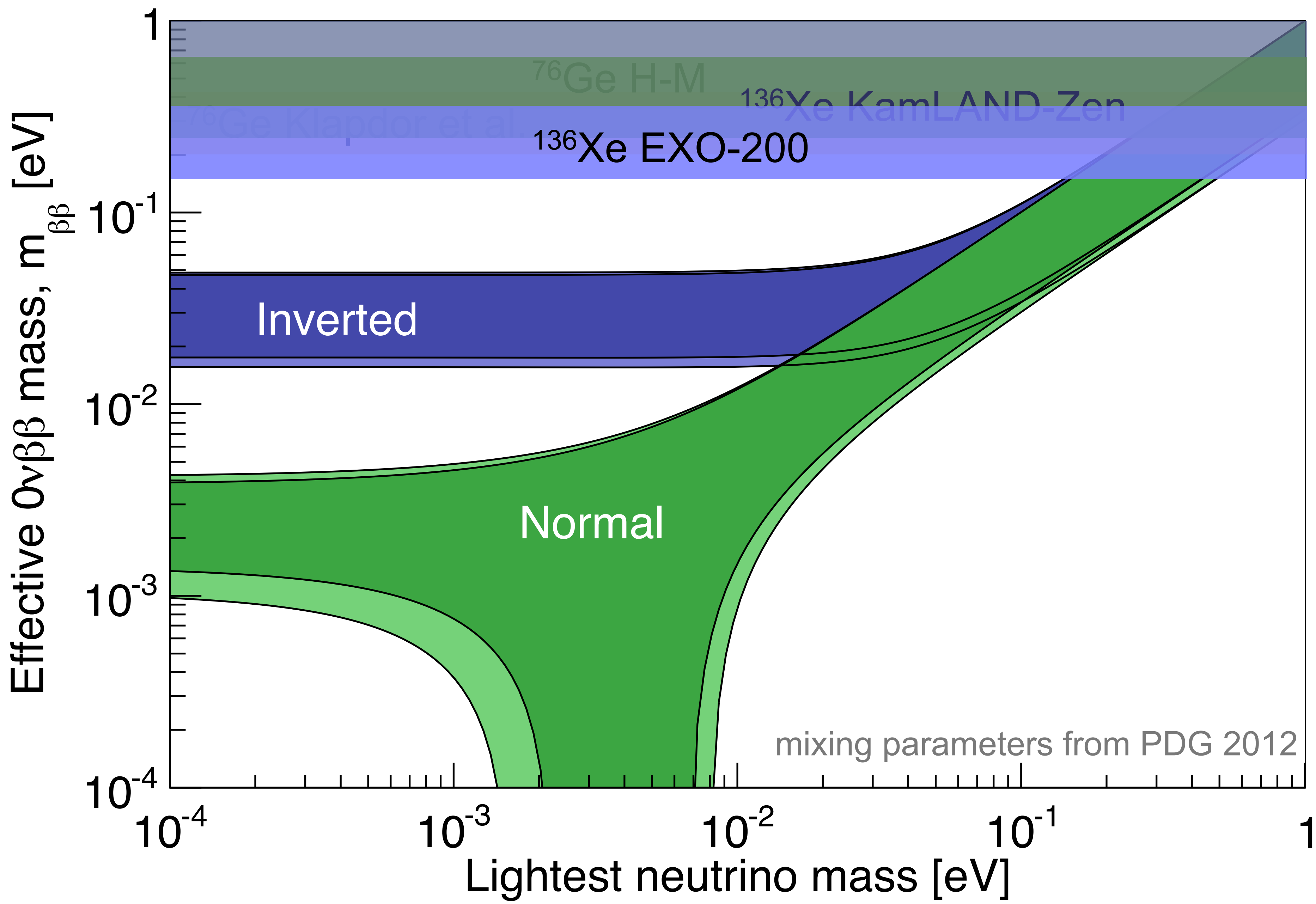

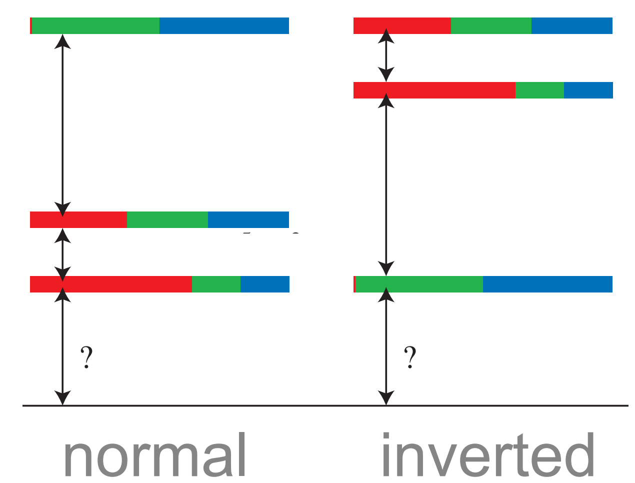

Klapdor: Mod. Phys. Lett. A21 (2006) 1547
HM: Eur Phys. Journal A12 (2001) 147
EXO-200: Phys. Rev. Lett. 109 (2012) 032505
KamLAND-Zen: Phys. Rev. C 86 (2012) 021601

Criteria for 0νββ experiment

- Large mass of source
- Extremely low background rate
- Best possible background identification techniques

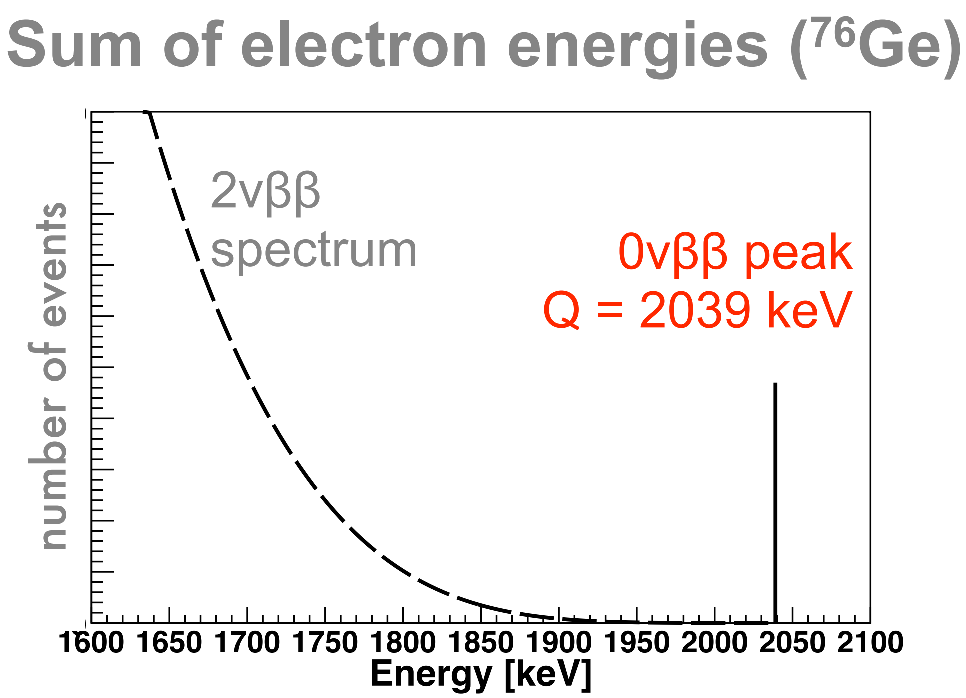

Criteria for 0νββ observation

- Peak at the correct energy
- Full energy spectrum, including backgrounds, understood
- Observe in several different isotopes in independent experiments

$0\nu\beta\beta$ experiments

EXO-200

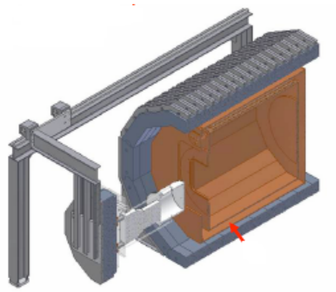

CUORE

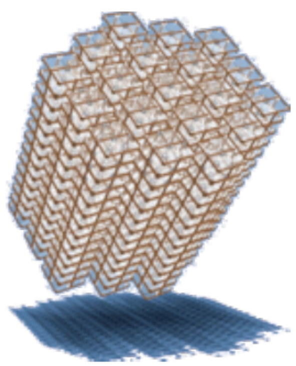

NEMO

Collaboration	Isotope	Technique	mass ($0\nu\beta\beta$ isotope)	Status
CANDLES	Ca-48	305 kg CaF_2 crystals - liq. scint	0.3 kg	Construction
CARVEL	Ca-48	$^{48}CaWO_4$ crystal scint.		
GERDA I	Ge-76	Ge diodes in LAr	15 kg	Operating
II		Point contact Ge in LAr or LN	30-35 kg	Construction
MAJORANA DEMONSTRATOR	Ge-76	Point contact Ge	30 kg	Construction
1TGe (GERDA & MAJORANA)	Ge-76	Best technology from GERDA and MAJORANA	~ tonne	R&D
NEMO3	Mo-100 Se-82	Foils with tracking	6.9 kg 0.9 kg	Complete
SuperNEMO Demonstrator	Se-82	Foils with tracking	7 kg	R&D
MOON	Mo-100	Mo sheets	200 kg	R&D
CAMEO	Cd-116	$CdWO_4$ crystals		
COBRA	Cd-116, Te-130	CdZnTe detectors	10 kg	R&D
CUORICINO	Te-130	TeO_2 Bolometer	10 kg	Complete
CUORE	Te-130	TeO_2 Bolometer	206 kg	Construction
KamLAND-ZEN	Xe-136	2.7% in liquid scint.	380 kg	Operating
NEXT-100	Xe-136	High pressure Xe TPC	80 kg	R&D
EXO200	Xe-136	Xe liquid TPC	160 kg	Operating
EXO	Xe-136	Xe liquid TPC	~ tonne	R&D
DCBA	Nd-150	Nd foils & tracking chambers	< kg	R&D
SNO+	Nd-150	0.1% ^{nat}Nd suspended in Scint	44 kg	Construction

Operating Commissioning Construction

GERDA

MAJORANA

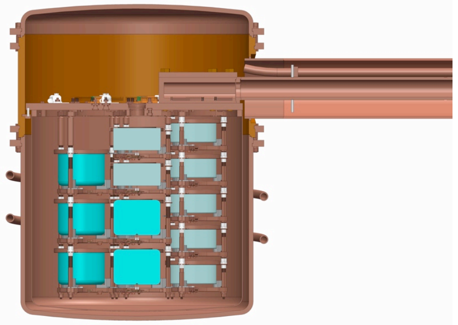

KamLAND-Zen

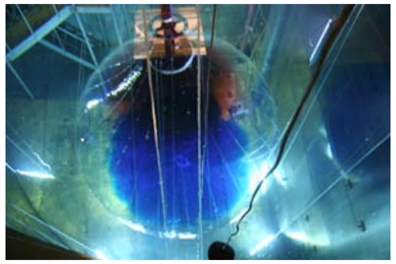

slide from J.F. Wilkerson

germanium detectors

- Detector is source: demonstrated ability to enrich from 7.4% to 86% ^{76}Ge
- Ge diodes are intrinsically high purity
- Excellent energy resolution: 0.13% FWHM at Q-value of 2039 keV
- Commercially available
- P-type point contact detectors
  - extremely low noise
  - low energy threshold

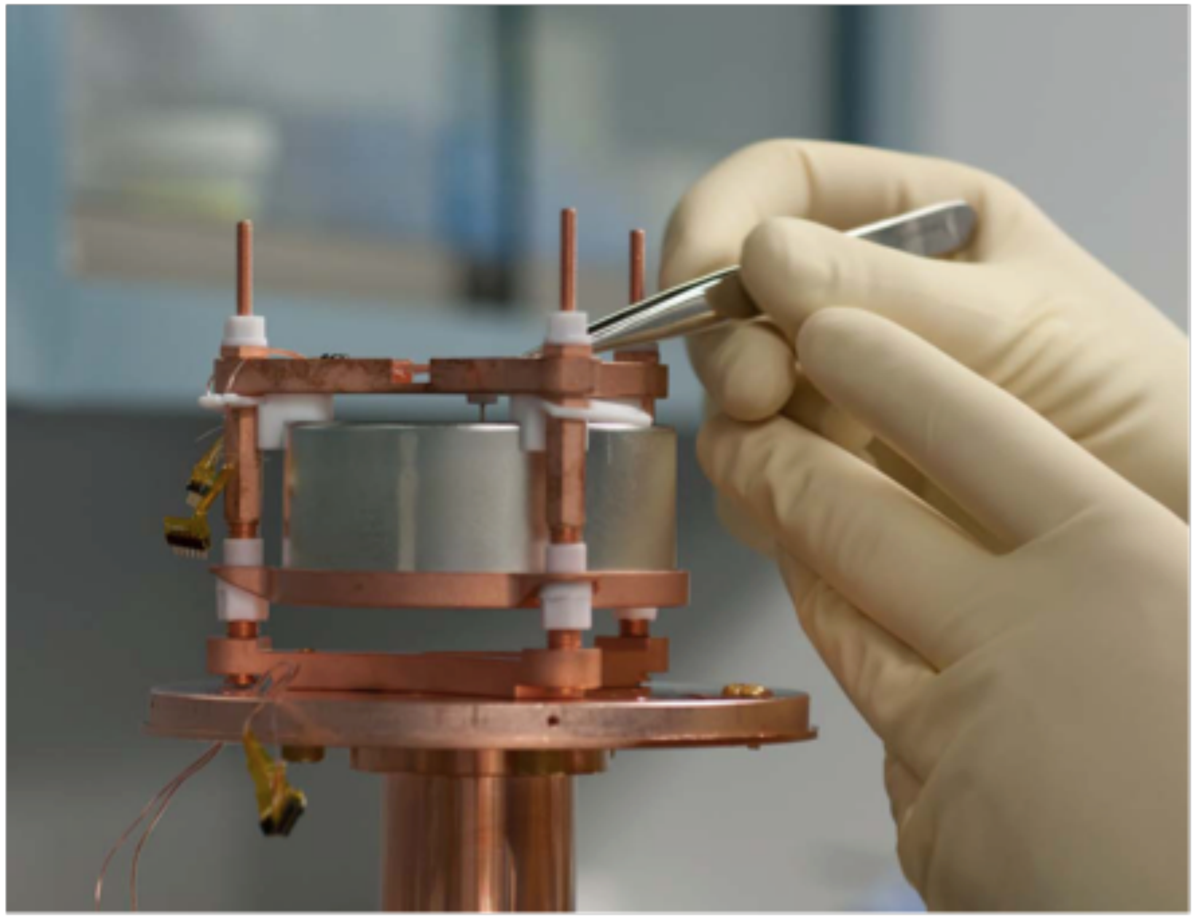

A stainless-steel detector blank in a prototype MAJORANA detector mount

GERDA

MAJORANA

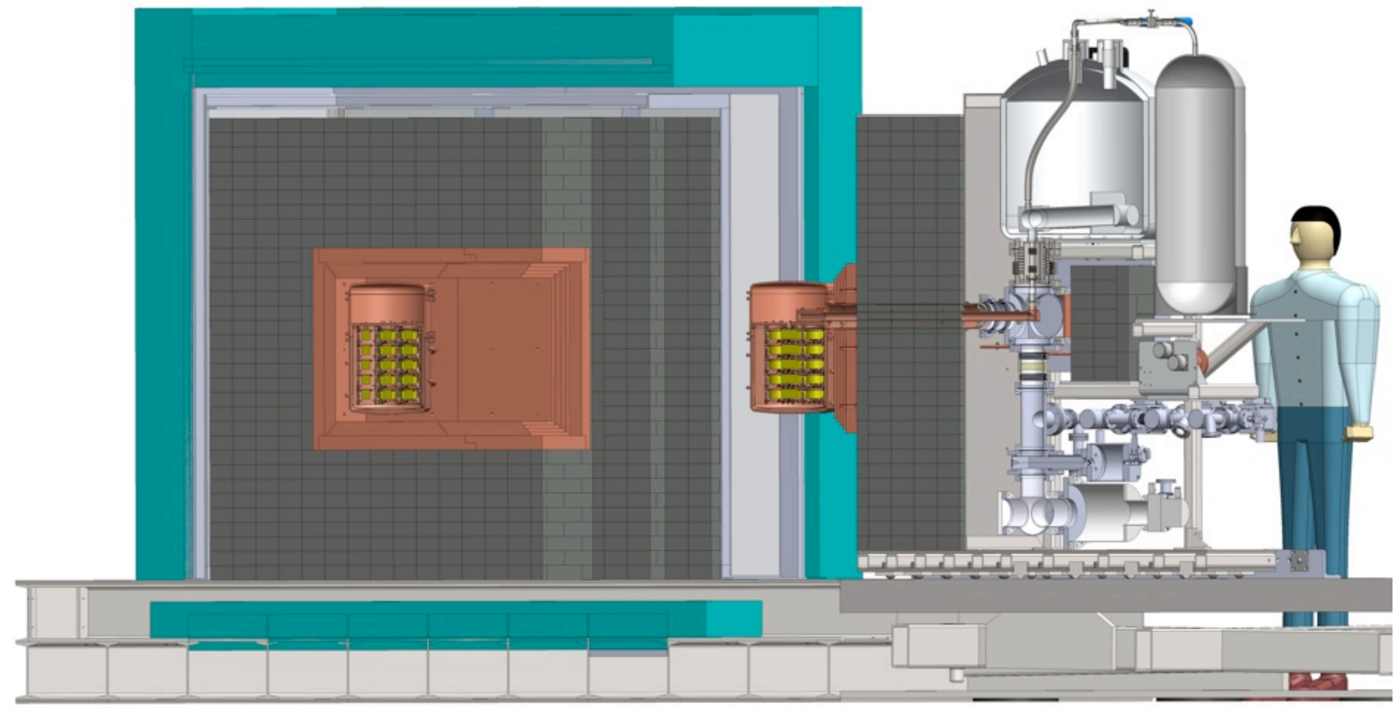

- **Design:** detectors submerged in liquid Argon at LNGS, Italy
- **Shield**: LAr, H_20
- **Phase I:** 18 kg enr-Ge (2011)
- **Phase II:** 20 kg enr-Ge (2013)

- **Design:** detectors in high-purity electroformed copper cryostats at Sanford Lab, US
- **Shield:** copper, lead
- **DEMONSTRATOR:** 30 kg of enr-Ge

Open exchange of knowledge and technologies
Future goal: merge for tonne-scale experiment

Sensitivity of a tonne-scale ^{76}Ge experiment

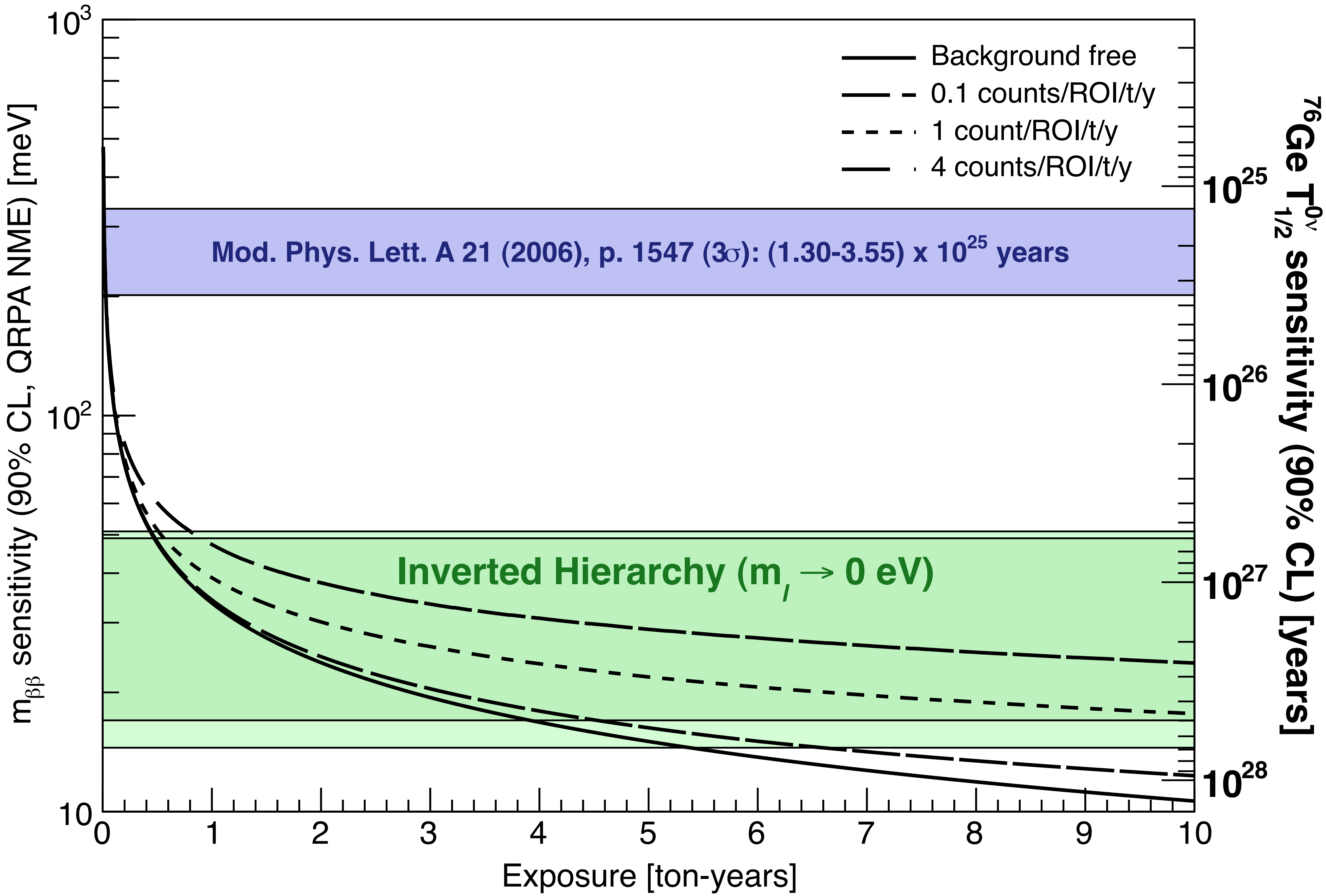

The MAJORANA DEMONSTRATOR

Funded by DOE Office of Nuclear Physics and NSF Particle and Nuclear Astrophysics,
with additional contributions from international collaborators.

Goals: - Demonstrate backgrounds low enough to justify building a tonne scale experiment
- Establish feasibility to construct & field modular arrays of Ge detectors
- Test Klapdor-Kleingrothaus claim
- Low-energy dark matter (light WIMPs) search

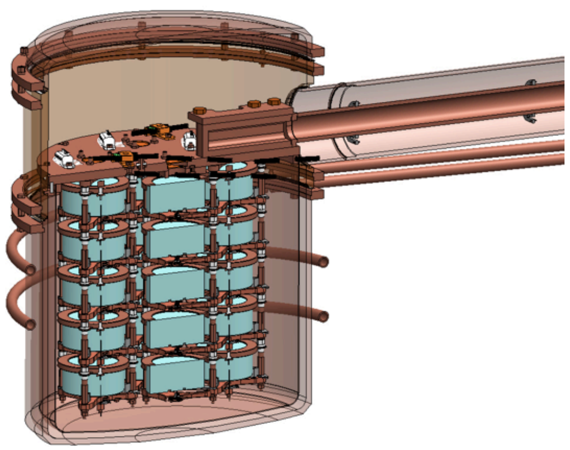

- **Located underground at 4850' Sanford Lab**
- **Background Goal in the 0νββ peak region of interest (4 keV at 2039 keV)**
  4 counts/ROI/t/y (after analysis cuts)
  scales to 1 count/ROI/t/y for a tonne experiment
- **40-kg of Ge detectors**
  – 30-kg of 86% enriched ^{76}Ge crystals & 10-kg of ^{nat}Ge
  – Detector Technology: P-type, point-contact.
- **2 independent cryostats**
  – ultra-clean, electroformed Cu
  – 20 kg of detectors per cryostat
  – naturally scalable
- **Compact Shield**
  – low-background passive Cu and Pb shield with active muon veto

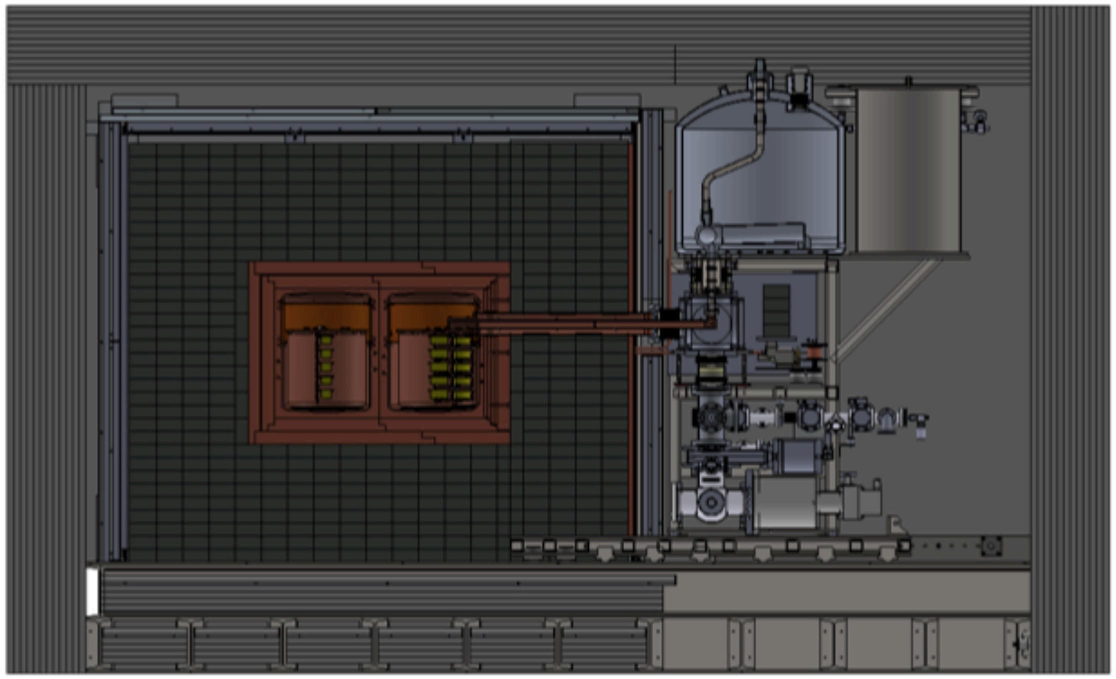

The MAJORANA DEMONSTRATOR

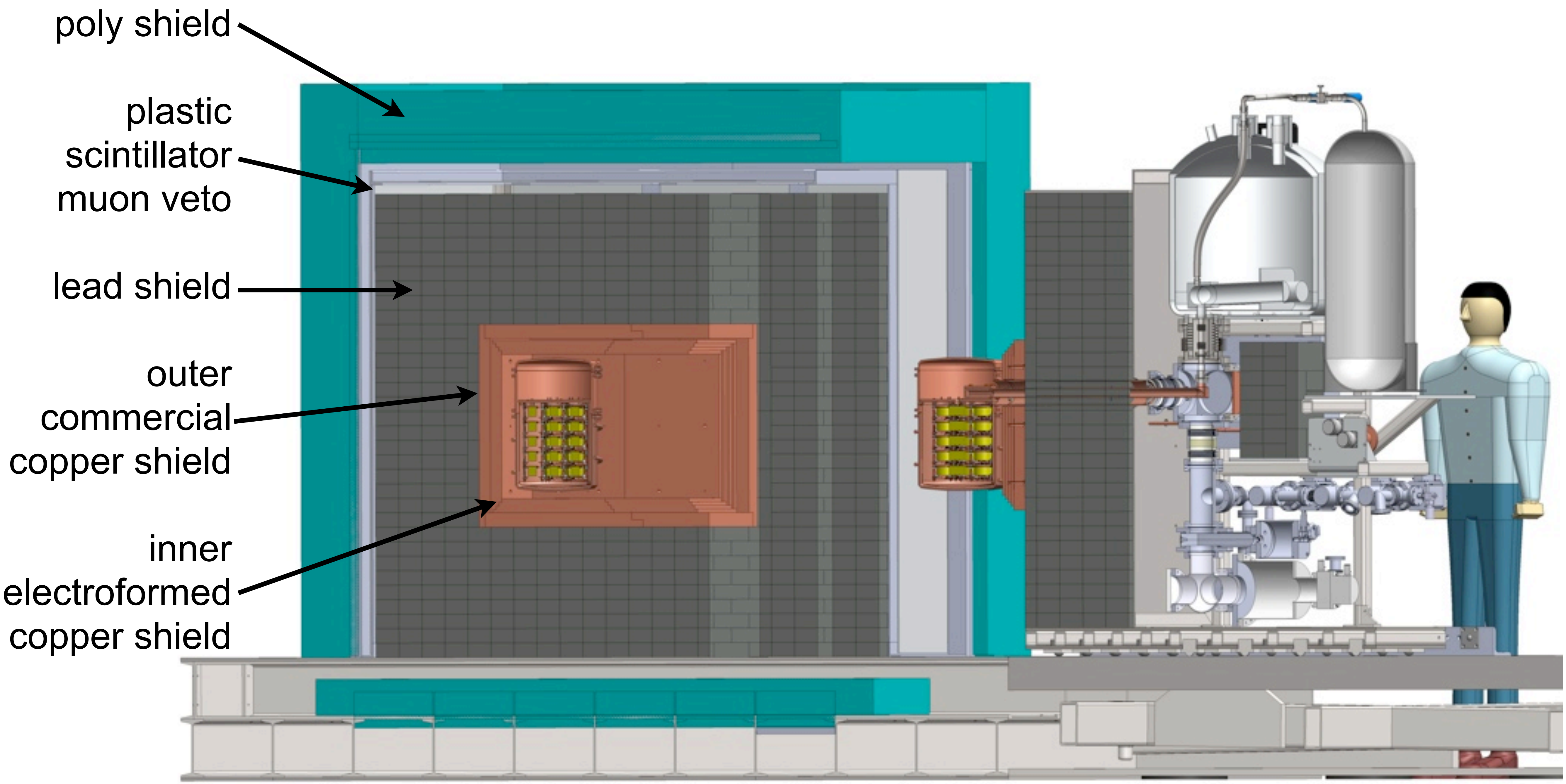

DEMONSTRATOR Schedule

- **Three steps:**
  - **Prototype cryostat:** 2 strings natural Ge — **Early 2013**
  - **Cryostat 1:** 3 strings enr. Ge, 4 strings nat. Ge — **Fall 2013**
  - **Cryostat 2:** 7 strings enr. Ge — **Fall 2014**

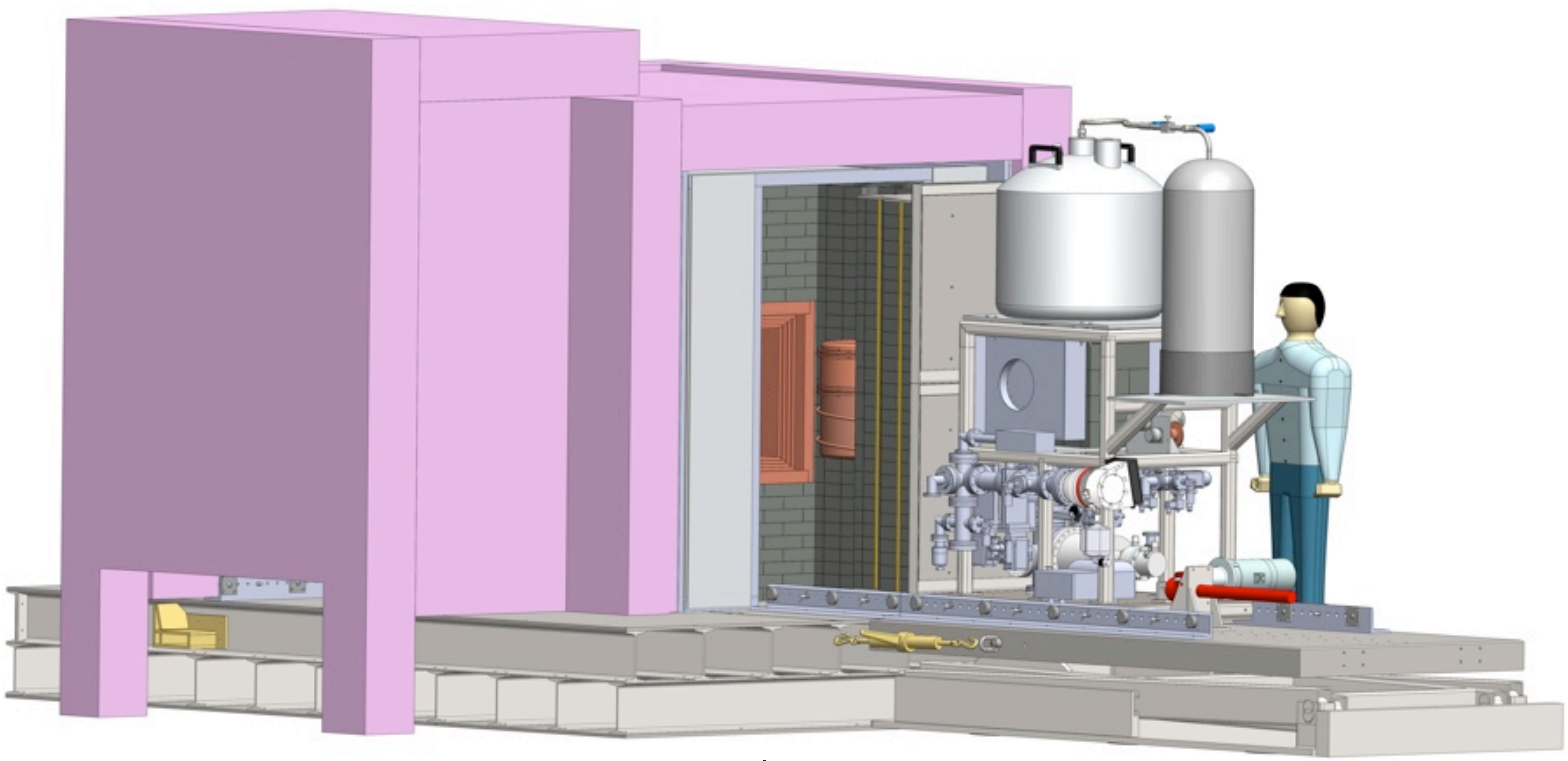

Sanford Underground Research Facility

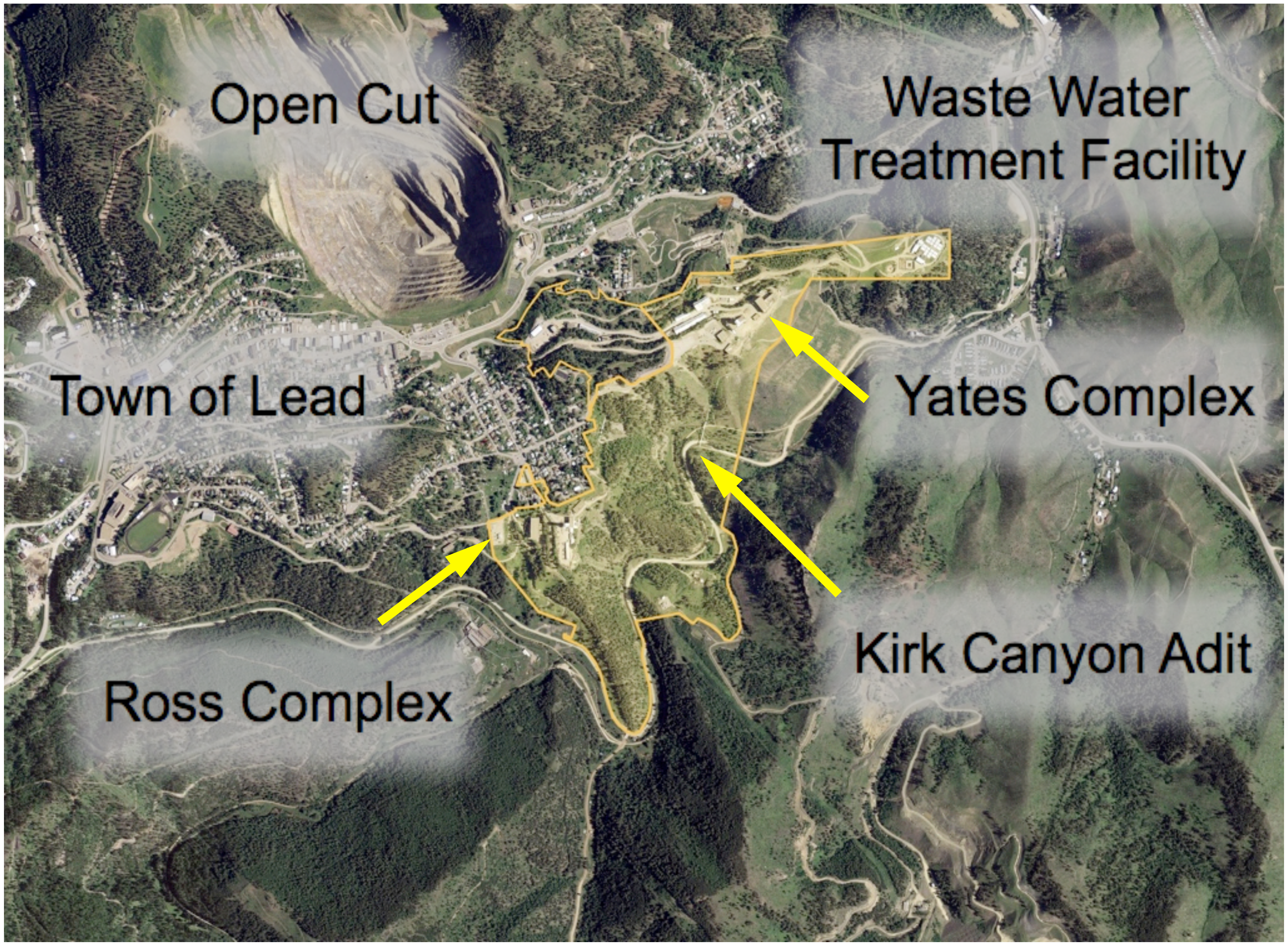

Home of the MAJORANA DEMONSTRATOR, Lead, SD

Recent DEMONSTRATOR progress

prototype cryostat

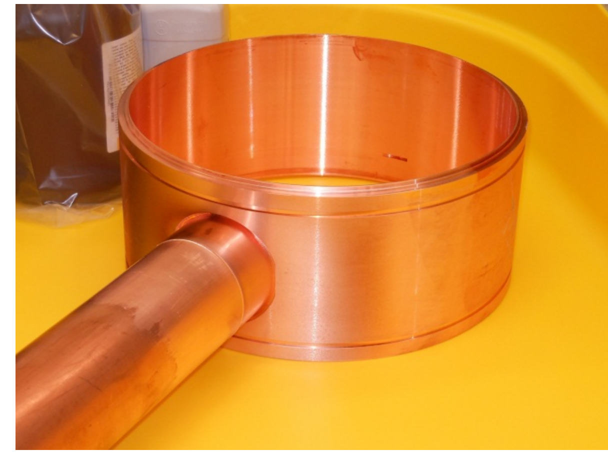

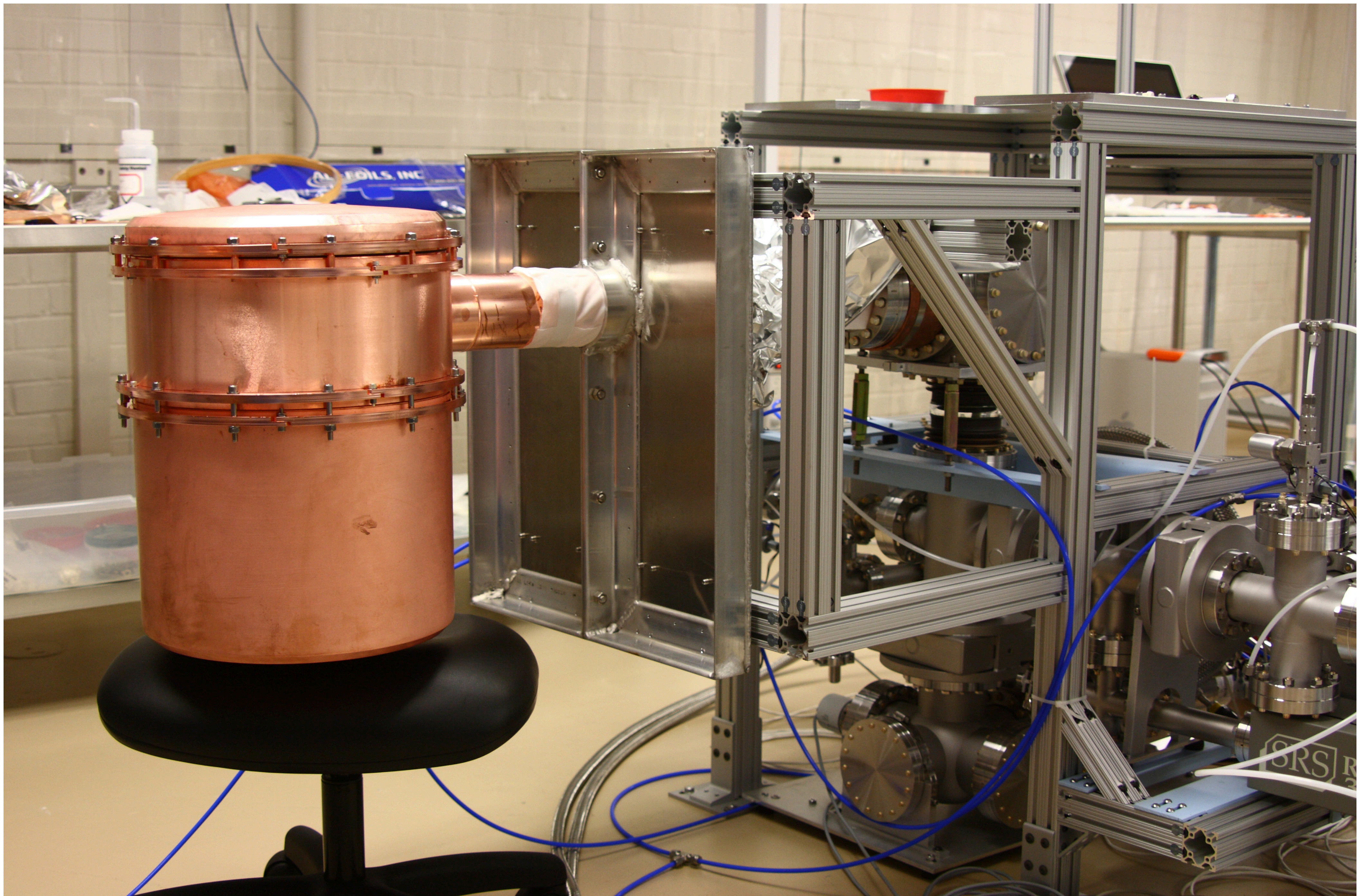

detector string evolution

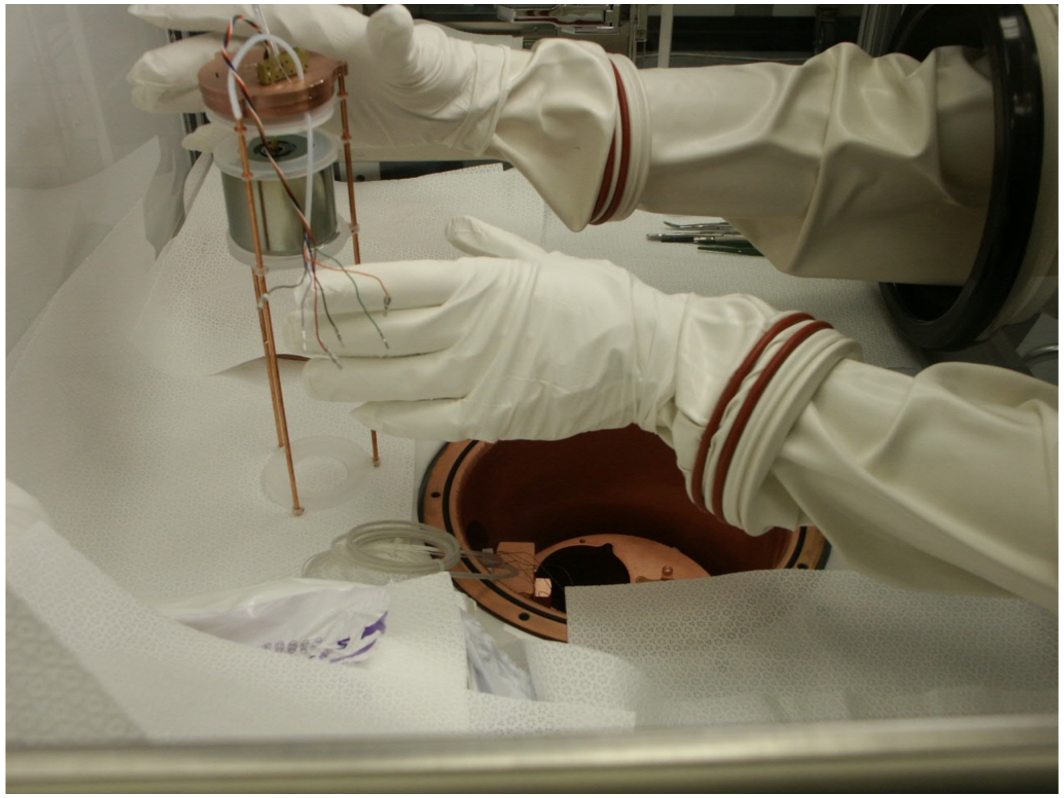

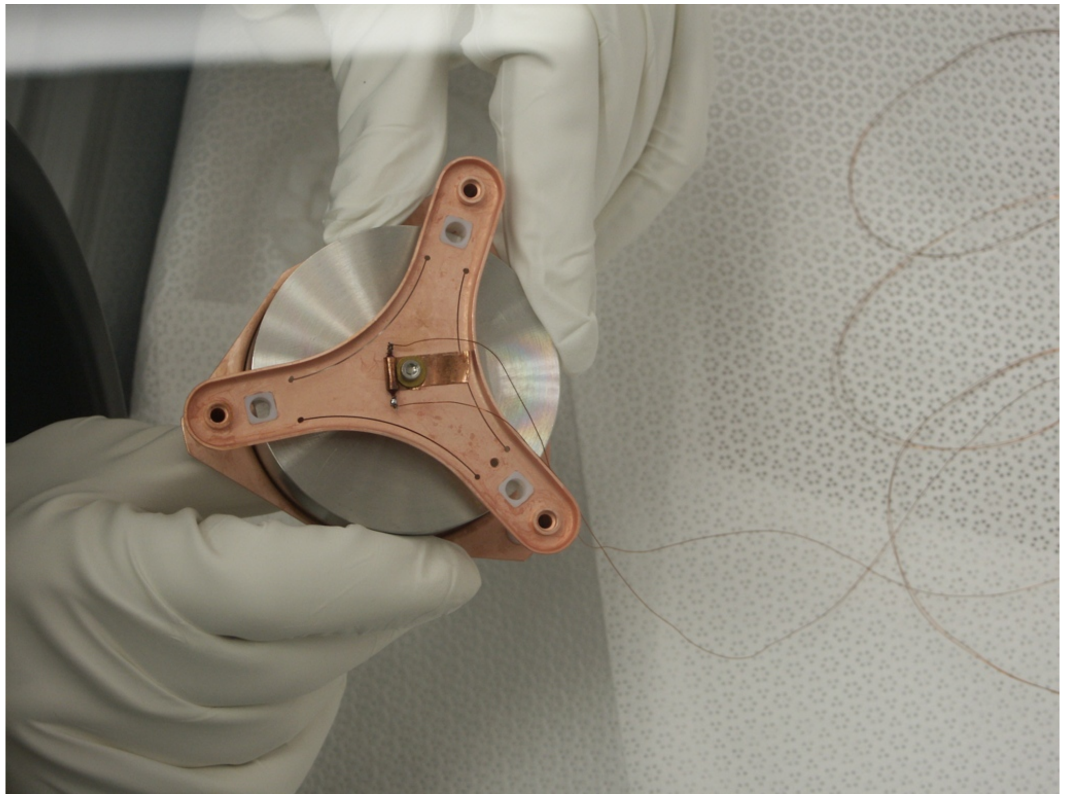

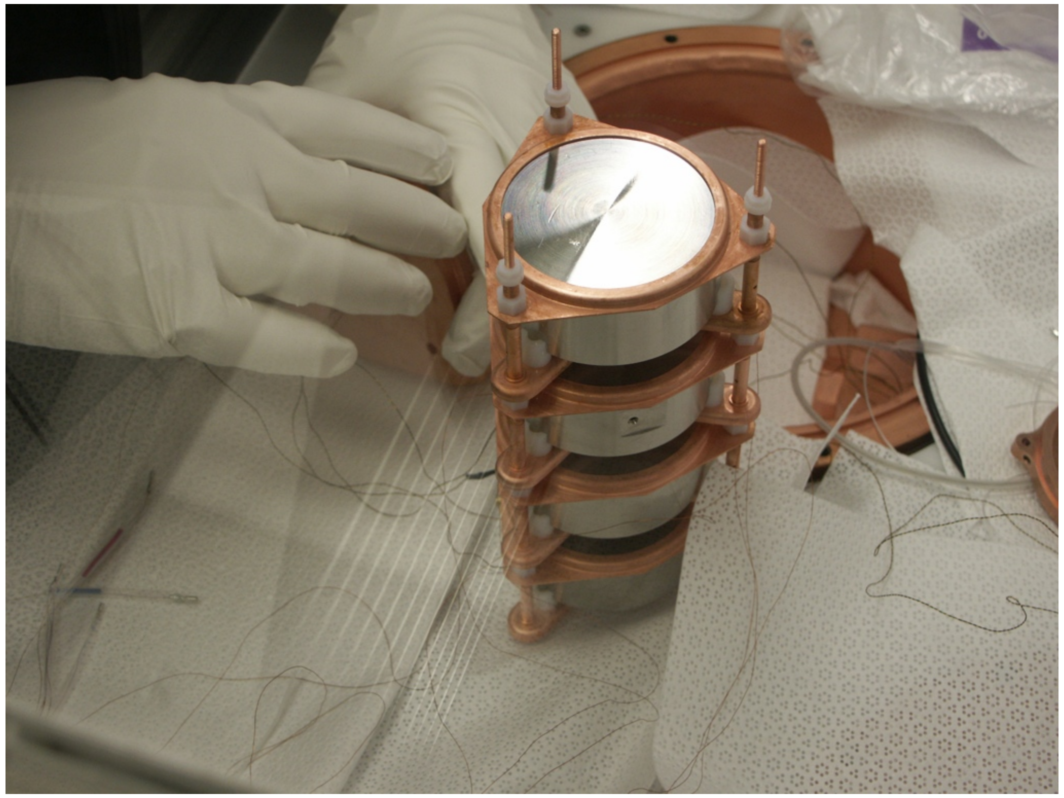

detector string evolution

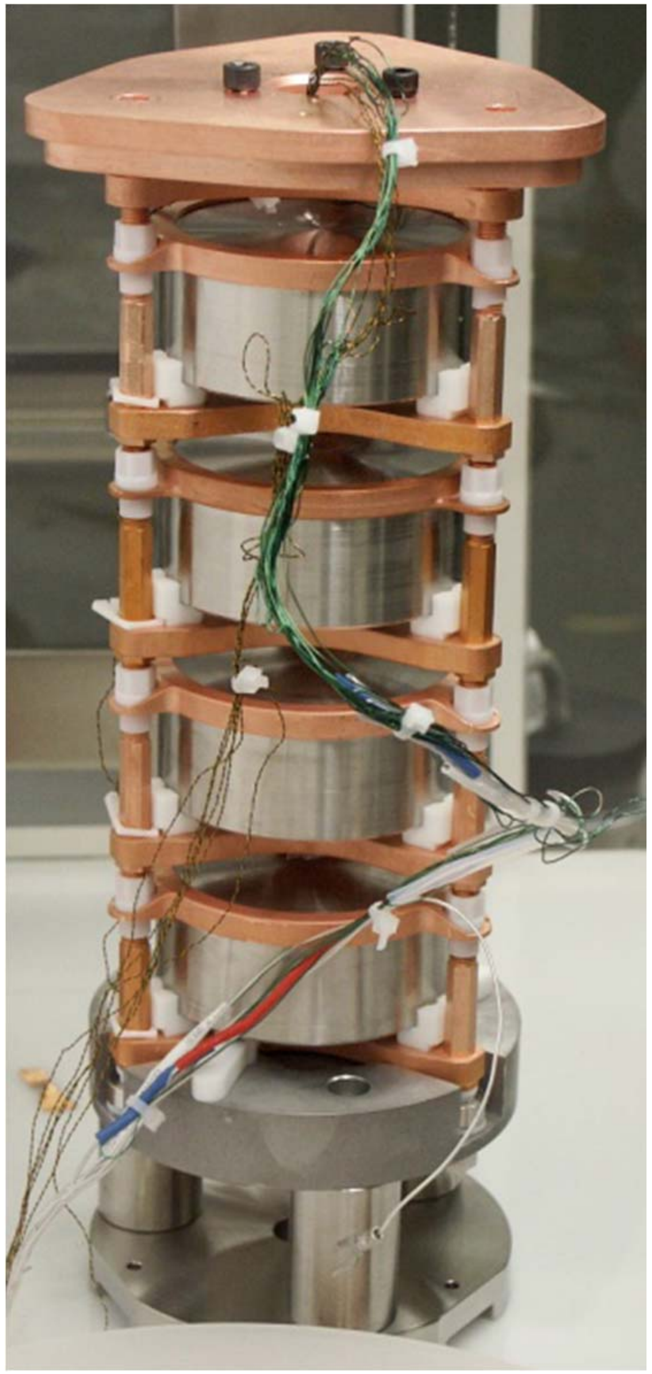

LANL thermal test string Jan 2011

LBNL March 2011 thermal tests

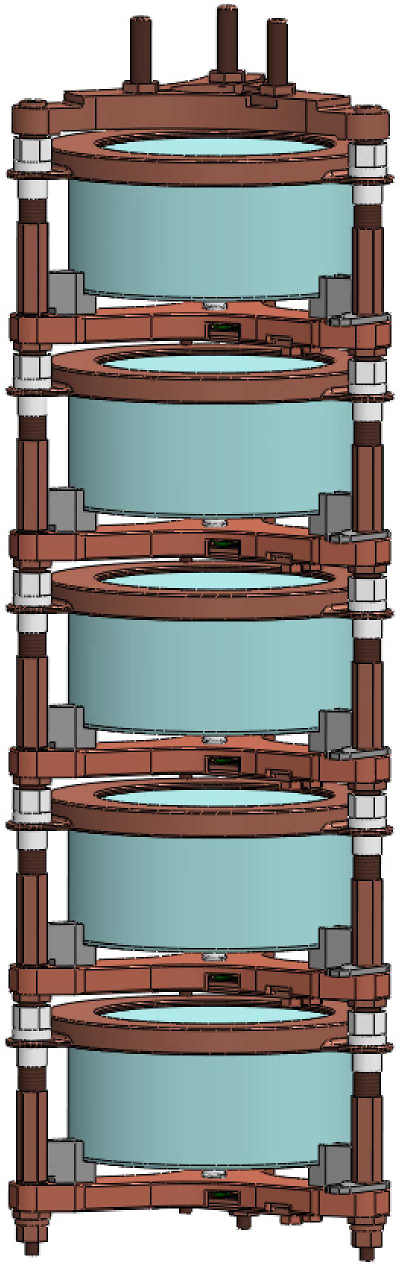

Design as released for Prototype production Feb 2012: MJ80-02-195

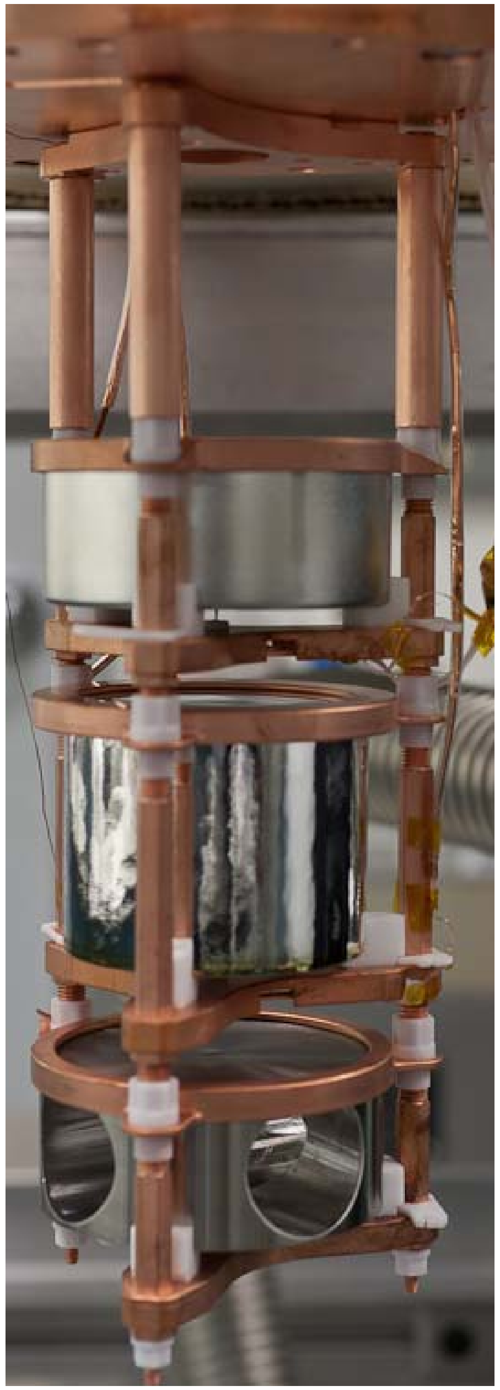

LBNL Jan 2012 tests

Slide from M. Busch

10 baths at Sanford producing copper since July 2011

about 50% of EFCu complete, including major parts for cryostat 1

M. Kapust

underground construction is underway

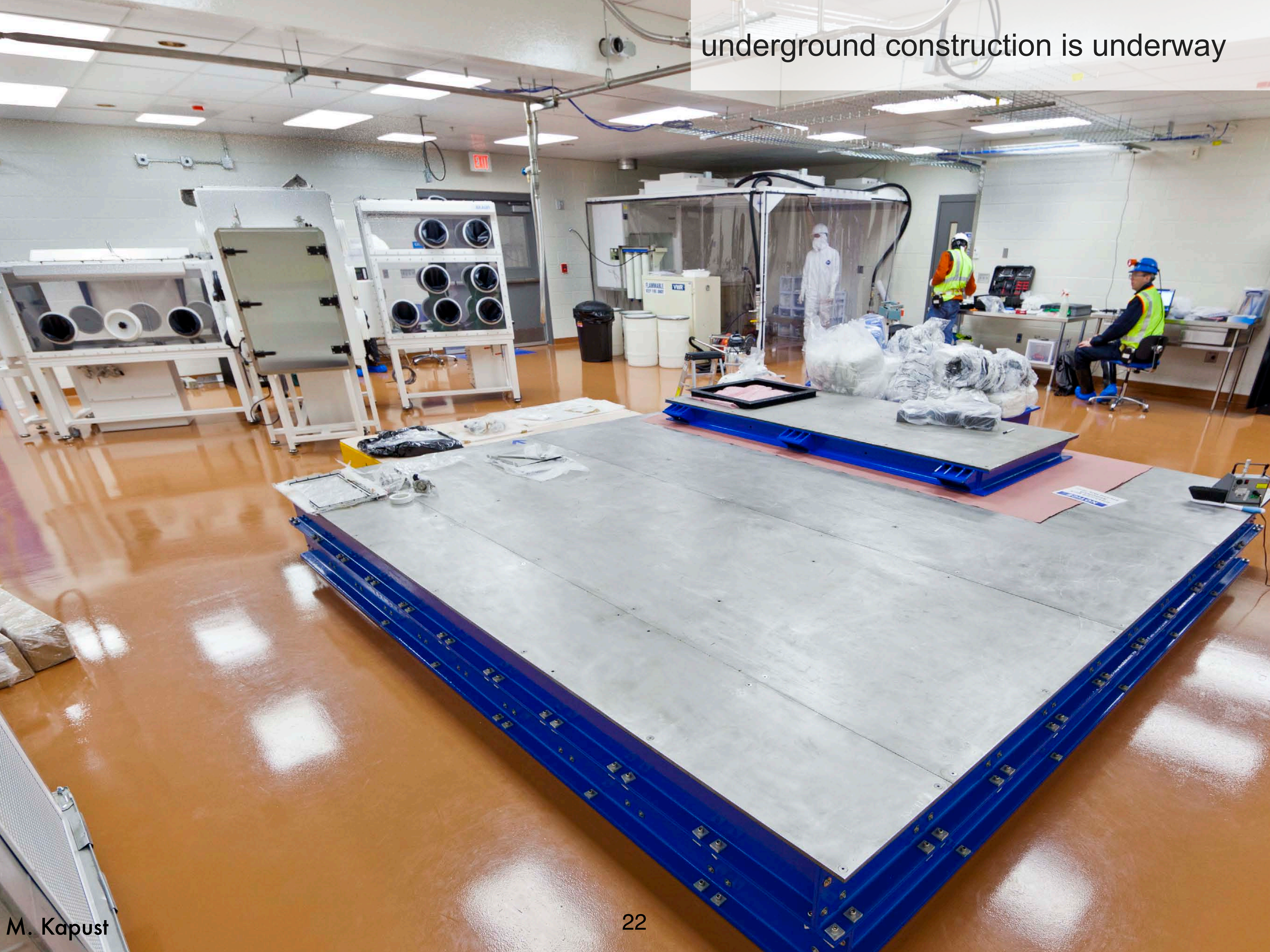

M. Kapust

M. Kapust

M. Kapust

Detector electronics

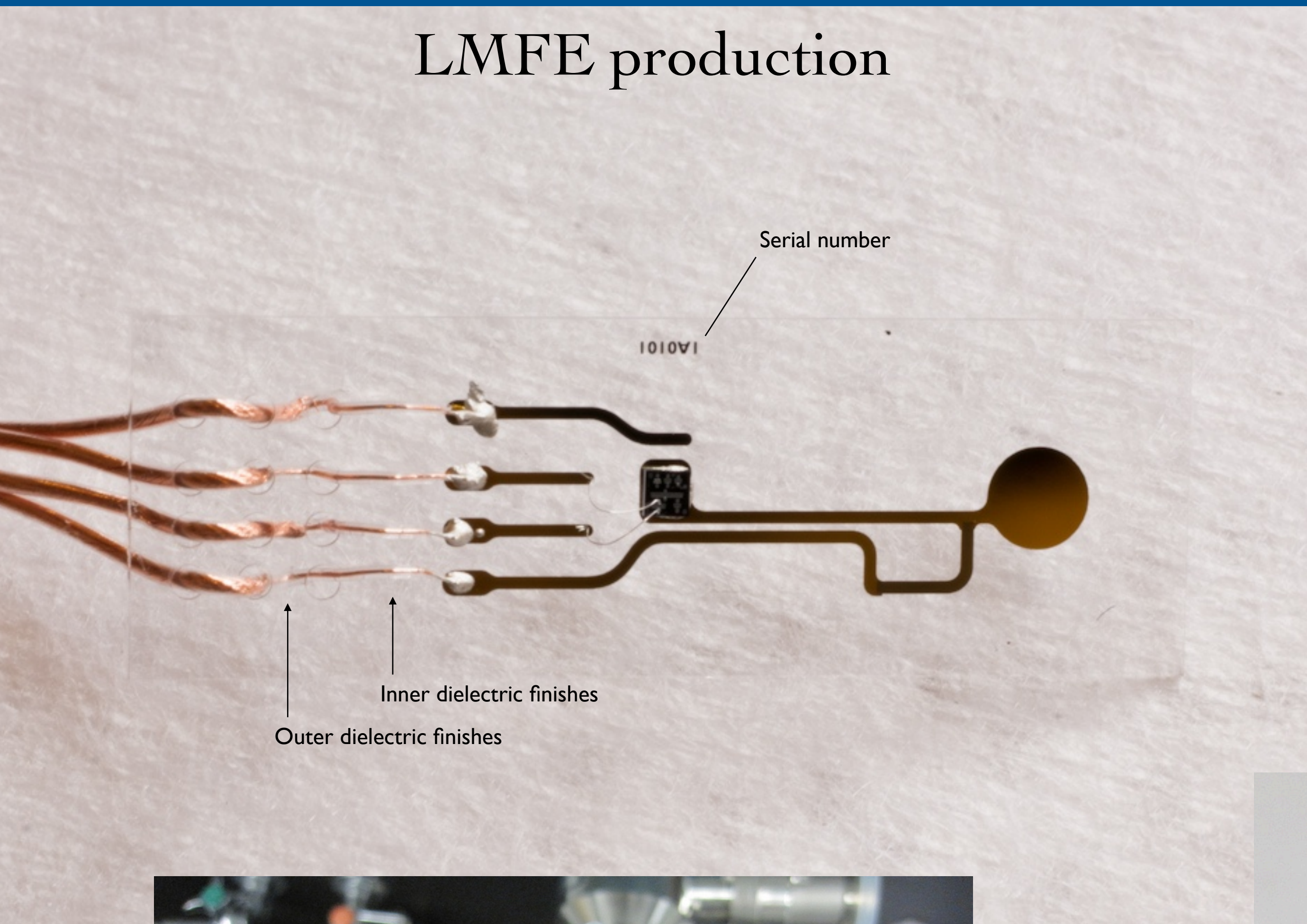

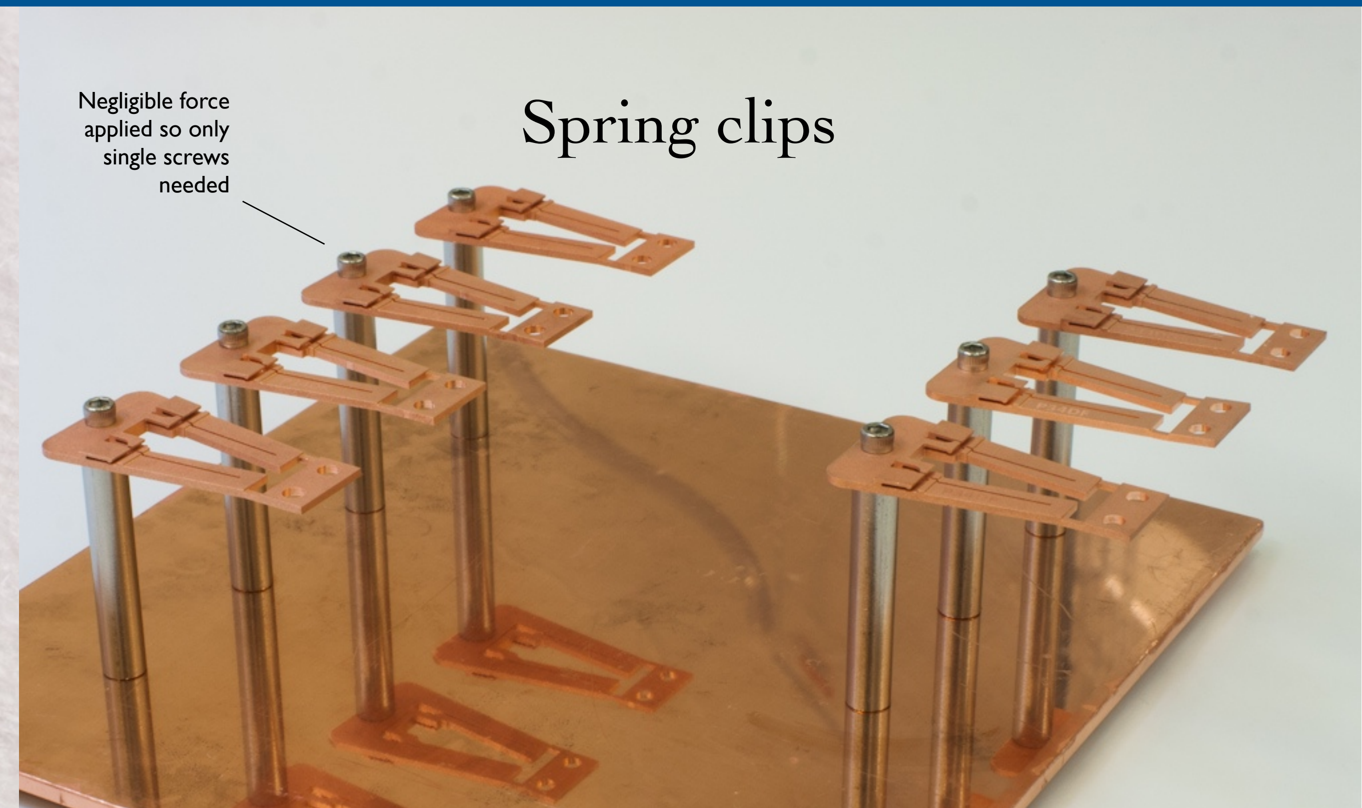

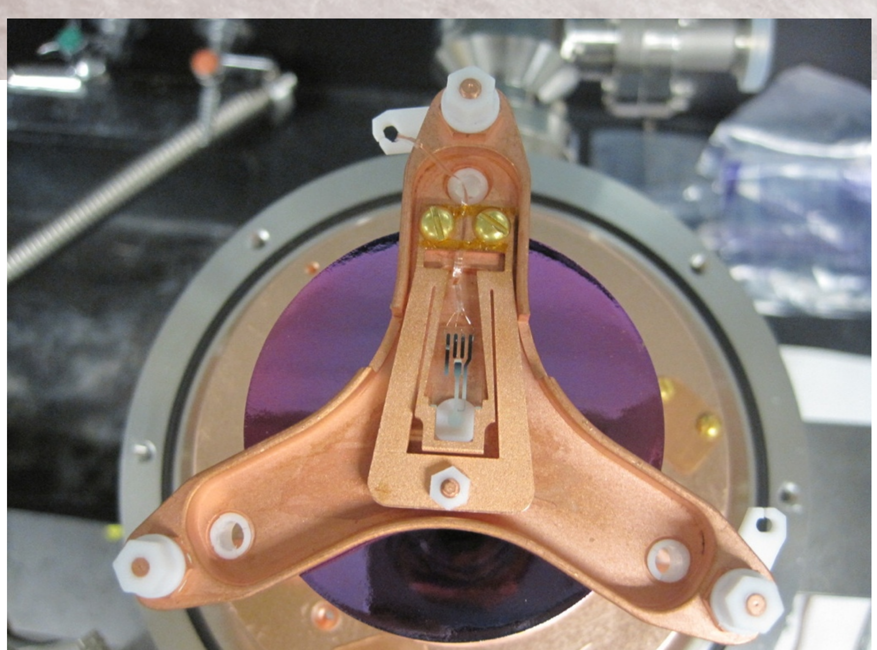

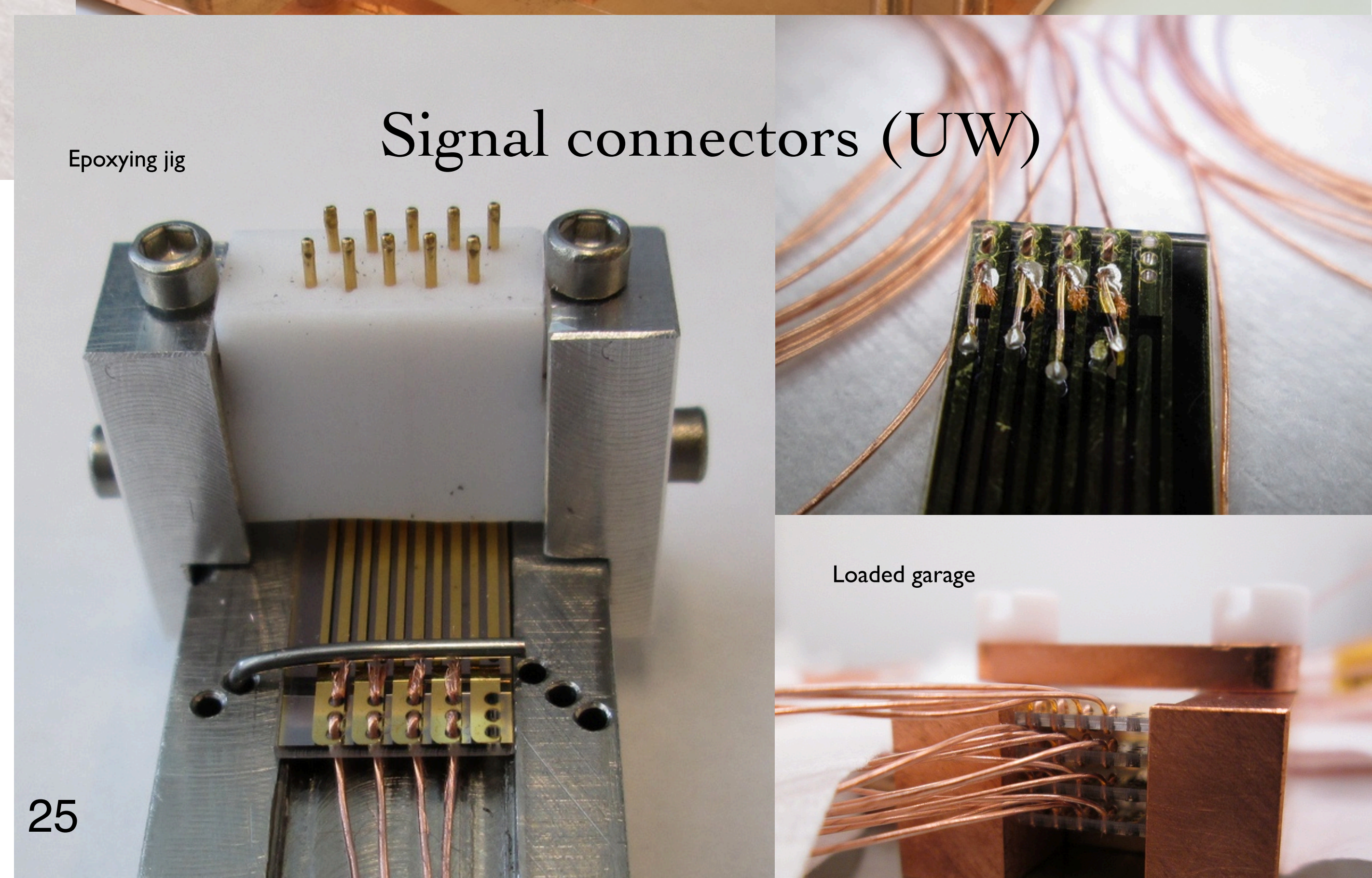

images from J. Loach

detection of $0\nu\beta\beta$

The 0νββ signal in germanium

- Ionizing energy deposits in germanium produce a charge signal
- The 0νββ signal:
  - Single site
  - Single crystal
  - Uncorrelated in time with other events
  - Near 2039-keV ^{76}Ge endpoint

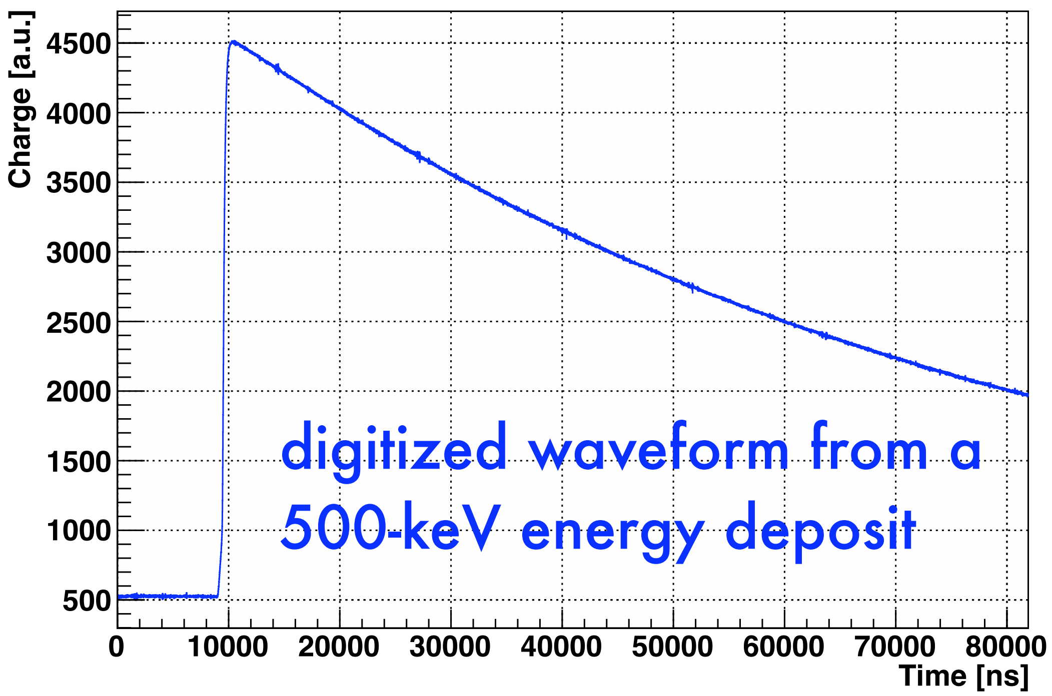

a germanium crystal in cross section

Sources of background

- Primordial contamination: ^{40}K, ^{238}U, ^{232}Th
- Long-lived cosmogenics: ^{68}Ge, ^{60}Co, ^{65}Zn
- Prompt cosmogenics: μ, μ-induced neutrons
- other: anthropogenic contaminants, radon, solar neutrinos

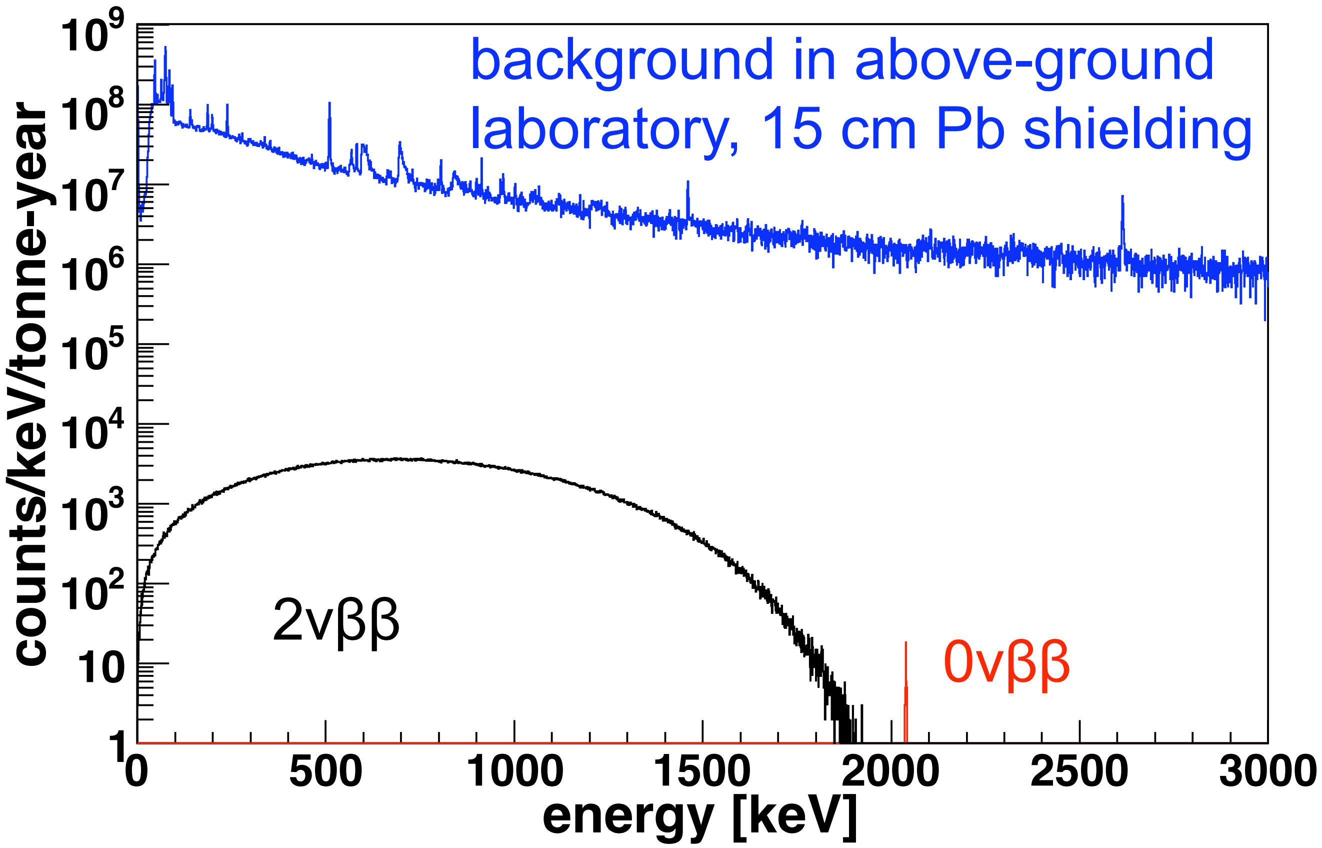

Background reduction techniques

- Minimize mass of non-germanium components
- Use passive and active shielding
- Fabricate parts in shielding from clean copper and plastic
  - Electroform and machine copper underground at Sanford and PNNL

Backgrounds in germanium detectors

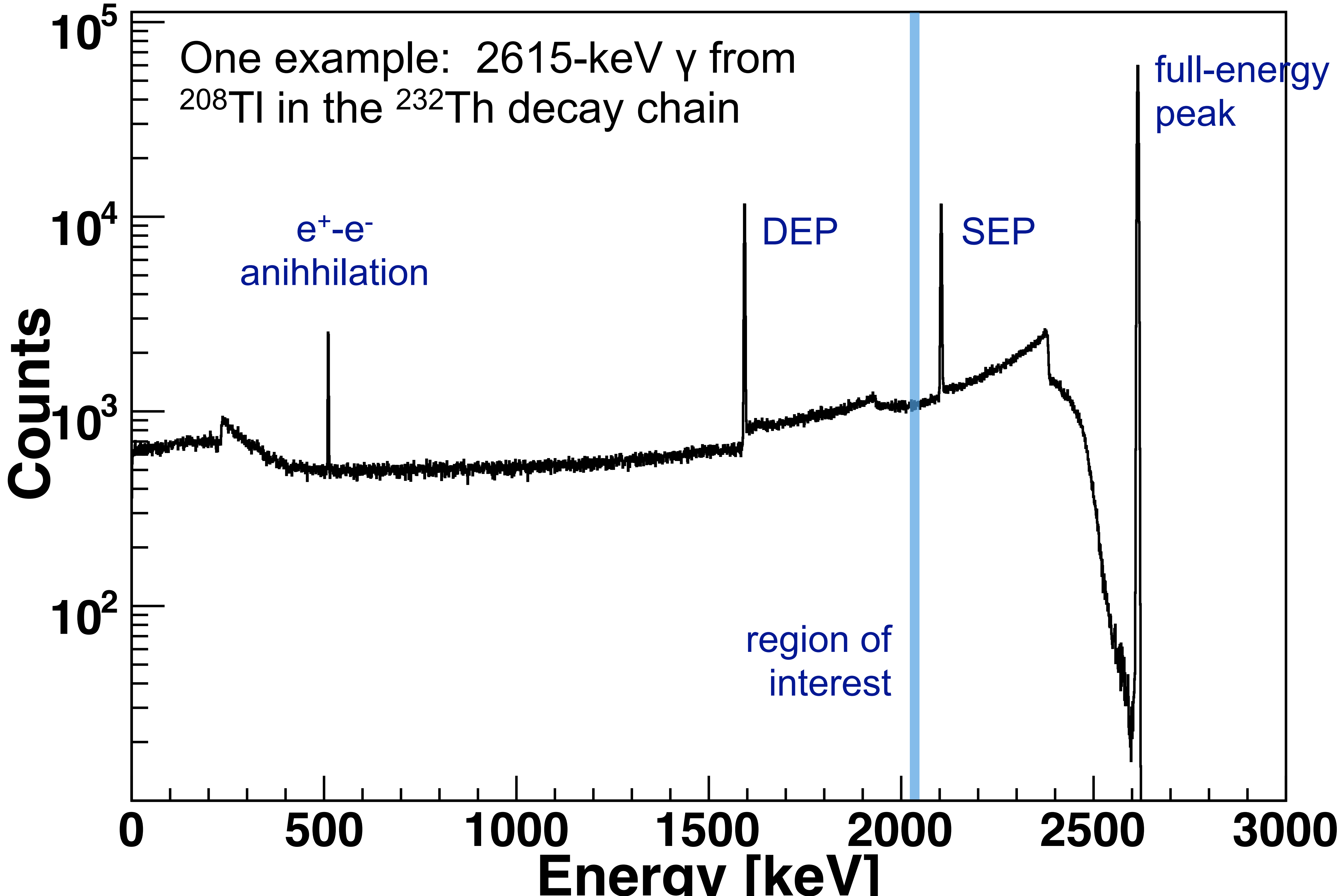

Background mitigation techniques

- Time correlation: identify ^{68}Ge to ^{68}Ga decays

$^{68}Ge \longrightarrow$ $^{68}Ga \longrightarrow$ ^{68}Zn

$T_{1/2}$ = 271 days
electron capture:
K-shell: 10.4 keV, 86%
L-shell: 1.2 keV, 11%

$T_{1/2}$ = 68 minutes
Q = 2.9 MeV

- Granularity: tag events that deposit energy in multiple detectors

- Pulse-shape discrimination: discriminate multi-site backgrounds

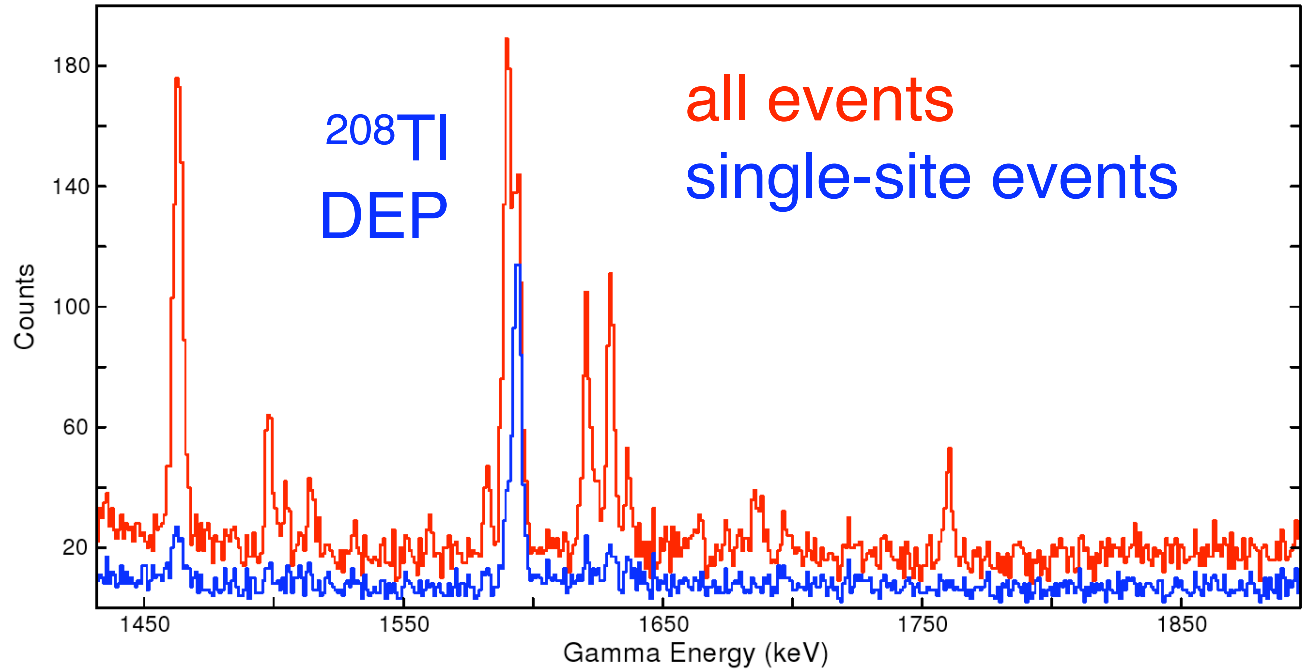

example of pulse-shape analysis

R&D detector: MALBEK

<u>M</u>A<u>J</u>ORANA <u>L</u>ow-background <u>BE</u>Ge detector at <u>K</u>imballton

- 0.4 kg natural germanium
- Customized CANBERRA <u>B</u>road-<u>E</u>nergy <u>Ge</u>rmanium (BEGe) detector
  - Modified geometry of crystal ditch, surrounding components to minimize capacitance
  - Low-background copper cryostat
- Kimballton Underground Research Facility in Ripplemeade, VA (1700', 1400 m.w.e.)
- R&D:
  - Dark matter search
  - MAJORANA-like data-acquisition system
  - Measurement & model of background energy spectrum

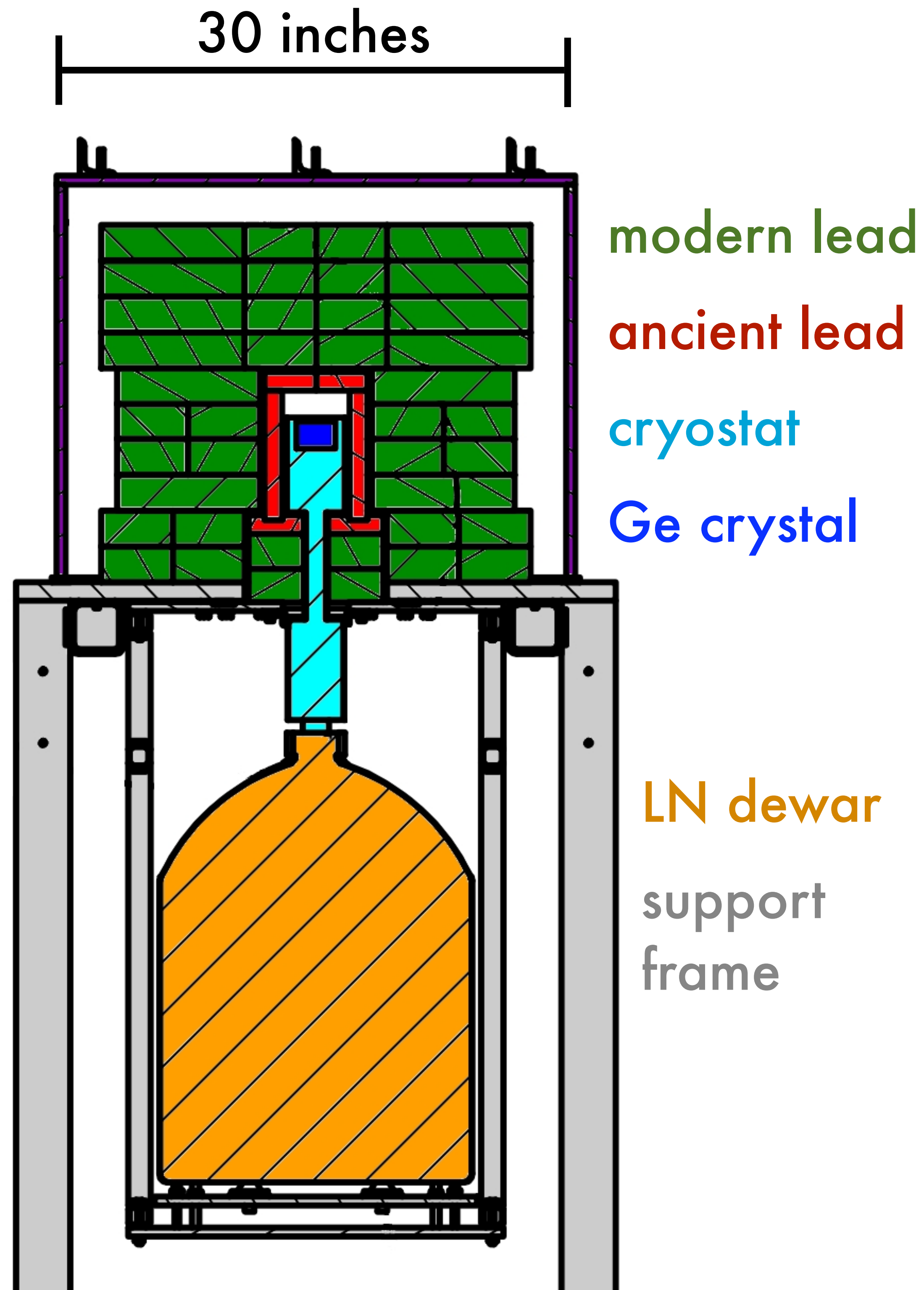

R&D detector: MALBEK

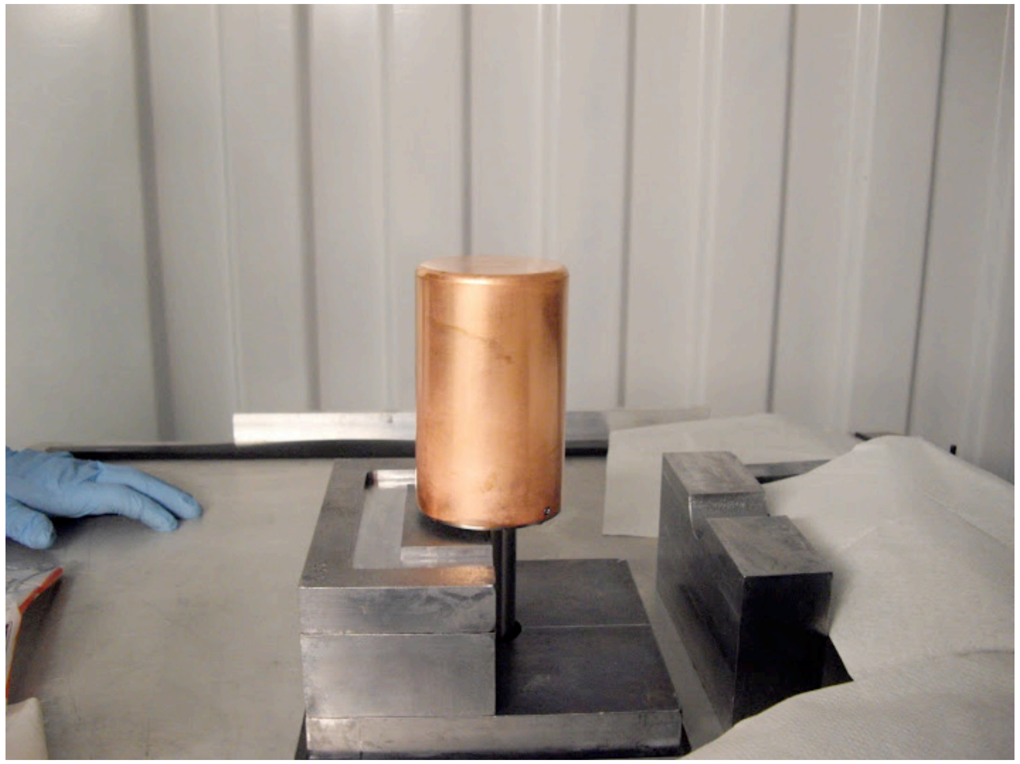

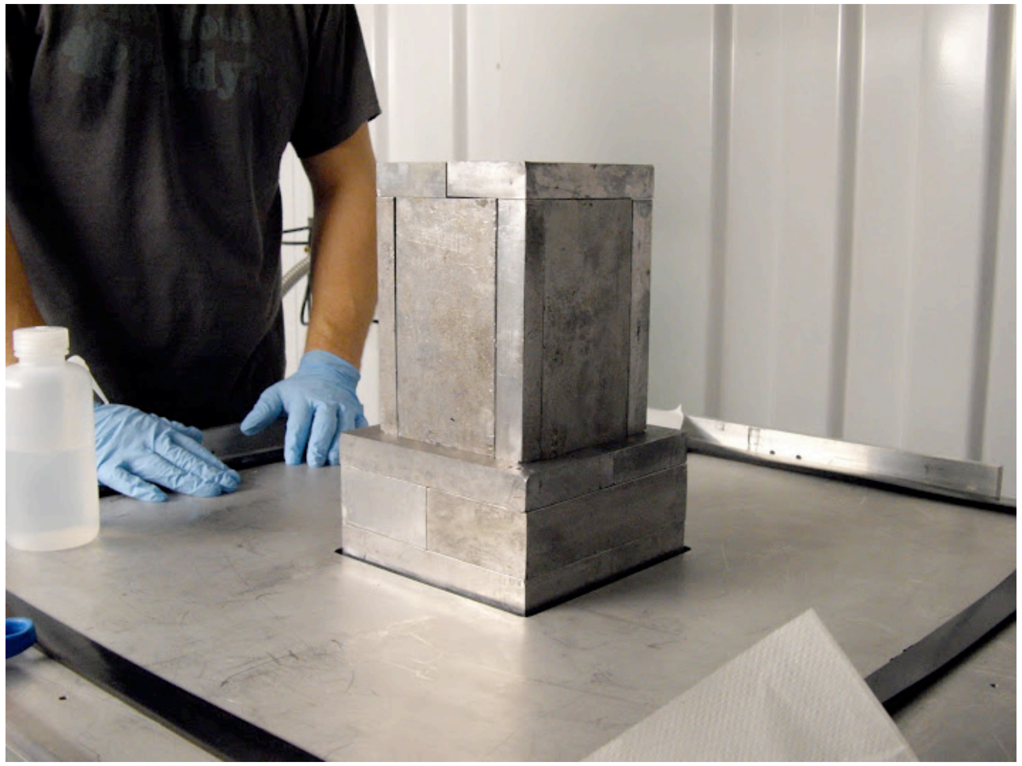

Kimballton Underground Research Facility

slow-rising, energy-degraded pulses

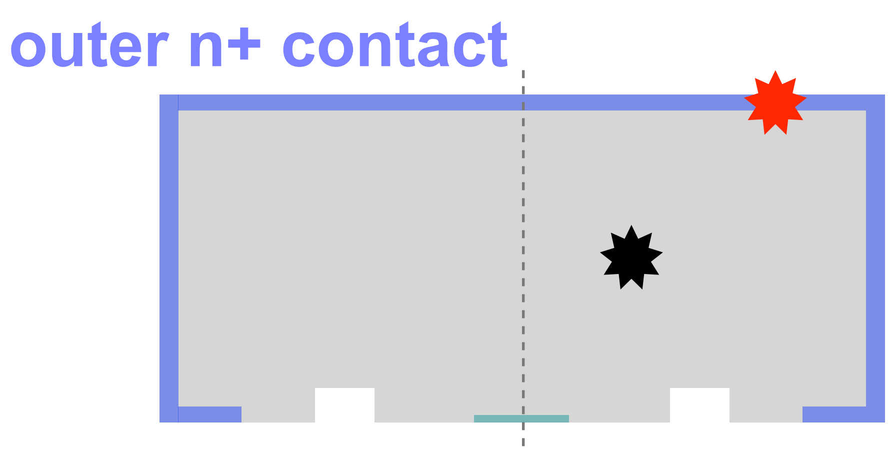

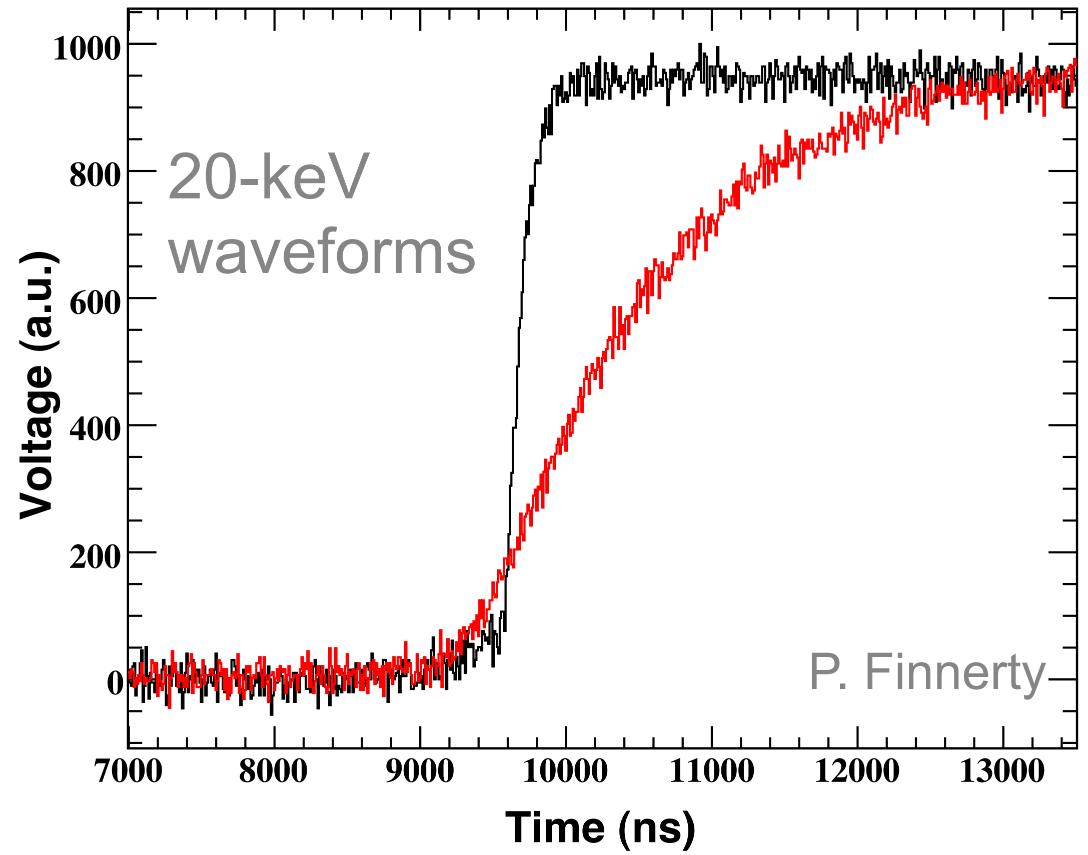

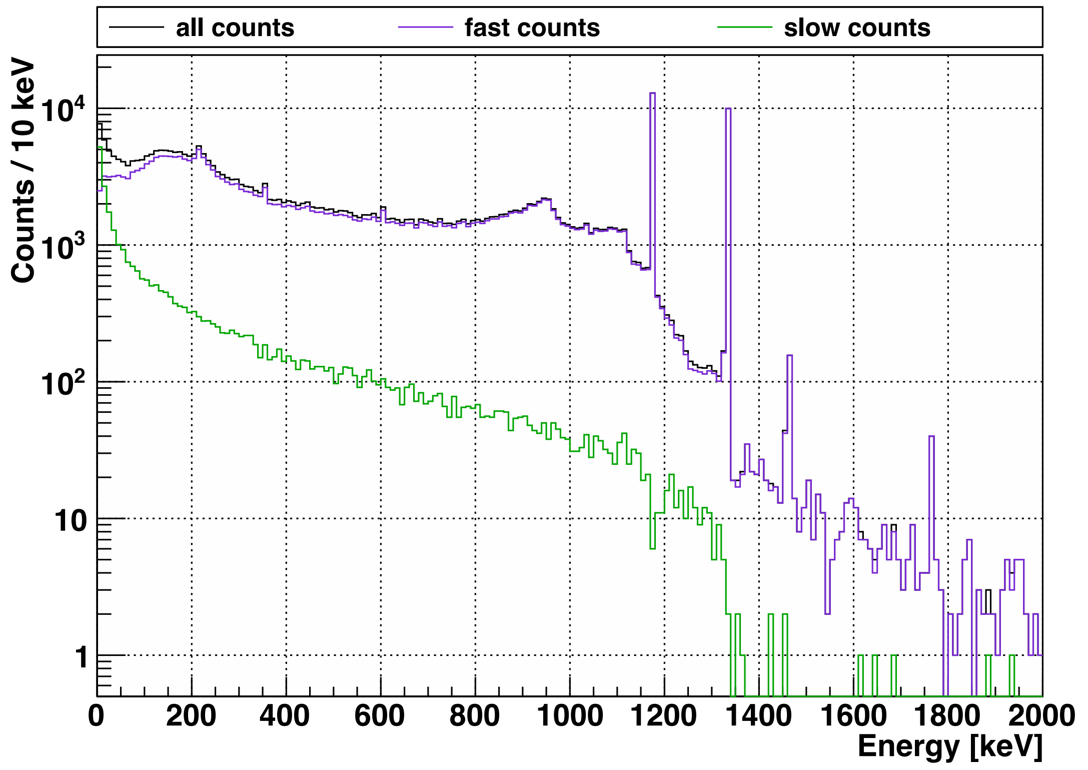

measured ^{60}Co spectrum

slow pulses contribute throughout the energy spectrum

MALBEK background model

Material purity information

cosmogenic contaminants: production rates from literature

primordial contaminants: material assay data from literature and direct measurements of bulk and surface contamination

cosmic muon flux: from literature

Monte Carlo simulation results

Geant4 simulations to determine efficiencies for contamination to deposit energy in our detectors

50k CPU hours

8k+ runs, 40+ contaminants, 56 components, 21 materials

Exposure history

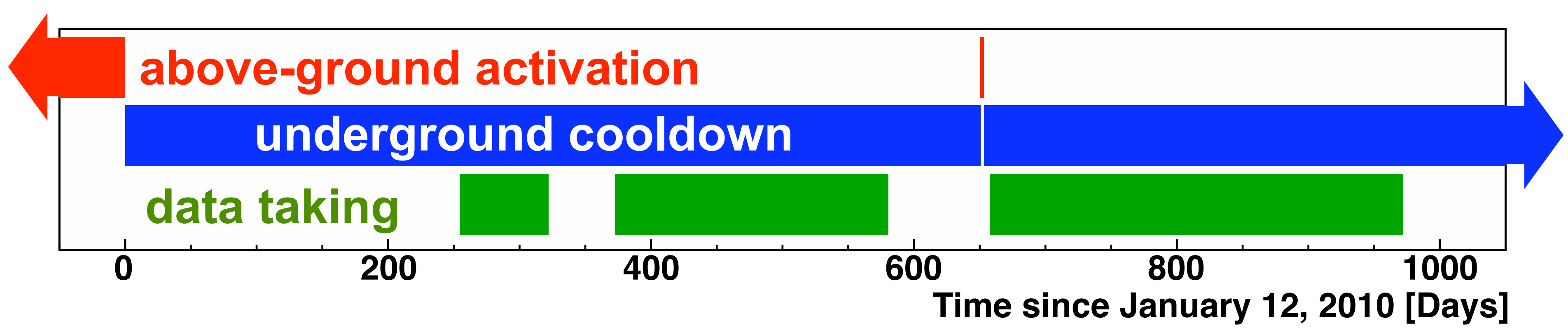

Detector characteristics

energy resolution: $\sigma(E) = (0.12^2 + 0.09\varepsilon E + E^2)^{1/2}$ keV

dead layer properties: 0.93 ± 0.09 mm outer n^+ contact [arXiv:1207.6716]

preamplifier effects: efficiency as a function of energy

Geant4 geometry model

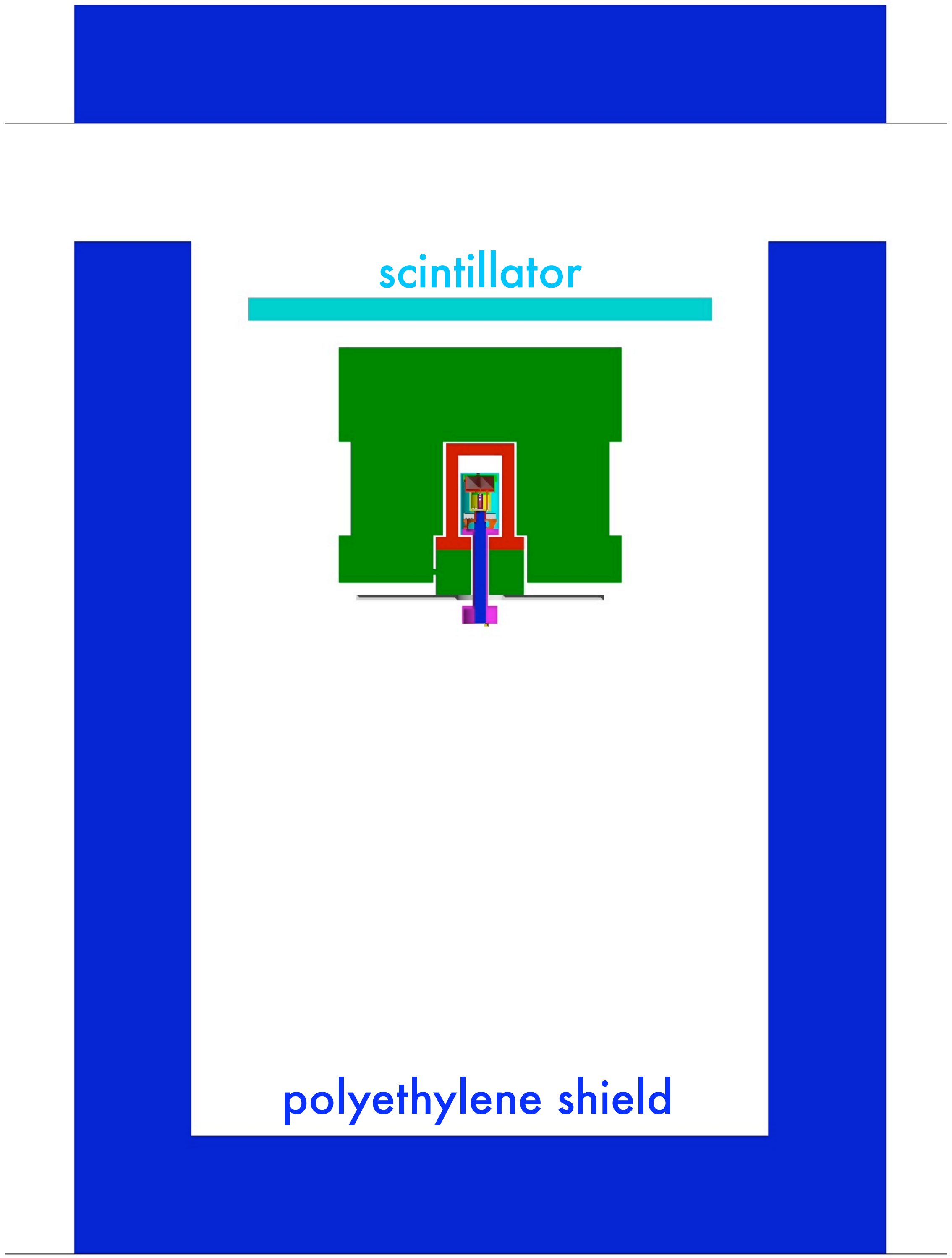

Geant4 geometry

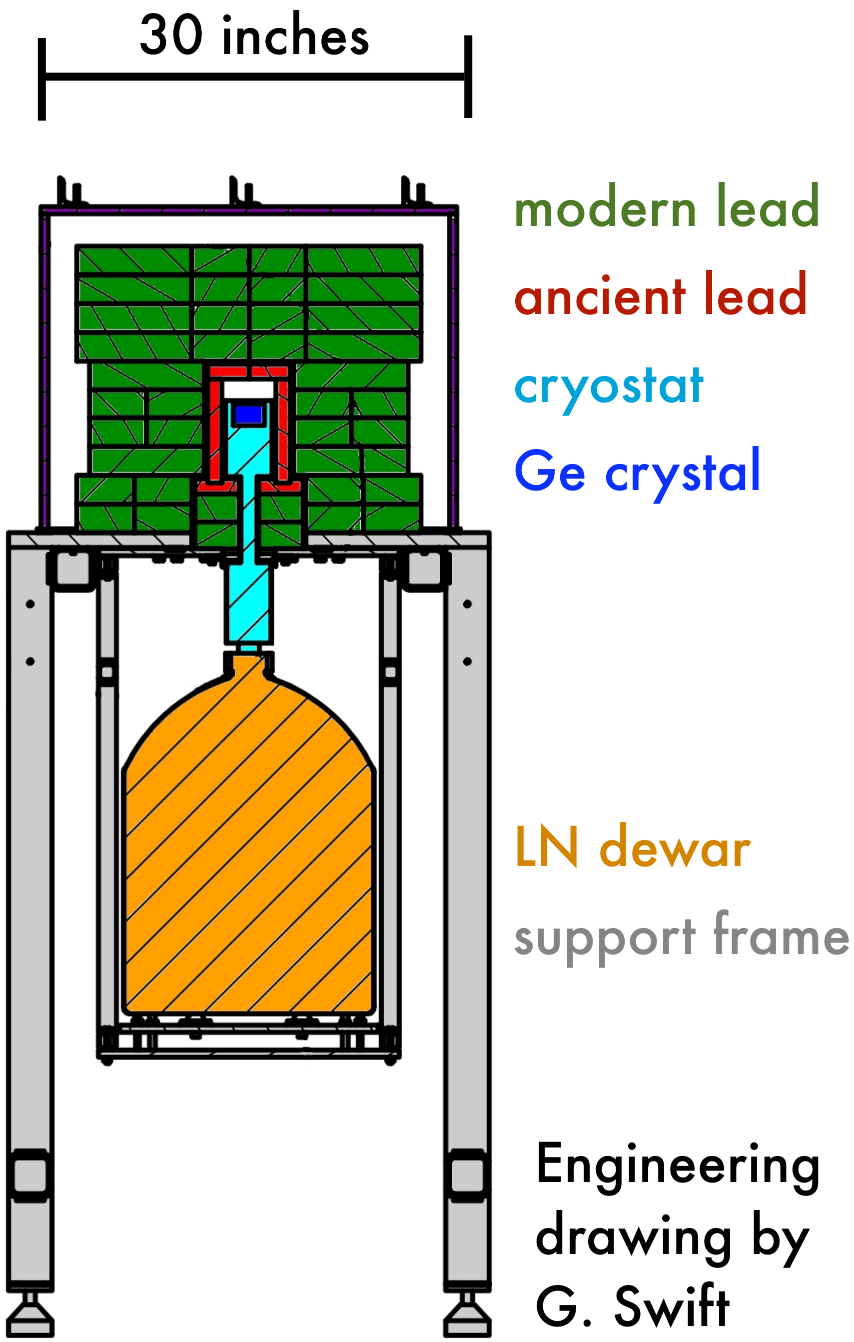

Engineering drawing by G. Swift

Geant4 geometry model

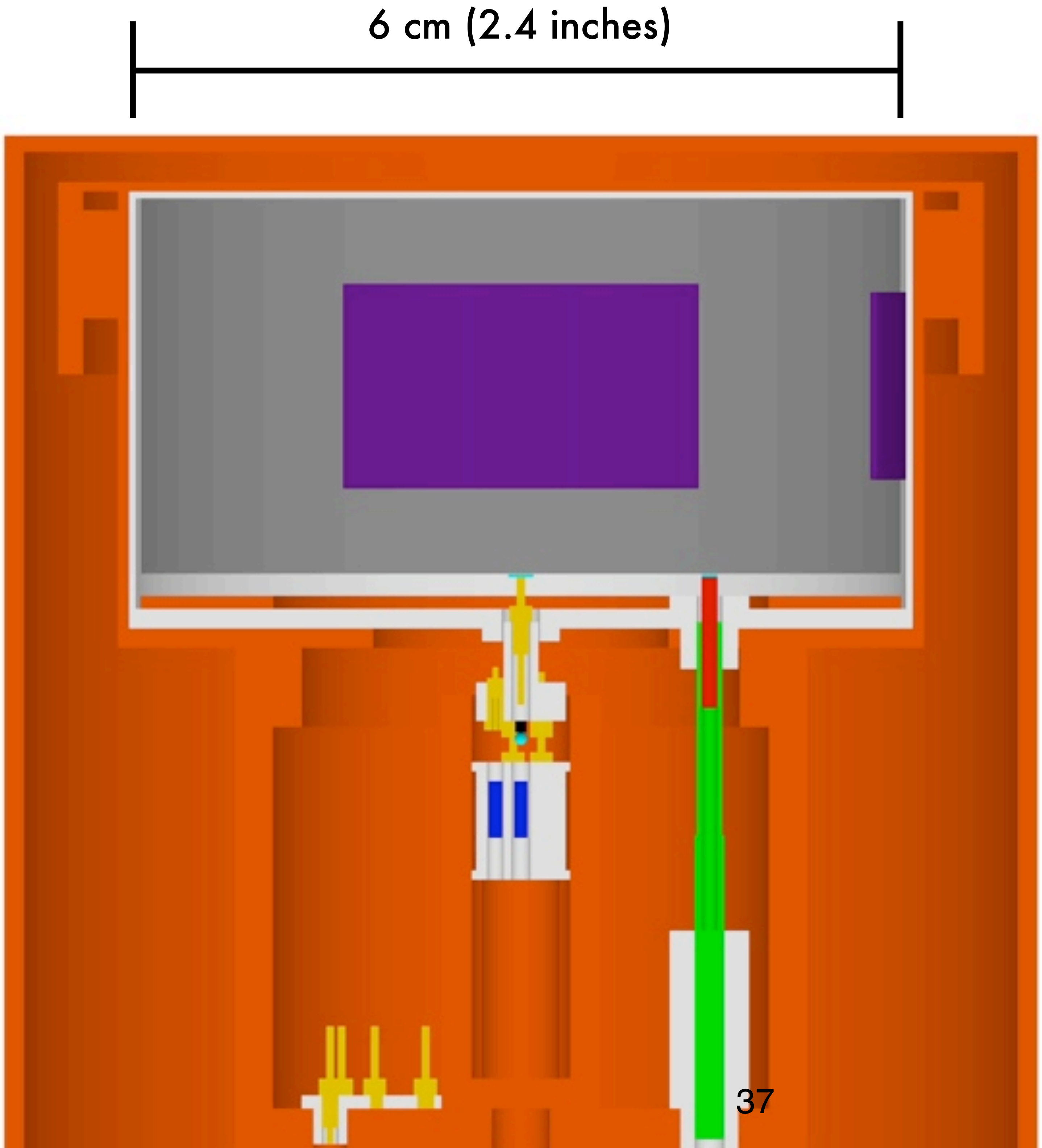

germanium
lead
copper
teflon (white)
brass
tin solder
resistors
beryllium copper
nickel silver

MALBEK background model

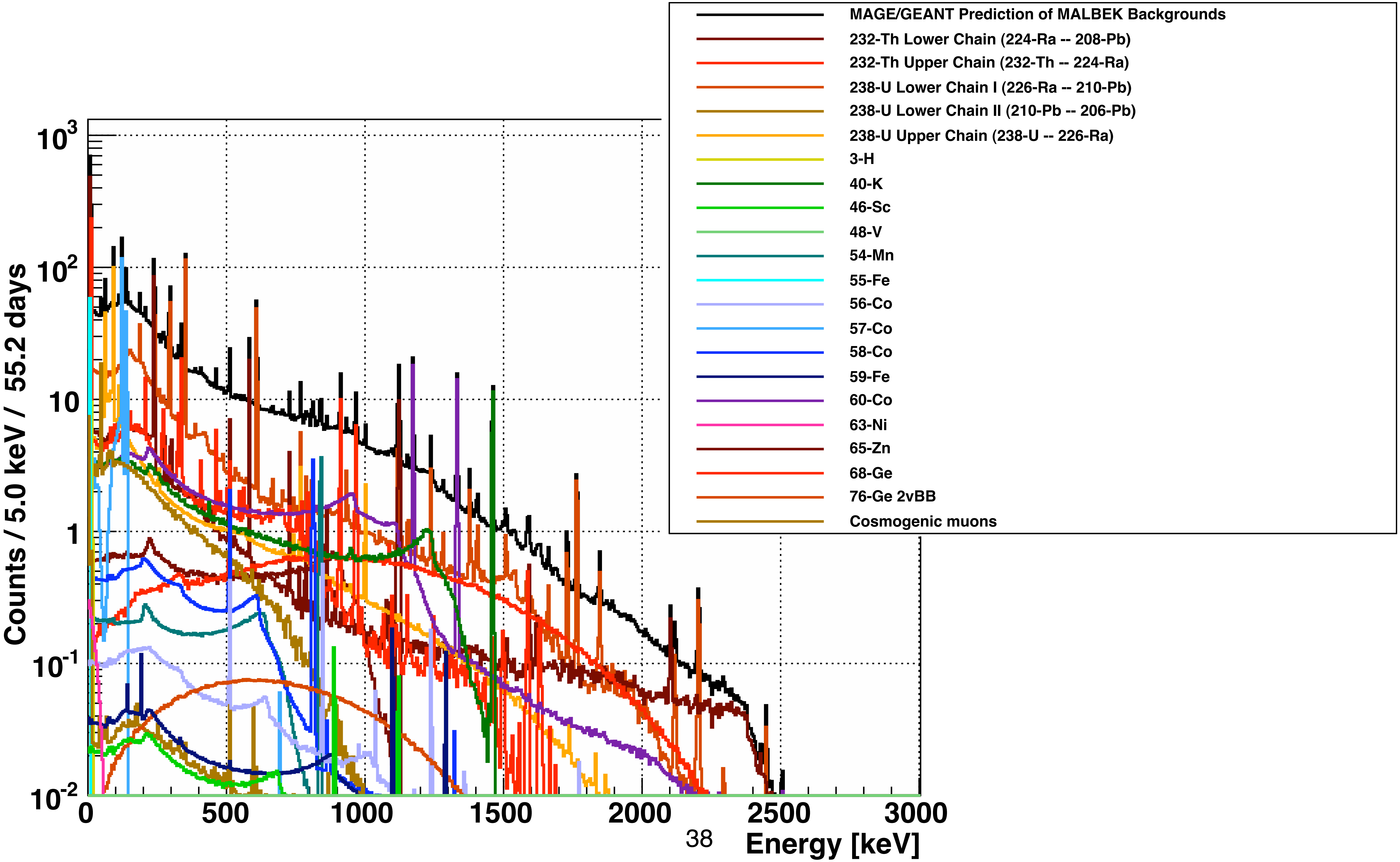

validation tests

^{60}Co: integral count rate agrees within 2% between 5 and 3000 keV

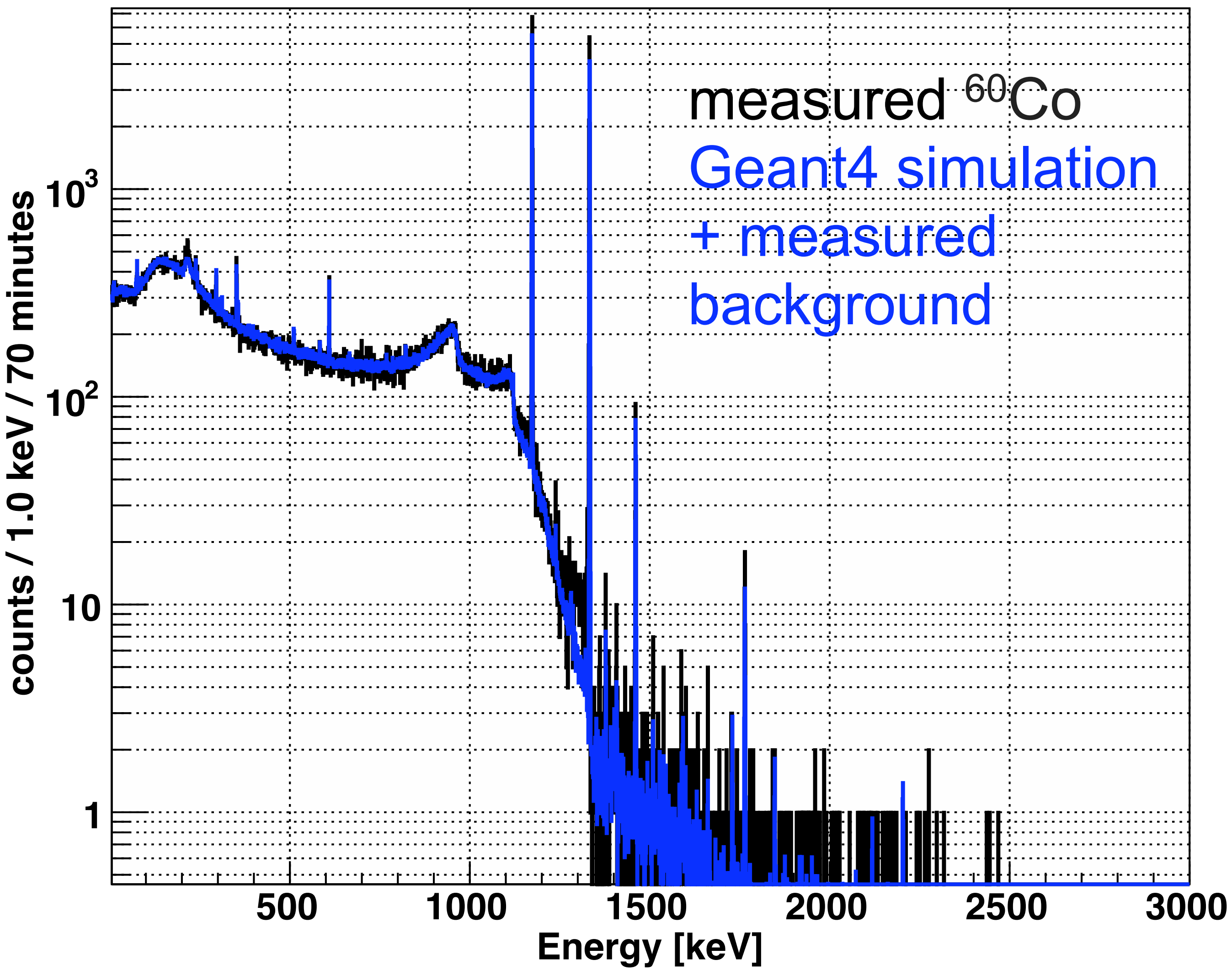

^{133}Ba: integral count rate agrees within 3% between 5 and 400 keV

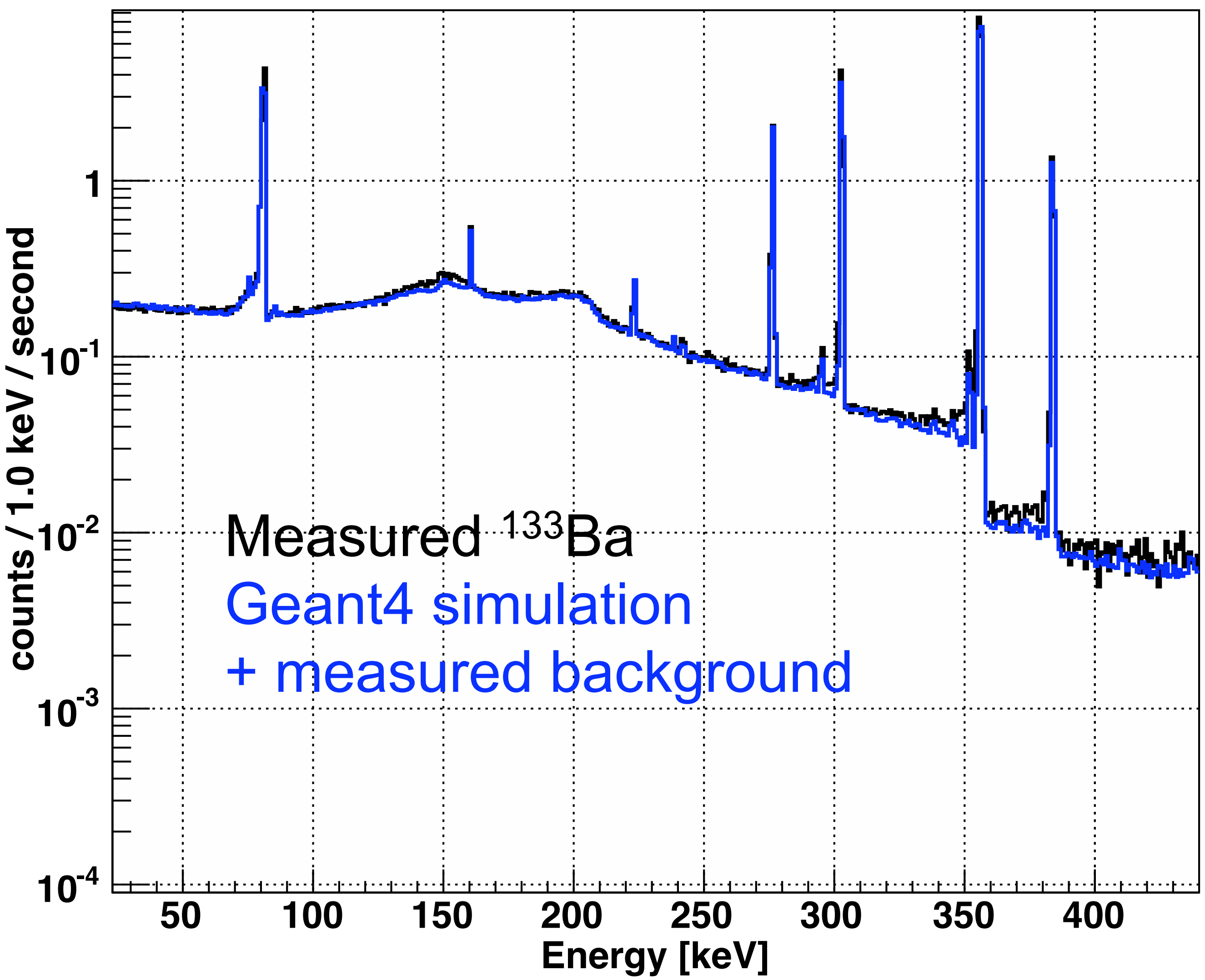

Shielded background energy spectrum measured at Kimballton

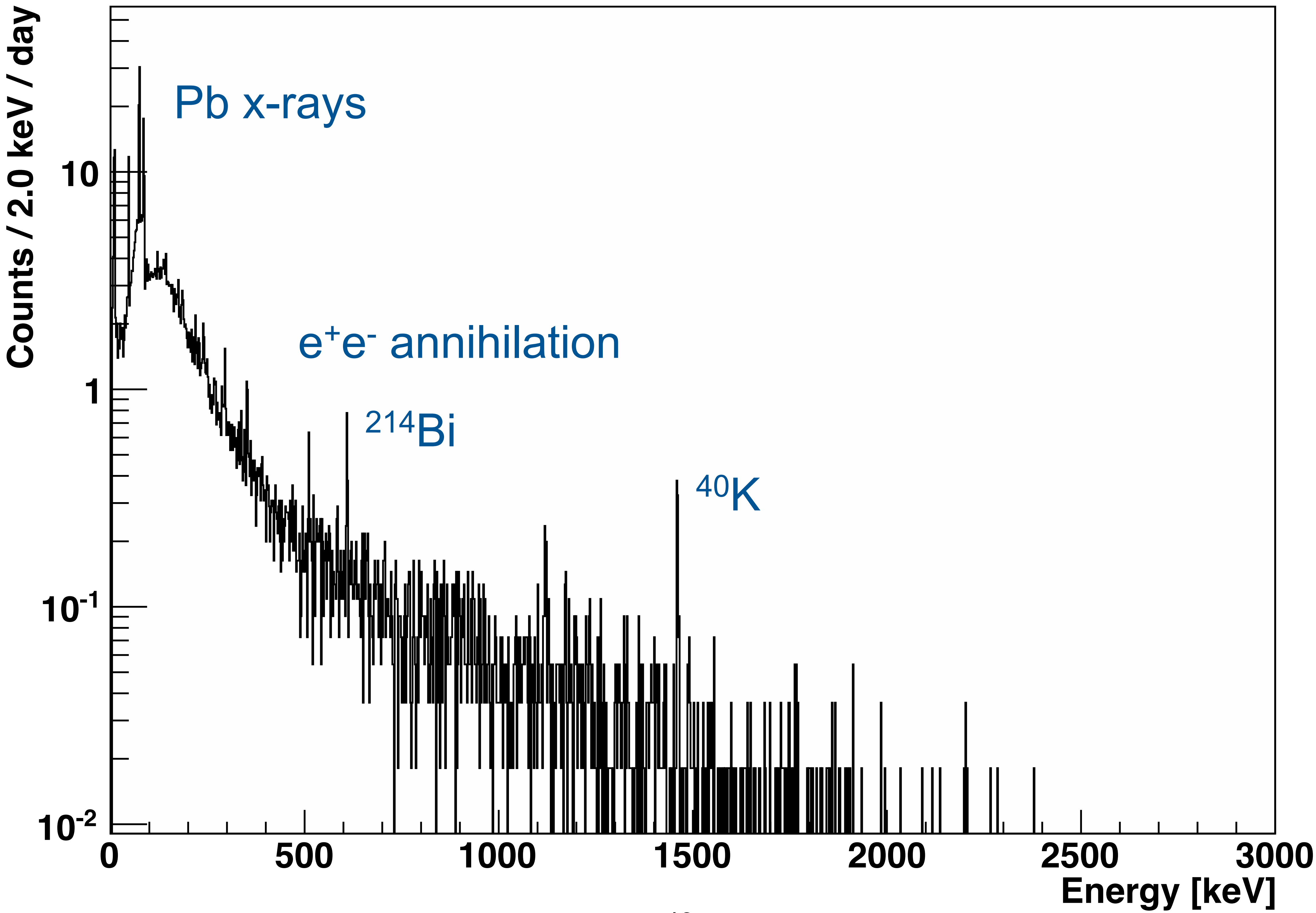

Measurement exceeded our expectations

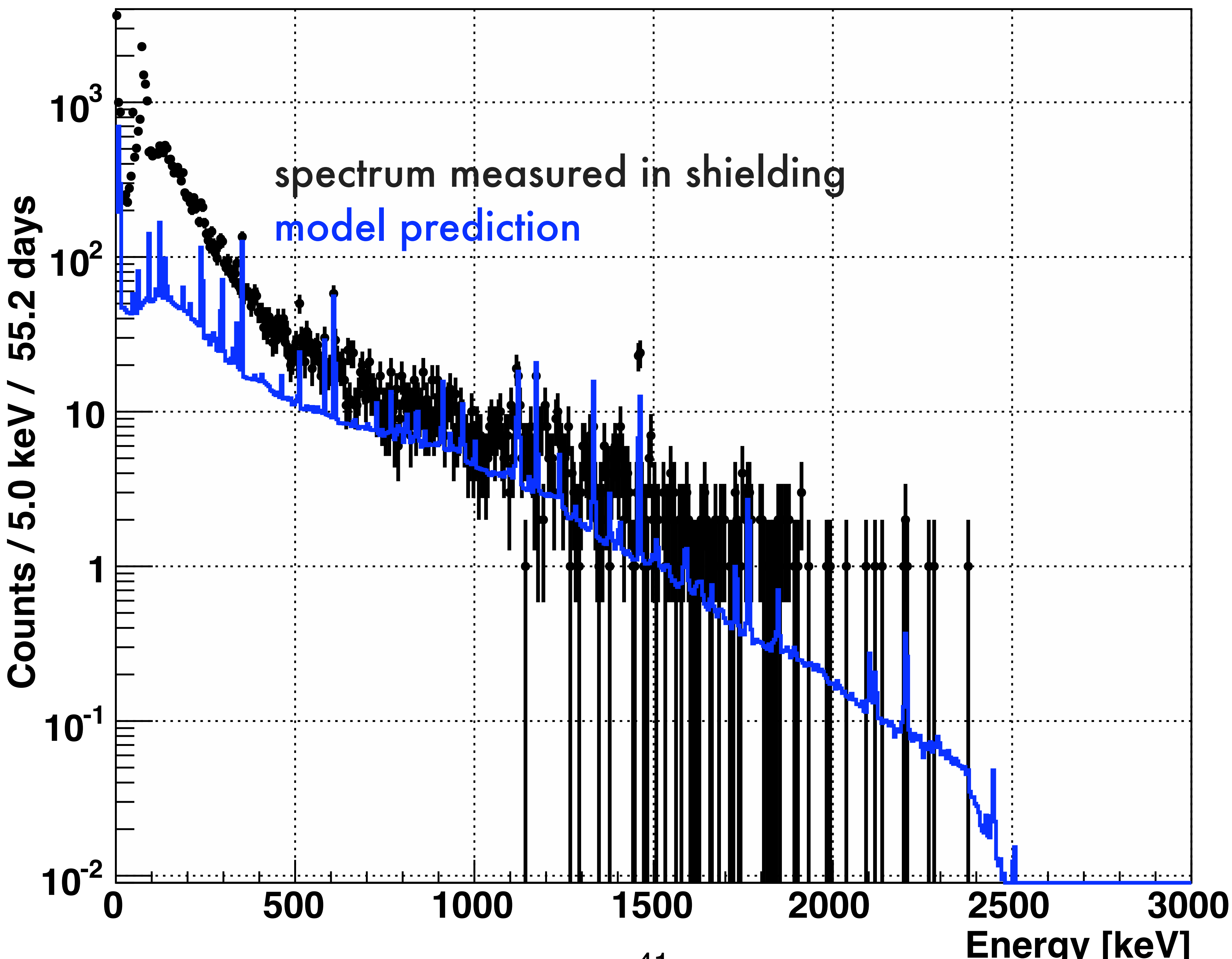

$^{210}Pb \rightarrow {}^{210}Bi \rightarrow {}^{210}Po \rightarrow {}^{206}Pb$

$T_{1/2}$ = 22 years
γ 46.5 keV

$T_{1/2}$ = 5 days
β 1162 keV end point

$T_{1/2}$ = 138 days
α 5.3 MeV

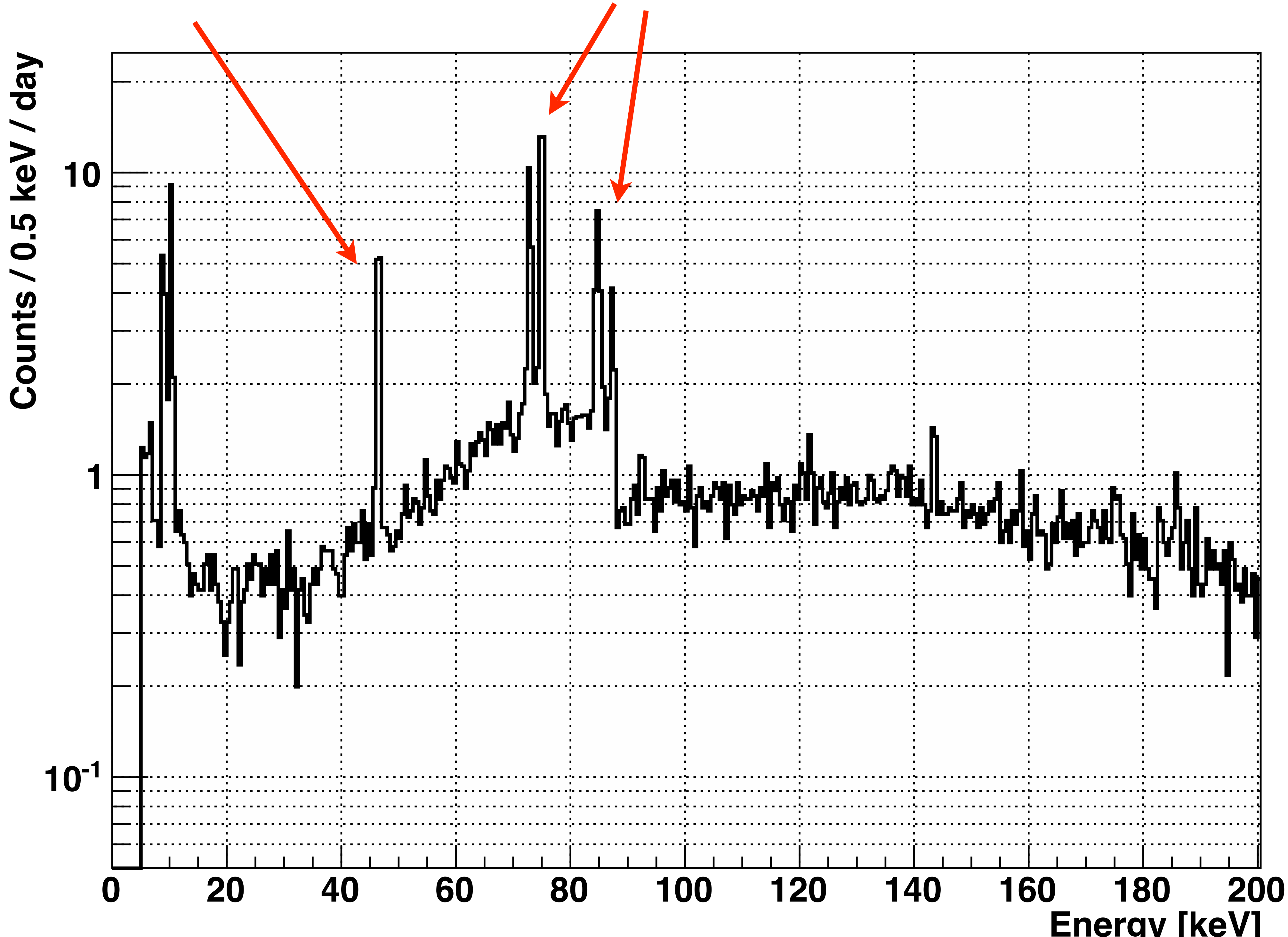

Possible sources of ^{210}Pb contamination

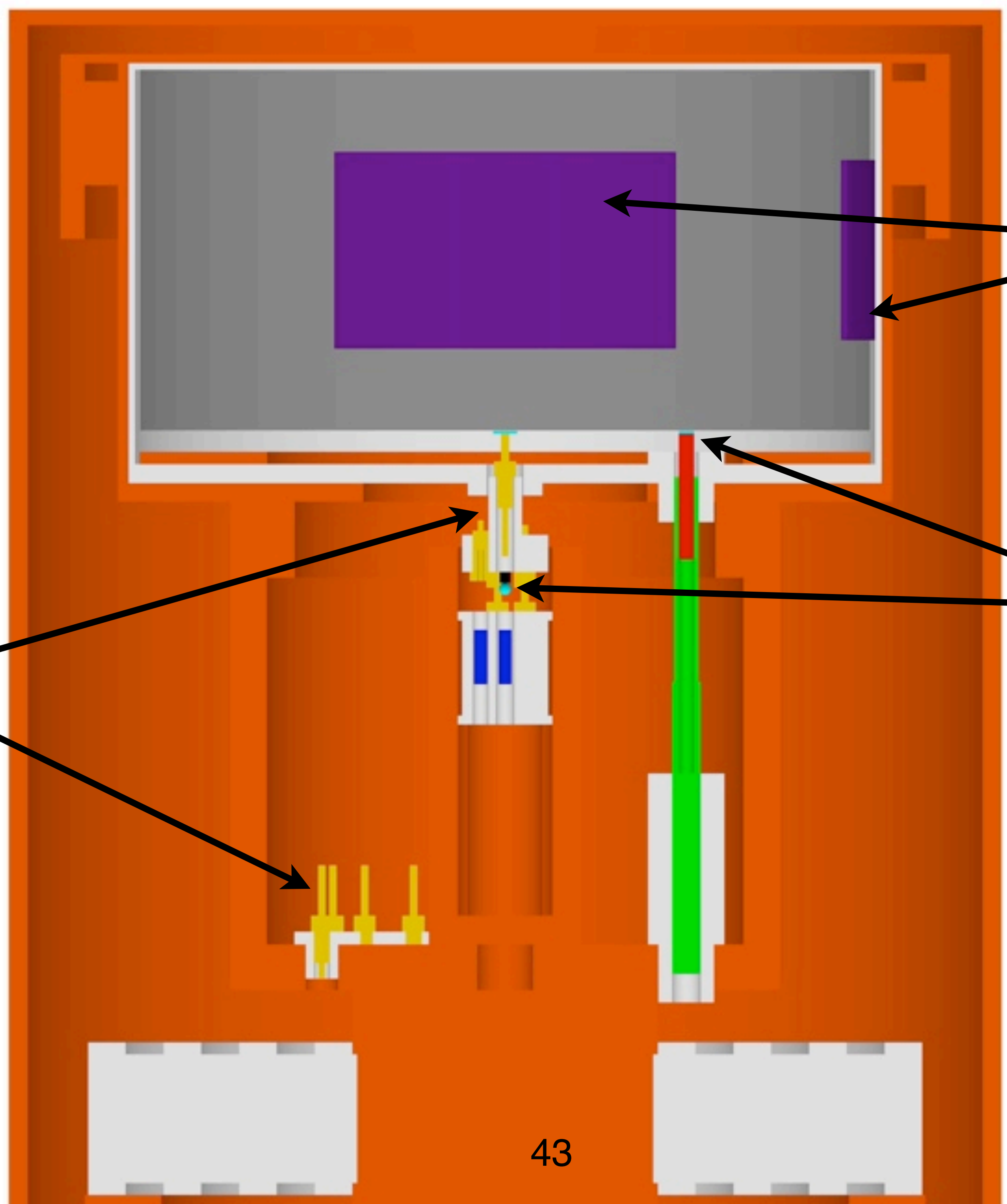

brass pins and connectors (< 4% lead)

ancient lead shims (< 1.3 x 10^{-5} Bq/g)

ultra-low-background tin solder

inner shielding: ancient lead bricks (< 1.3 x 10^{-5} Bq/g)

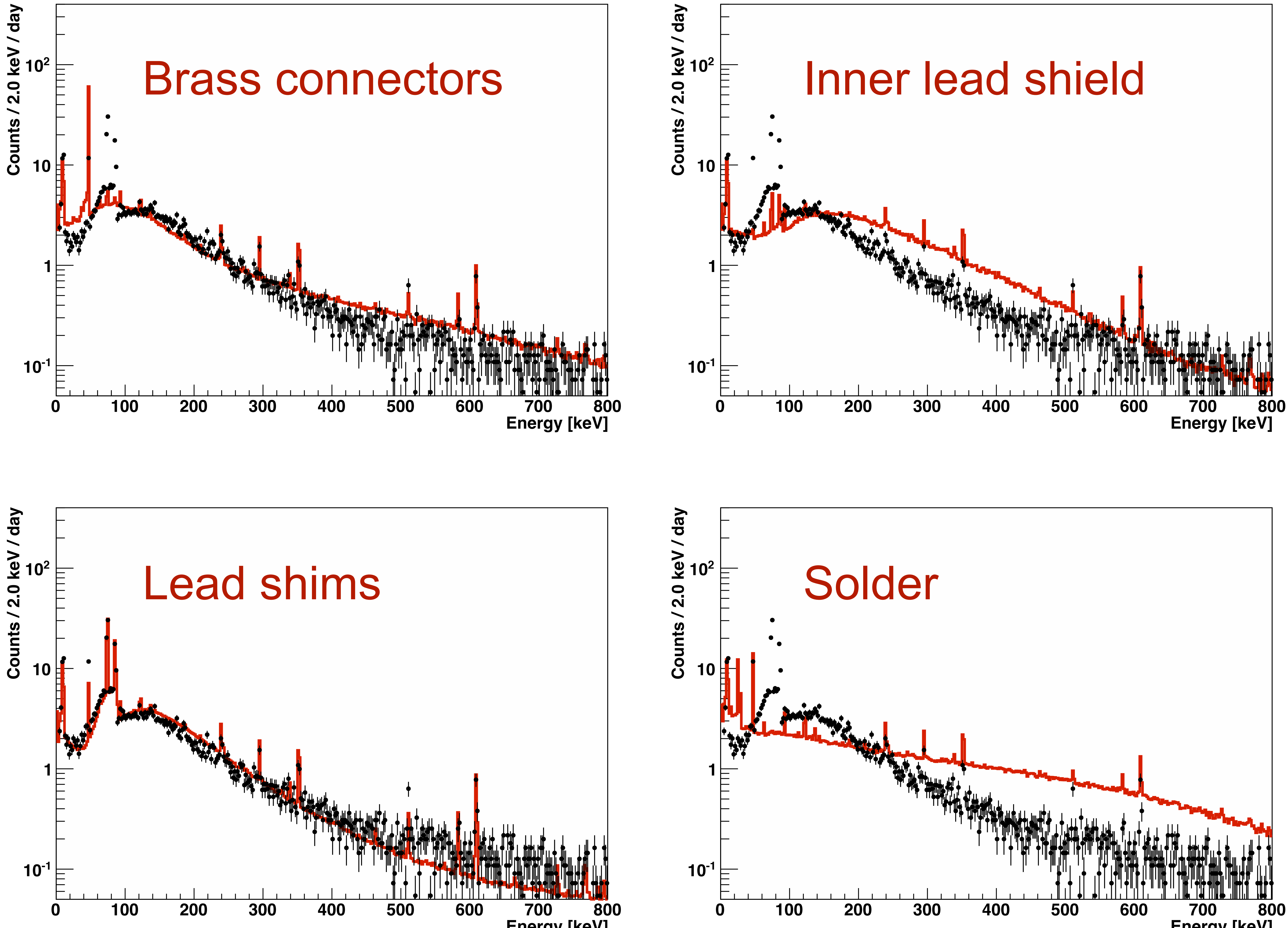
Brass connectors
Inner lead shield
Lead shims
Solder
Counts / 2.0 keV / day
Energy [keV]

Background model fit of energy spectrum

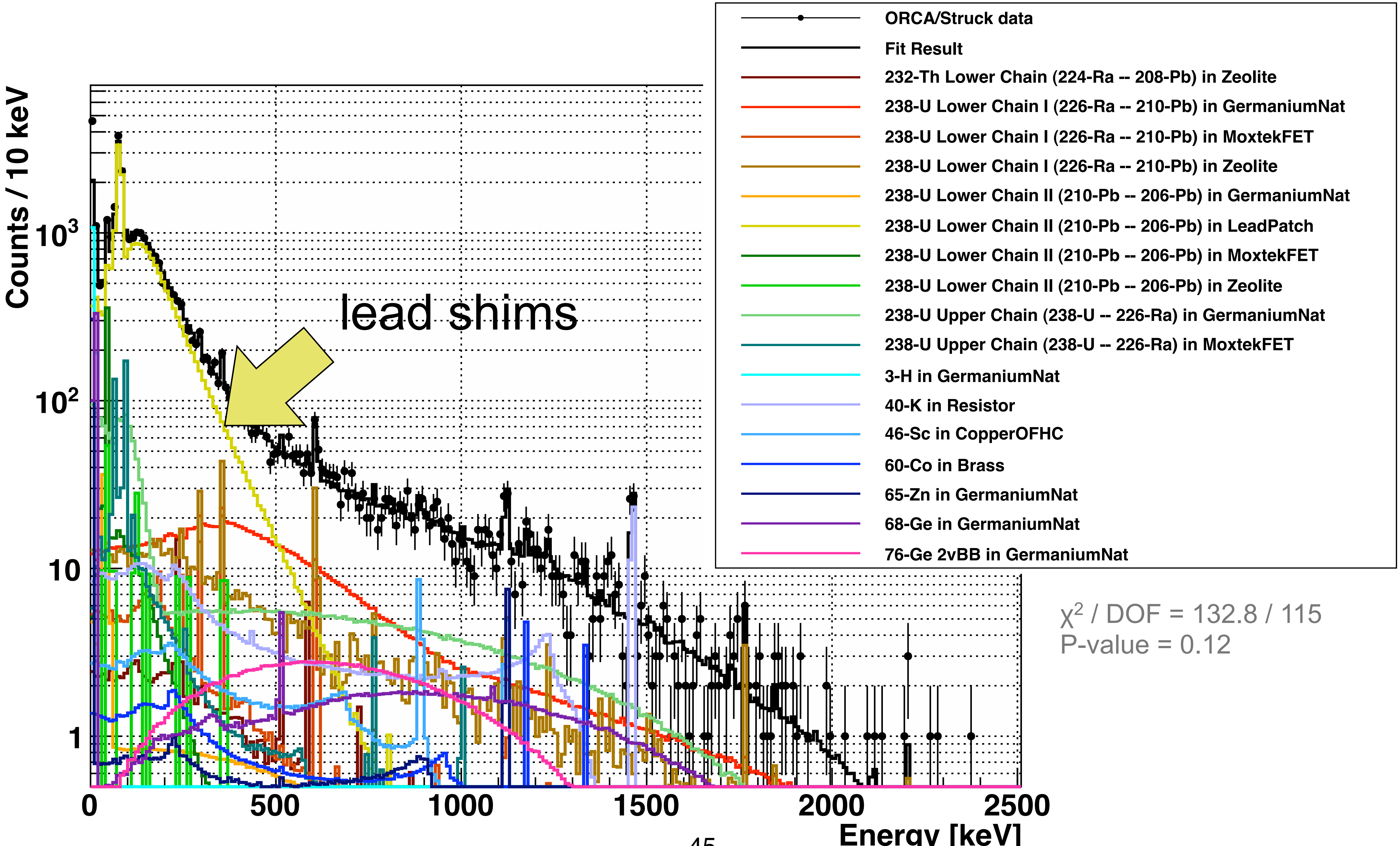

χ^2 / DOF = 132.8 / 115
P-value = 0.12

Lead shim removal

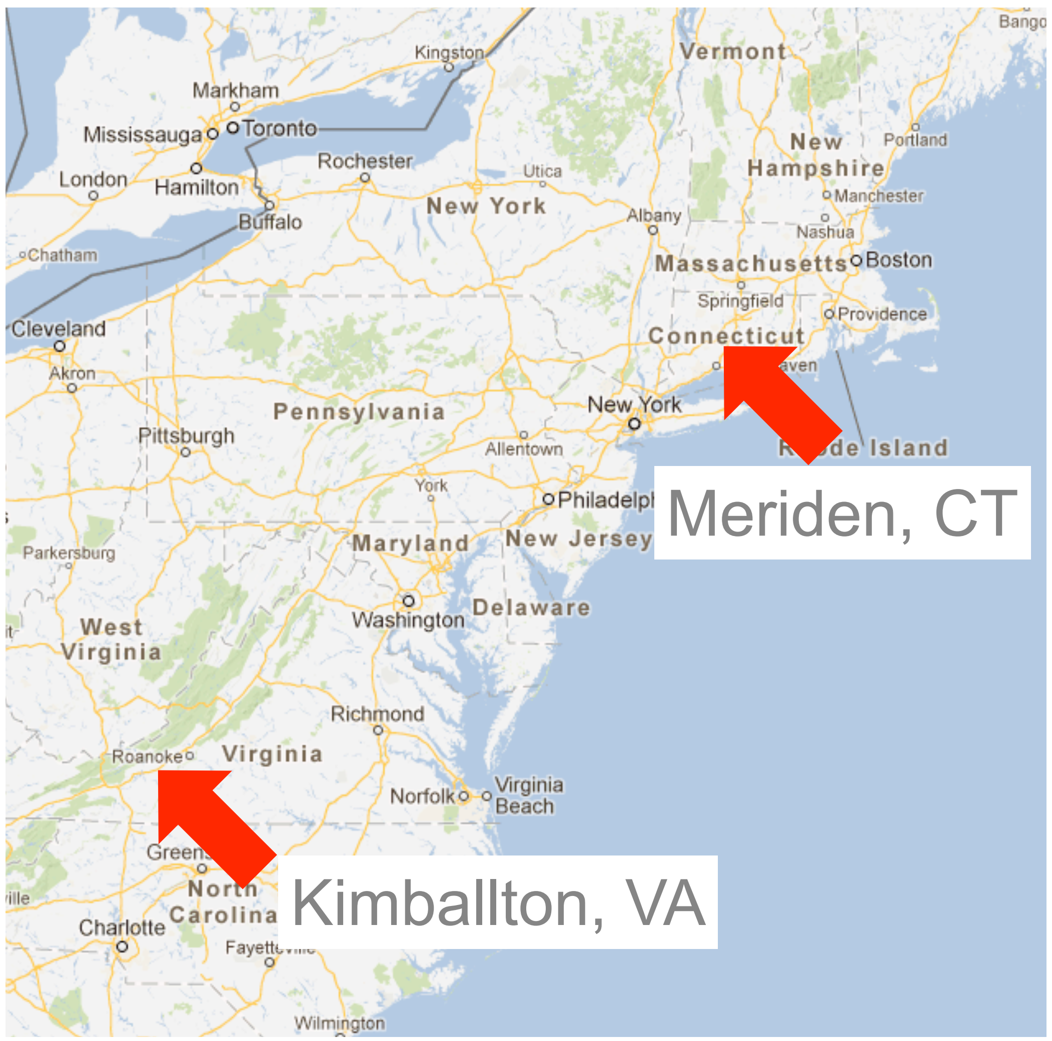

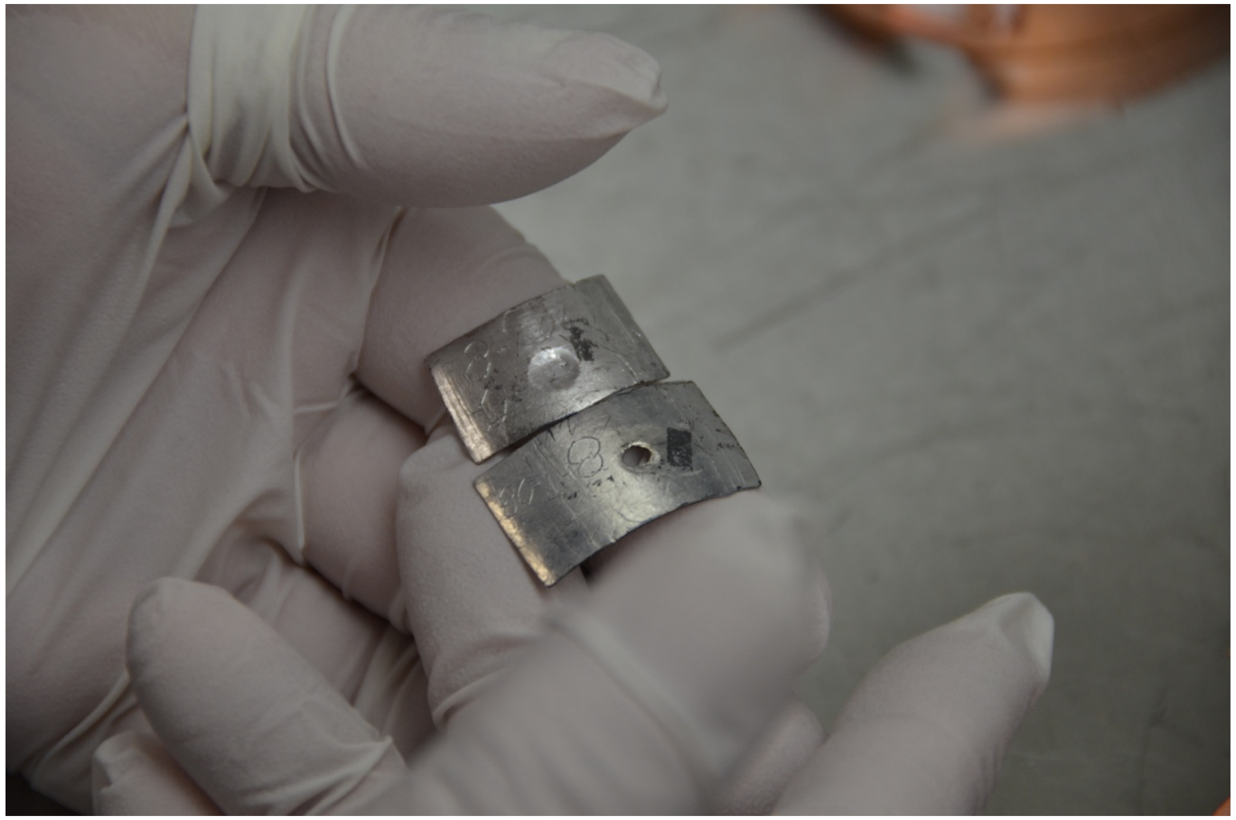

Removed 3g of lead from cryostat

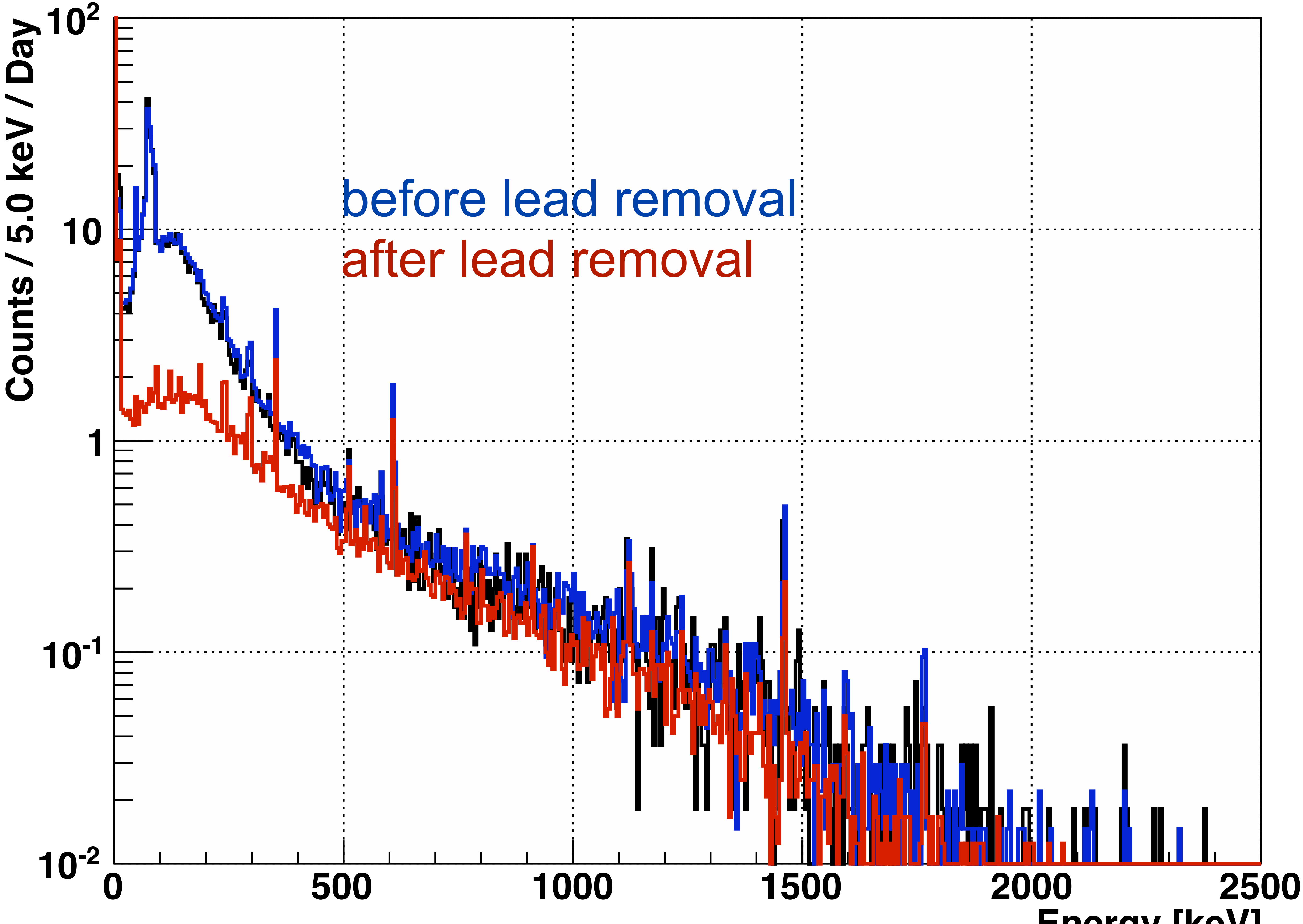

Counts / 5.0 keV / Day
10^2
10
1
10^{-1}
10^{-2}
0
500
1000
1500
2000
2500
Energy [keV]
before lead removal
after lead removal

Background model fit of spectrum after shim removal

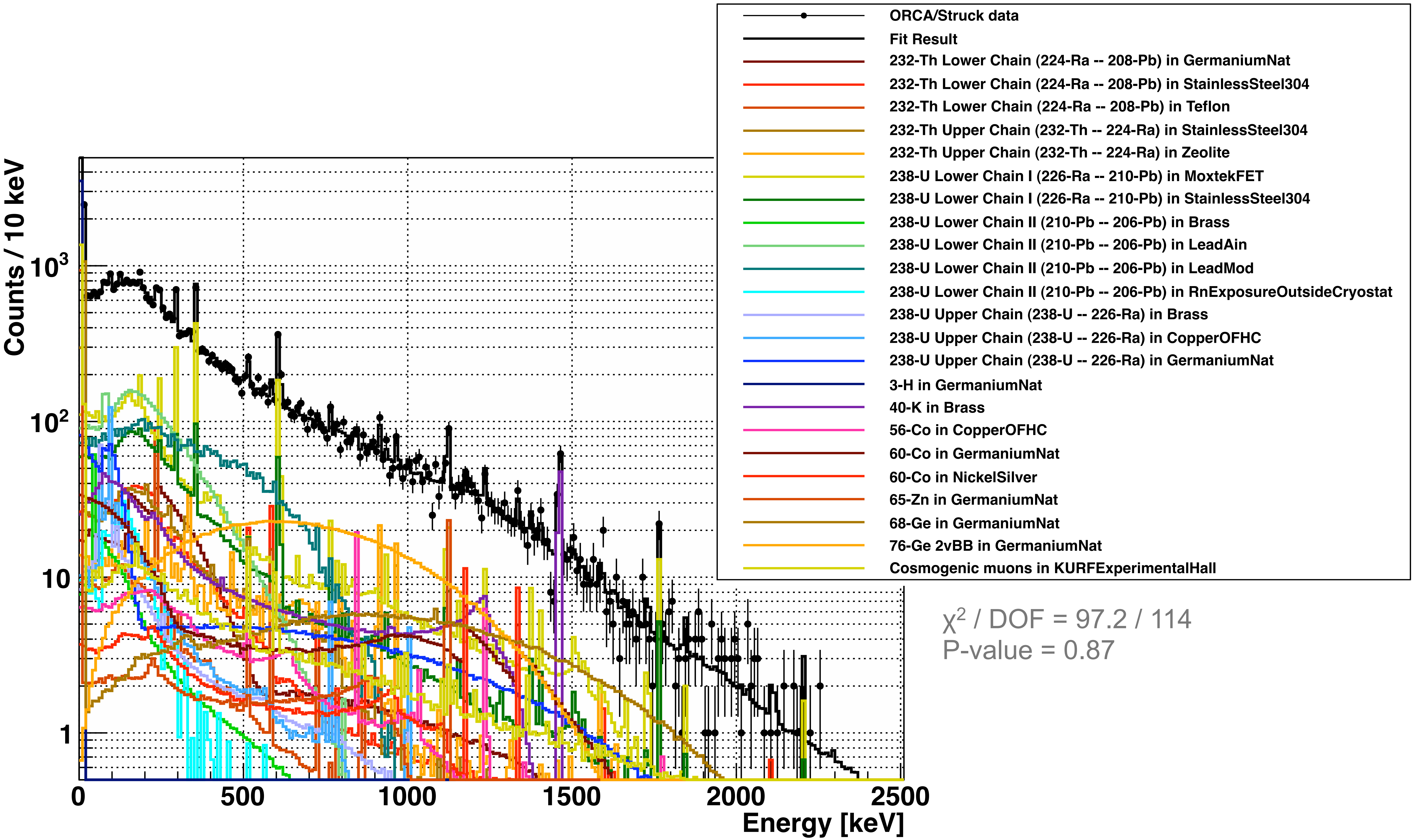

χ^2 / DOF = 97.2 / 114
P-value = 0.87

Results from R&D detector

- Validated background model of the energy spectrum
- Identified and removed contaminated component from cryostat
- Studied slow pulses and developed a cut to remove them throughout the energy spectrum
- Tested MAJORANA data-acquisition system
- Developed and tested software for simulations and analysis of data

DEMONSTRATOR background model

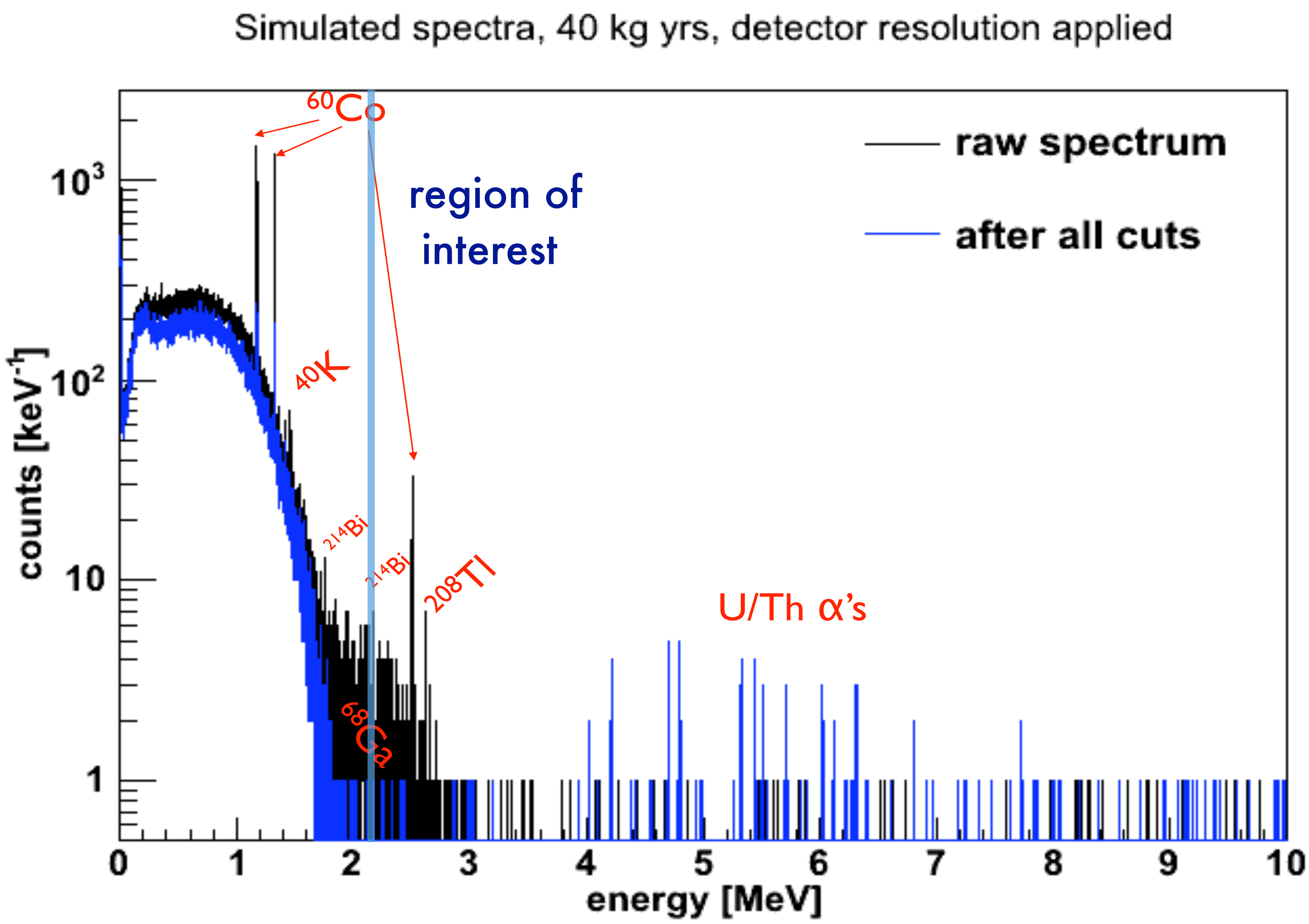

Conclusions

- Observation of neutrinoless double beta decay would determine Majorana nature of the neutrino, demonstrate lepton number violation, and provide information about neutrino mass
- MAJORANA DEMONSTRATOR is a 40-kg detector array searching for $0\nu\beta\beta$ of ^{76}Ge
  - Under construction at Sanford Underground Laboratory
  - On track to begin taking data in September 2013
  - Tests of data taking, data analysis, and background modeling with an R&D detector have been successful

Thank you!

supplemental slides

Airborne radioactivity in Seattle after the 2011 Fukushima earthquake

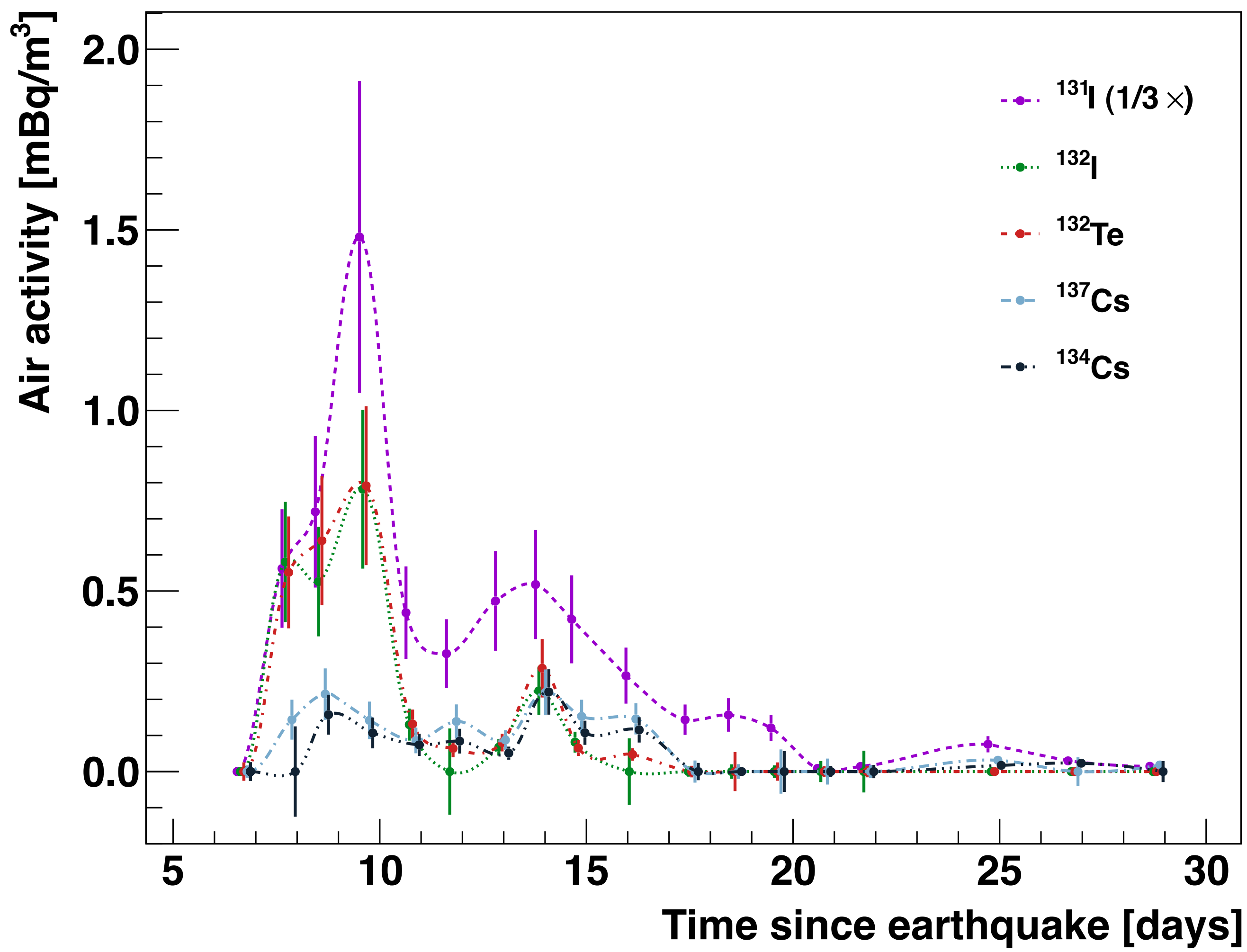

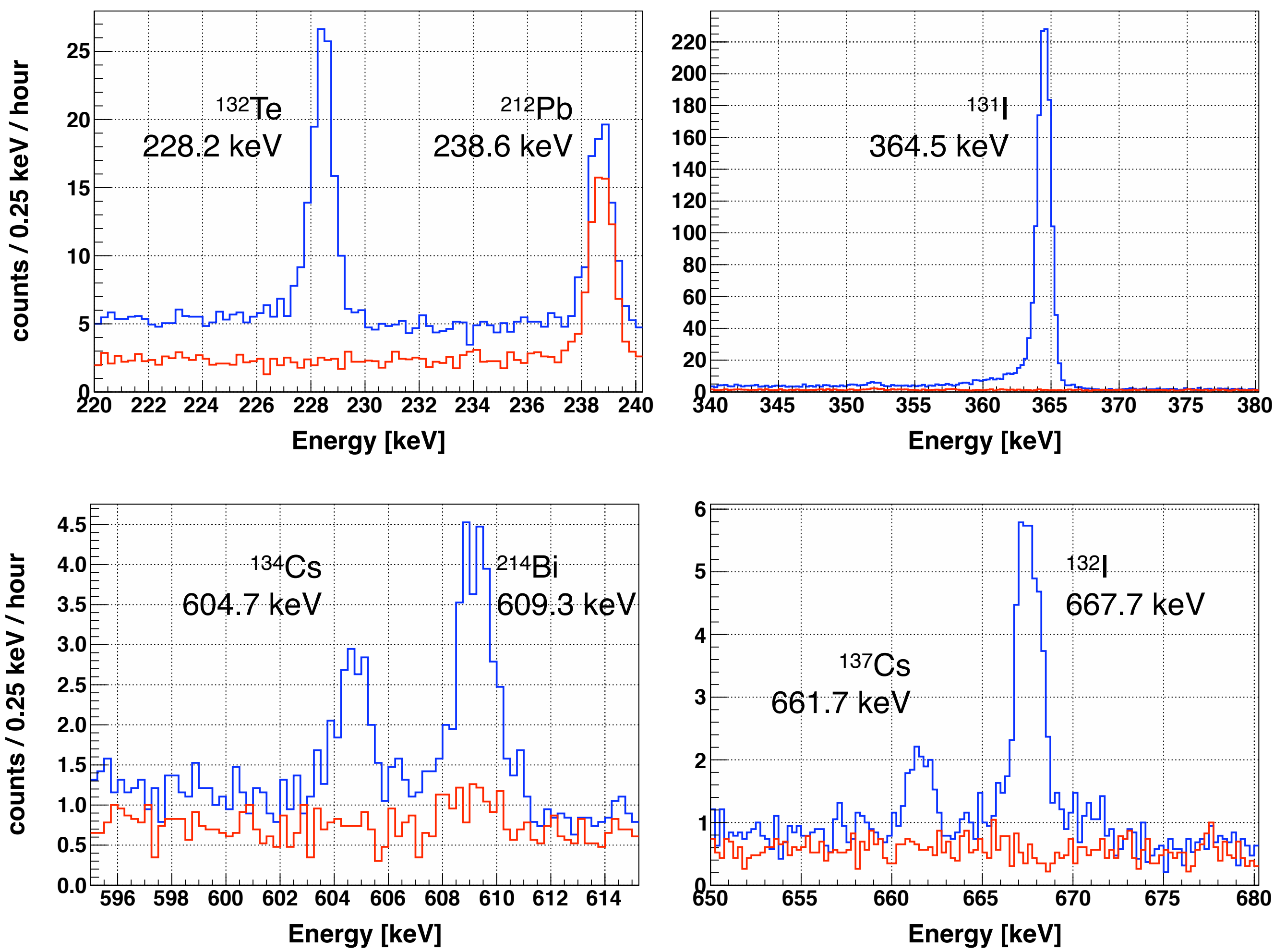

J. Diaz Leon et al., Journal of Environmental Radioactivity 102 (2011) 1032-1038
arXiv:1103.4853

energy calibration

Energy Linearity

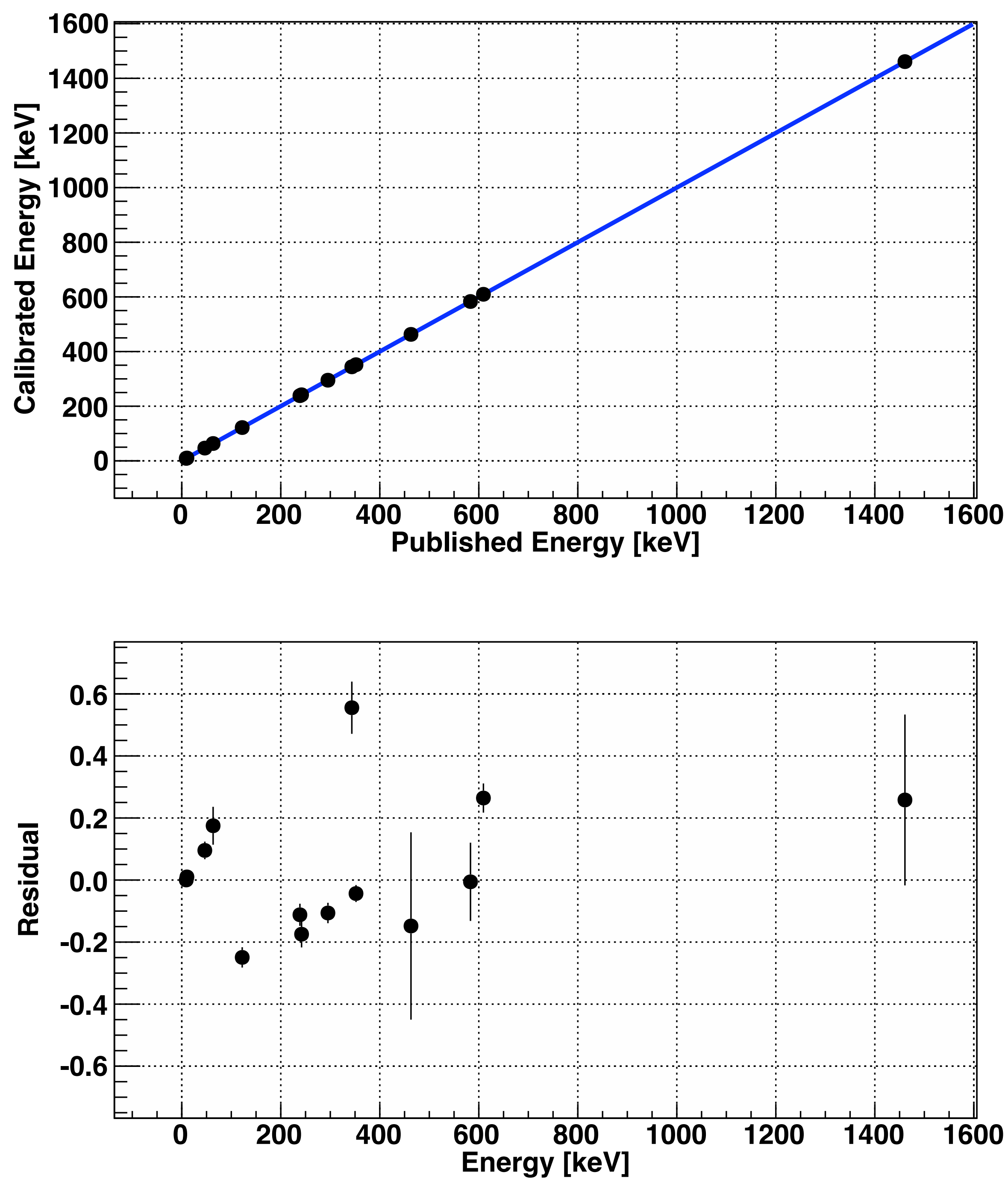

FIG. 47: Energy linearity.

χ^2/DOF: 194.21 / 14 (13.87), p-val: 8.33E-34

identified peaks

Peak	Energy [keV]	Centroid [keV]	Sigma [eV]	Count Rate [μHz]	χ^2 / DOF	P-value
^{65}Zn[1]	8.98	8.98 $\pm$ 0.01	143.4 $\pm$ 7.6	23.7 $\pm$ 1.3		
^{68}Ga	9.66	9.66 $\pm$ 0.03	141.7 $\pm$ 33.3	3.8 $\pm$ 0.8	39.3 / 53 (0.74)	0.920
^{68}Ge[1]	10.37	10.38 $\pm$ 0.00	131.8 $\pm$ 2.9	74.7 $\pm$ 2.0		
^{210}Pb[1]	46.54	46.63 $\pm$ 0.03	162.1 $\pm$ 25.0	4.1 $\pm$ 0.6	21.4 / 36 (0.59)	0.975
^{234}U, ^{72}Ge(n,γ)	53.20, 53.53	53.91 $\pm$ 0.03	71.8 $\pm$ 19.8	1.0 $\pm$ 0.3	19.5 / 36 (0.54)	0.989
^{234}Th[1]	63.29	63.46 $\pm$ 0.06	224.5 $\pm$ 44.3	2.2 $\pm$ 0.0	19.3 / 36 (0.54)	0.989
Bi $K_{\alpha 2}$	74.81	75.06 $\pm$ 0.06	223.4 $\pm$ 54.0	2.3 $\pm$ 0.6	34.3 / 59 (0.58)	0.996
Bi $K_{\alpha 1}$	77.11	77.23 $\pm$ 0.06	221.7 $\pm$ 50.5	2.7 $\pm$ 0.6		
^{234}Th	92.38, 92.80	92.76 $\pm$ 0.05	440.9 $\pm$ 41.4	9.0 $\pm$ 0.0	28.3 / 36 (0.79)	0.816
^{57}Co[1]	122.06	121.81 $\pm$ 0.03	280.4 $\pm$ 27.8	8.3 $\pm$ 0.0	43.1 / 36 (1.20)	0.193
^{57}Co + atomic	143.58	143.52 $\pm$ 0.06	305.8 $\pm$ 65.7	4.0 $\pm$ 0.8	26.1 / 36 (0.73)	0.887
?[1]	-	185.60 $\pm$ 0.04	334.7 $\pm$ 30.6	8.9 $\pm$ 0.0	19.0 / 36 (0.53)	0.991
^{228}Ac	209.25	209.56 $\pm$ 0.16	226.5 $\pm$ 97.8	0.7 $\pm$ 0.0	20.5 / 36 (0.57)	0.982
^{212}Pb[1]	238.63	238.52 $\pm$ 0.03	304.2 $\pm$ 33.2	8.0 $\pm$ 0.8	33.9 / 54 (0.63)	0.985
^{214}Pb[1]	242.00	241.82 $\pm$ 0.04	338.1 $\pm$ 41.1	7.3 $\pm$ 0.8		
^{214}Pb[1]	295.22	295.12 $\pm$ 0.03	408.5 $\pm$ 29.7	13.8 $\pm$ 1.0	14.0 / 36 (0.39)	1.000
^{228}Ac	338.32	338.13 $\pm$ 0.10	265.5 $\pm$ 88.3	1.3 $\pm$ 0.4	28.1 / 36 (0.78)	0.822
^{206}Pb$(n,n'\gamma)$[1]	343.51	344.07 $\pm$ 0.08	387.7 $\pm$ 72.4	2.9 $\pm$ 0.6	26.3 / 36 (0.73)	0.881
^{214}Pb[1]	351.93	351.89 $\pm$ 0.03	442.9 $\pm$ 21.5	20.8 $\pm$ 0.0	25.4 / 36 (0.71)	0.905
^{228}Ac[1]	463.00	462.86 $\pm$ 0.30	1022.9 $\pm$ 217.2	2.1 $\pm$ 0.0	29.5 / 36 (0.82)	0.768
^{208}Tl + annih.	510.77, 511.00	510.88 $\pm$ 0.20	1217.0 $\pm$ 190.1	5.2 $\pm$ 0.0	23.5 / 36 (0.65)	0.946
^{208}Tl[1]	583.19	583.18 $\pm$ 0.13	620.8 $\pm$ 100.0	2.7 $\pm$ 0.5	17.2 / 36 (0.48)	0.997
^{214}Bi[1]	609.32	609.58 $\pm$ 0.05	703.7 $\pm$ 40.2	15.6 $\pm$ 1.0	21.2 / 36 (0.59)	0.976
^{214}Bi	768.36	768.36 $\pm$ 0.24	1106.2 $\pm$ 216.0	2.6 $\pm$ 0.5	15.1 / 36 (0.42)	0.999
^{206}Pb$(n,n'\gamma)$	803.10	803.61 $\pm$ 0.35	1042.7 $\pm$ 280.8	1.3 $\pm$ 0.4	14.4 / 36 (0.40)	0.999
^{228}Ac	911.20	911.80 $\pm$ 0.22	1025.3 $\pm$ 183.3	2.3 $\pm$ 0.5	13.9 / 36 (0.39)	1.000
?	-	1086.22 $\pm$ 0.24	608.4 $\pm$ 161.2	0.7 $\pm$ 0.0	13.4 / 36 (0.37)	1.000
^{214}Bi	1120.29	1122.00 $\pm$ 0.52	2129.8 $\pm$ 477.1	2.5 $\pm$ 0.6	23.6 / 36 (0.65)	0.945
^{40}K[1]	1460.82	1461.08 $\pm$ 0.28	1887.3 $\pm$ 244.6	3.3 $\pm$ 0.5	12.7 / 36 (0.35)	1.000
^{214}Bi	1764.49	1765.05 $\pm$ 0.41	1042.3 $\pm$ 354.4	0.8 $\pm$ 0.2	11.1 / 36 (0.31)	1.000
^{214}Bi	2204.06	2257.12 $\pm$ 0.00	14567.5 $\pm$ 0.0	1.3 $\pm$ 0.0	2.4 / 36 (0.07)	1.000

sigma vs. energy

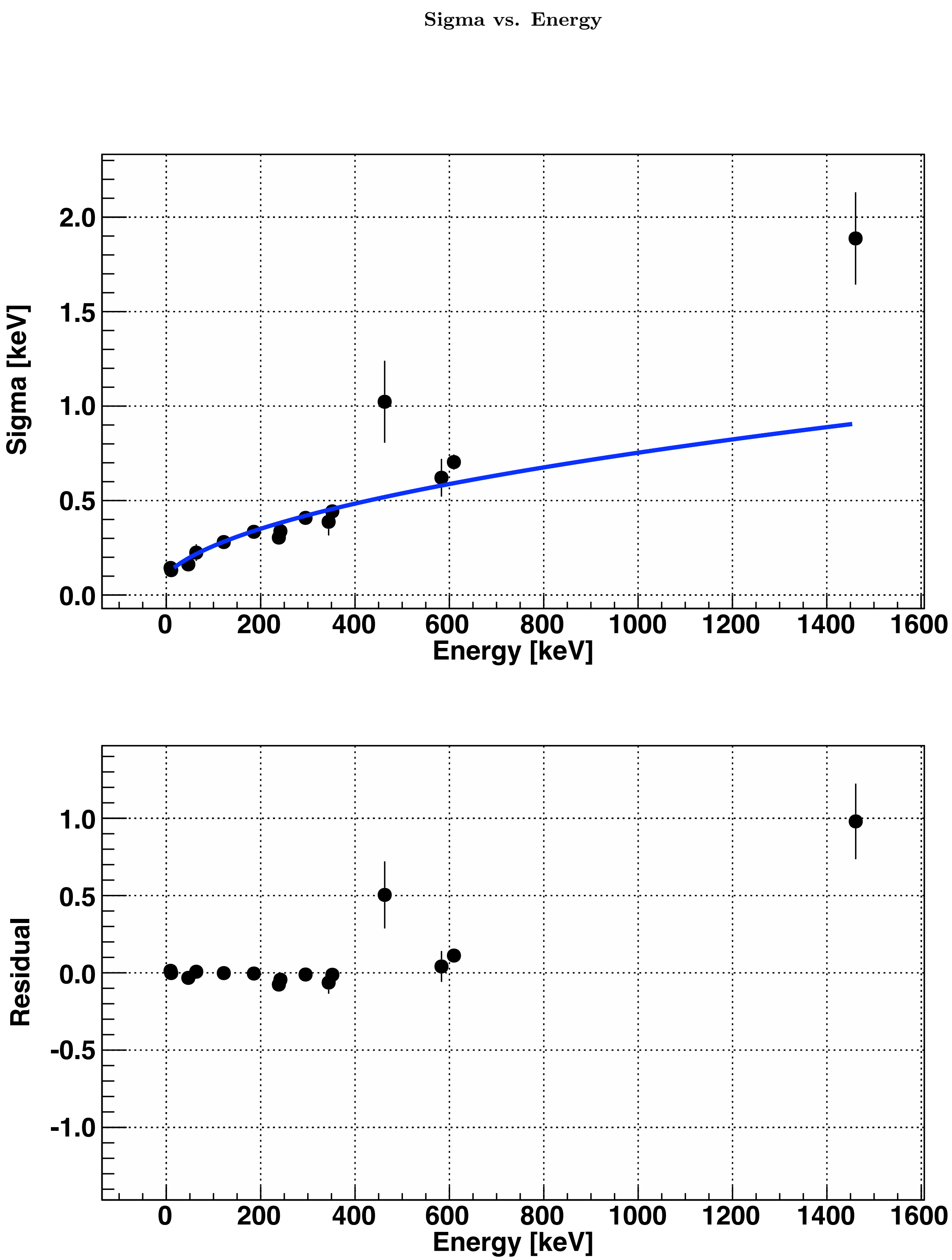

FIG. 51:

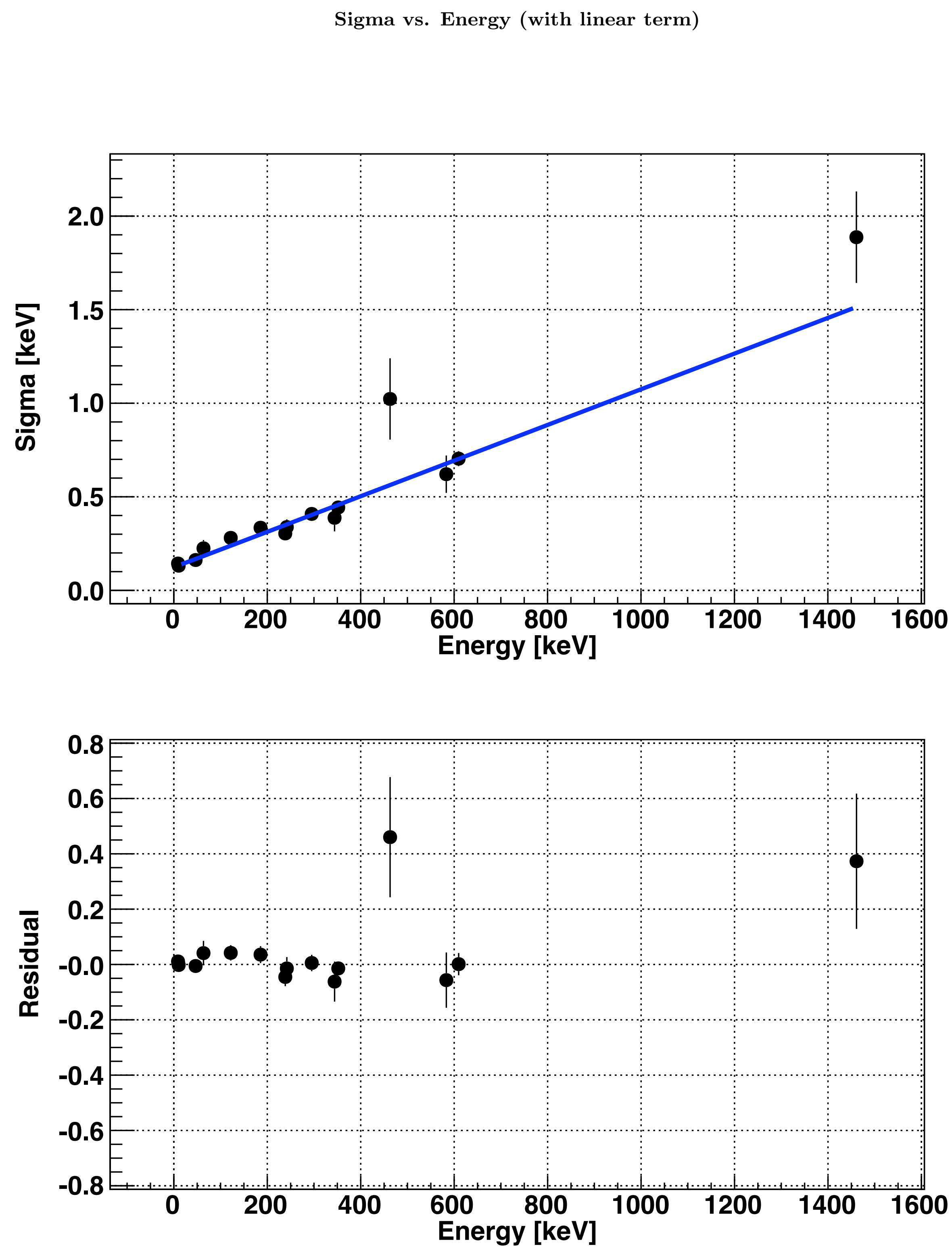

FIG. 52:

radiopurity info

Table J.4: Radiopurity information for Copper-OFHC. Table generated by *MJBMDbInfo.-ComponentsStore*.

Contaminant	**Activity/ Production Rate**	**Reference**
^{232}Th to ^{228}Ra (^{232}Th step 1)	9.00E-01 μBq/kg	DEMONSTRATOR Table [78]
^{228}Ra to ^{228}Th (^{232}Th step 2)	9.00E-01 μBq/kg	DEMONSTRATOR Table [78]
^{228}Th to ^{224}Ra (^{232}Th step 3)	9.00E-01 μBq/kg	DEMONSTRATOR Table [78]
^{224}Ra to ^{208}Pb (^{232}Th step 4)	9.00E-01 μBq/kg	DEMONSTRATOR Table [78]
^{238}U to ^{234}Th (^{238}U step 1)	3.00E+00 μBq/kg	DEMONSTRATOR Table [78]
^{234}Th to ^{234}U (^{238}U step 2)	3.00E+00 μBq/kg	DEMONSTRATOR Table [78]
^{234}U to ^{230}Th (^{238}U step 3)	3.00E+00 μBq/kg	DEMONSTRATOR Table [78]
^{230}Th to ^{226}Ra (^{238}U step 4)	3.00E+00 μBq/kg	DEMONSTRATOR Table [78]
^{226}Ra to ^{222}Rn (^{238}U step 5)	3.00E+00 μBq/kg	DEMONSTRATOR Table [78]
^{222}Rn to ^{210}Tl or ^{210}Pb (^{238}U step 6)	3.00E+00 μBq/kg	DEMONSTRATOR Table [78]
^{210}Tl to ^{210}Pb (^{238}U step 6a)	6.30E-04 μBq/kg	DEMONSTRATOR Table [78]
^{210}Pb to ^{210}Bi or ^{206}Pb (^{238}U step 7)	3.00E+00 μBq/kg	DEMONSTRATOR Table [78]
^{210}Bi to ^{210}Po or ^{206}Pb (^{238}U step 8)	3.00E+00 μBq/kg	DEMONSTRATOR Table [78]
^{210}Po to ^{206}Pb (^{238}U step 9)	3.00E+00 μBq/kg	DEMONSTRATOR Table [78]
^{40}K	1.24E+01 μBq/kg	EXO [75]
^{46}Sc	4.58E+00 atoms/kg/day	Heusser et al. [79]
^{48}V	9.50E+00 atoms/kg/day	Heusser et al. [79]
^{56}Co	1.99E+01 atoms/kg/day	Heusser et al. [79]
^{57}Co	1.56E+02 atoms/kg/day	Heusser et al. [79]
^{58}Co	1.43E+02 atoms/kg/day	Heusser et al. [79]
^{59}Fe	3.93E+01 atoms/kg/day	Heusser et al. [79]
^{60}Co	2.00E+02 atoms/kg/day	DEMONSTRATOR Table [78]

Table J.5: Radiopurity information for Germanium-Nat. Table generated by *MJBMDbInfo.-ComponentsStore*.

Contaminant	**Activity/ Production Rate**	**Reference**
^{232}Th to ^{228}Ra (^{232}Th step 1)	1.42E-02 μBq/kg	DEMONSTRATOR Table [78]
^{228}Ra to ^{228}Th (^{232}Th step 2)	1.42E-02 μBq/kg	DEMONSTRATOR Table [78]
^{228}Th to ^{224}Ra (^{232}Th step 3)	1.42E-02 μBq/kg	DEMONSTRATOR Table [78]
^{224}Ra to ^{208}Pb (^{232}Th step 4)	1.42E-02 μBq/kg	DEMONSTRATOR Table [78]
^{238}U to ^{234}Th (^{238}U step 1)	1.38E-02 μBq/kg	DEMONSTRATOR Table [78]
^{234}Th to ^{234}U (^{238}U step 2)	1.38E-02 μBq/kg	DEMONSTRATOR Table [78]
^{234}U to ^{230}Th (^{238}U step 3)	1.38E-02 μBq/kg	DEMONSTRATOR Table [78]
^{230}Th to ^{226}Ra (^{238}U step 4)	1.38E-02 μBq/kg	DEMONSTRATOR Table [78]
^{226}Ra to ^{222}Rn (^{238}U step 5)	1.38E-02 μBq/kg	DEMONSTRATOR Table [78]
^{222}Rn to ^{210}Tl or ^{210}Pb (^{238}U step 6)	1.38E-02 μBq/kg	DEMONSTRATOR Table [78]
^{210}Tl to ^{210}Pb (^{238}U step 6a)	2.89E-06 μBq/kg	DEMONSTRATOR Table [78]
^{210}Pb to ^{210}Bi or ^{206}Pb (^{238}U step 7)	1.38E-02 μBq/kg	DEMONSTRATOR Table [78]
^{210}Bi to ^{210}Po or ^{206}Pb (^{238}U step 8)	1.38E-02 μBq/kg	DEMONSTRATOR Table [78]
^{210}Po to ^{206}Pb (^{238}U step 9)	1.38E-02 μBq/kg	DEMONSTRATOR Table [78]
^{3}H	2.77E+01 atoms/kg/day	D.-M. Mei [80]
^{54}Mn	9.10E+00 atoms/kg/day	Avg. from Table I [81]
^{55}Fe	8.40E+00 atoms/kg/day	MAJORANA BSD – GENIUS [61]
^{57}Co	6.84E+00 atoms/kg/day	Avg. from Table I [81]
^{58}Co	1.61E+01 atoms/kg/day	MAJORANA BSD – GENIUS [61]
^{60}Co	5.00E+00 atoms/kg/day	DEMONSTRATOR Table [78]
^{63}Ni	4.60E+00 atoms/kg/day	MAJORANA BSD – GENIUS [61]
^{65}Zn	7.90E+01 atoms/kg/day	MAJORANA BSD – GENIUS [61]
^{68}Ge	3.00E+01 atoms/kg/day	DEMONSTRATOR Table [78]
^{76}Ge $2\nu\beta\beta$	9.03E+00 μBq/kg	A.S. Barabash [1]

Pulsed-reset preamplifier

Pulsed-reset preamplifier

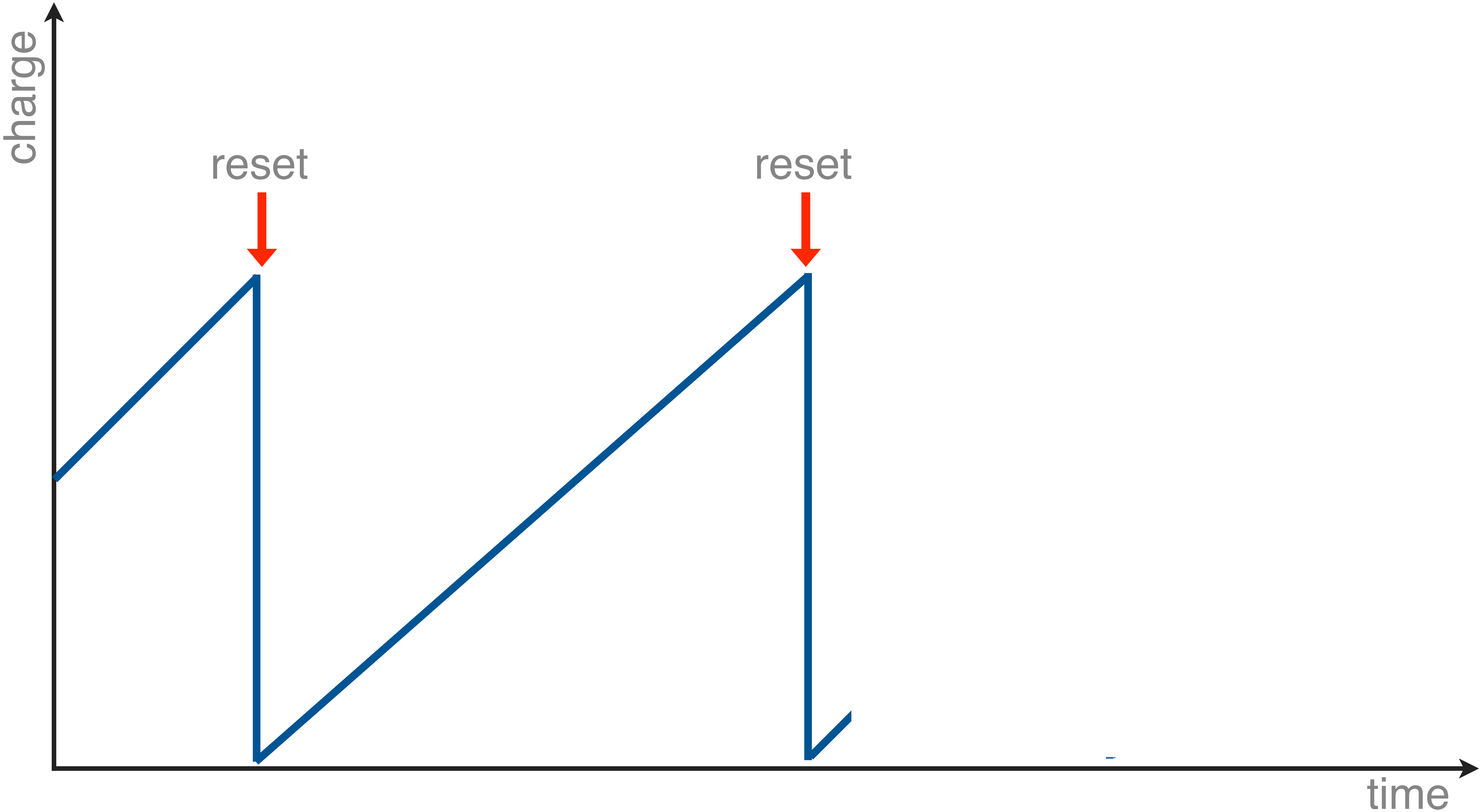

Pulsed-reset preamplifier

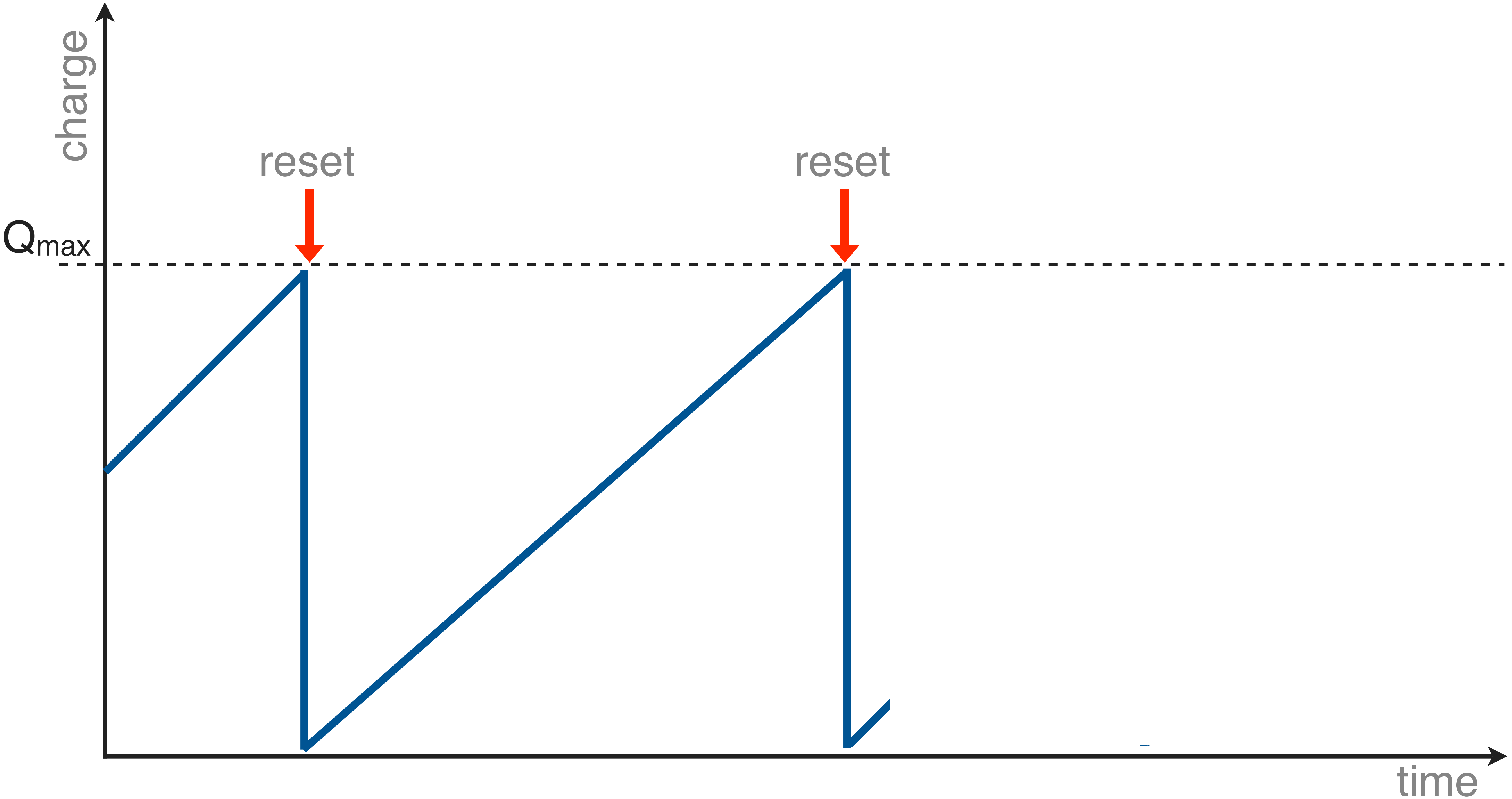

Pulsed-reset preamplifier

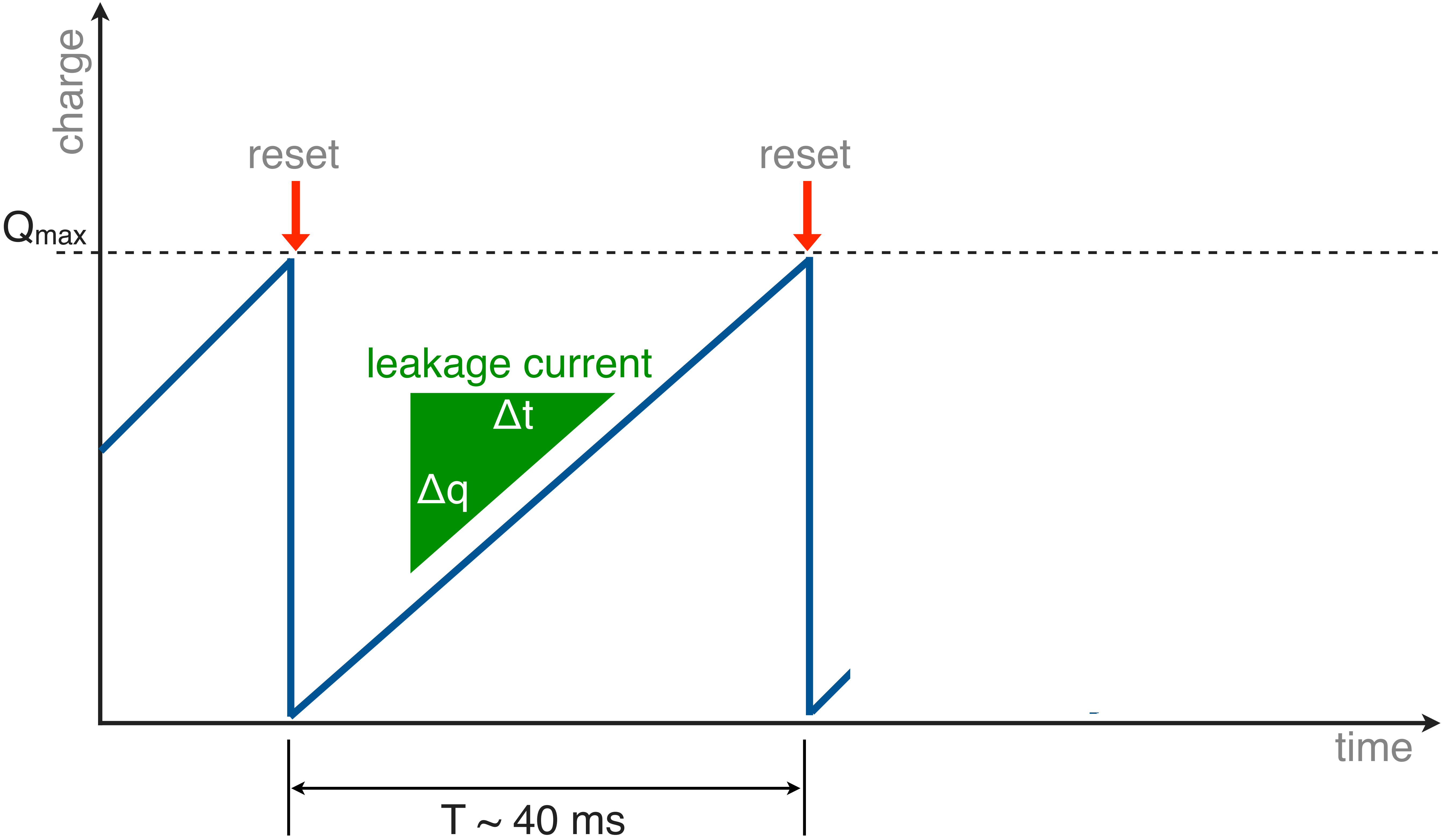

Pulsed-reset preamplifier

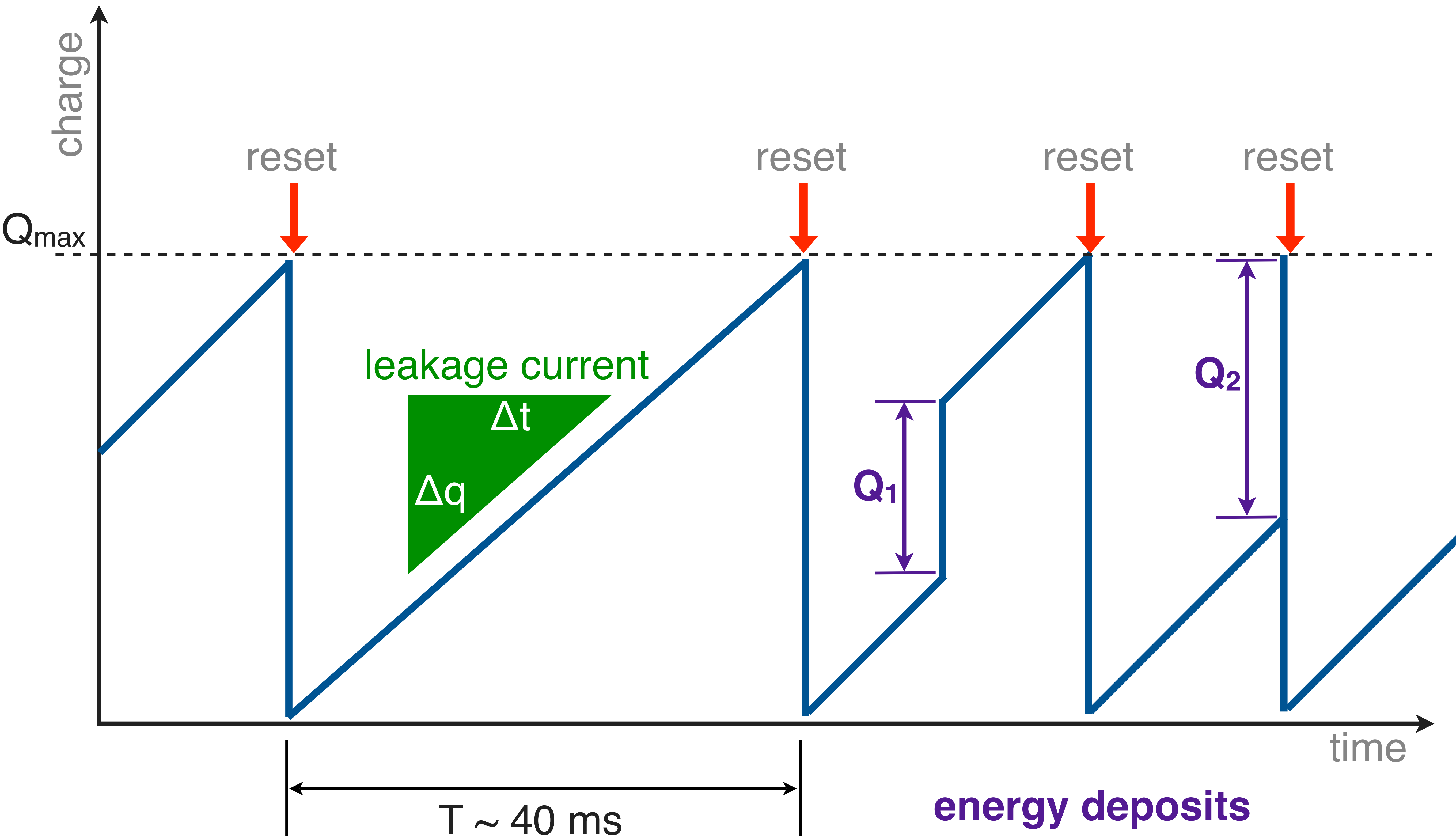

Energy-dependent efficiency

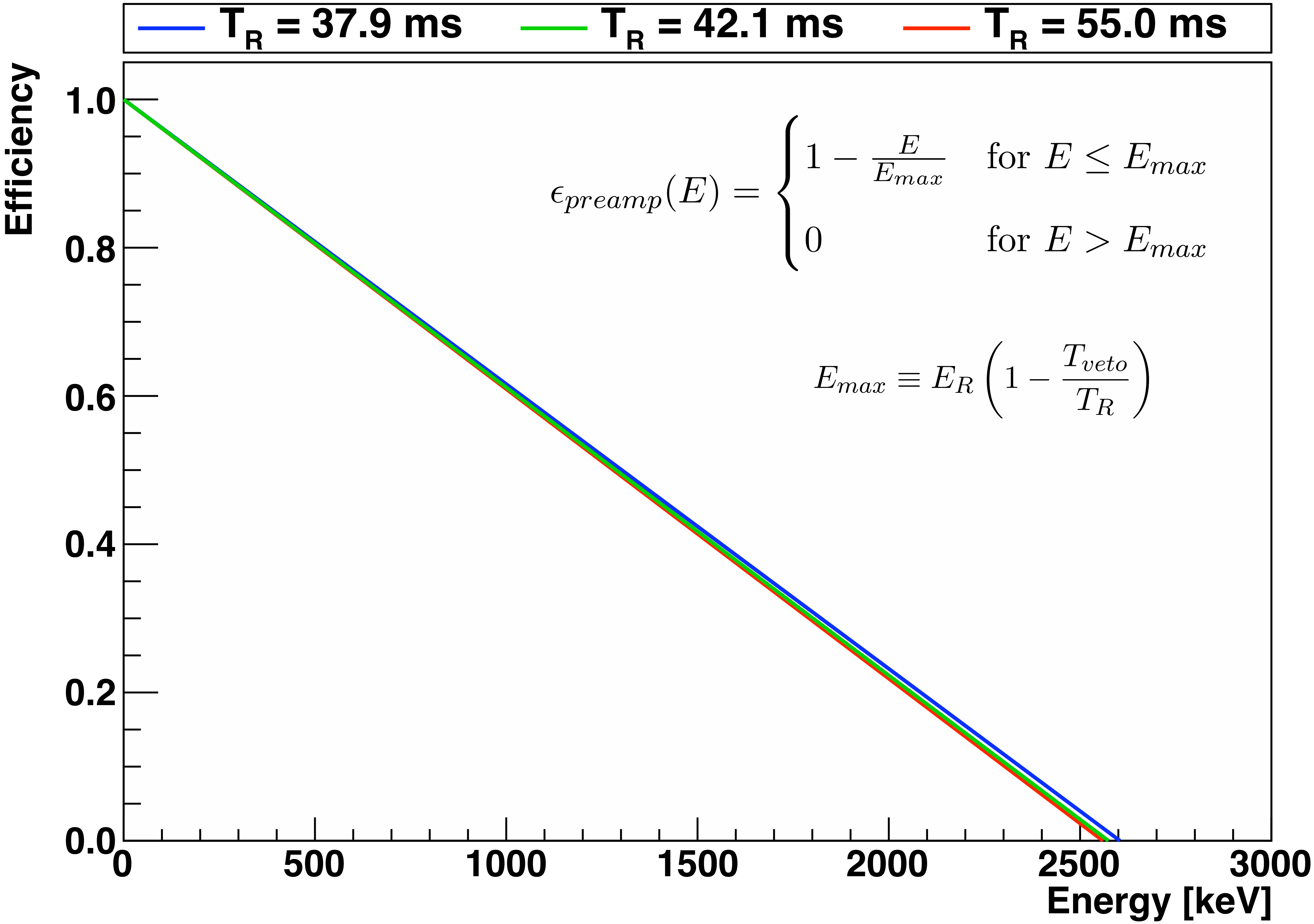

DEMONSTRATOR WIMP sensitivity

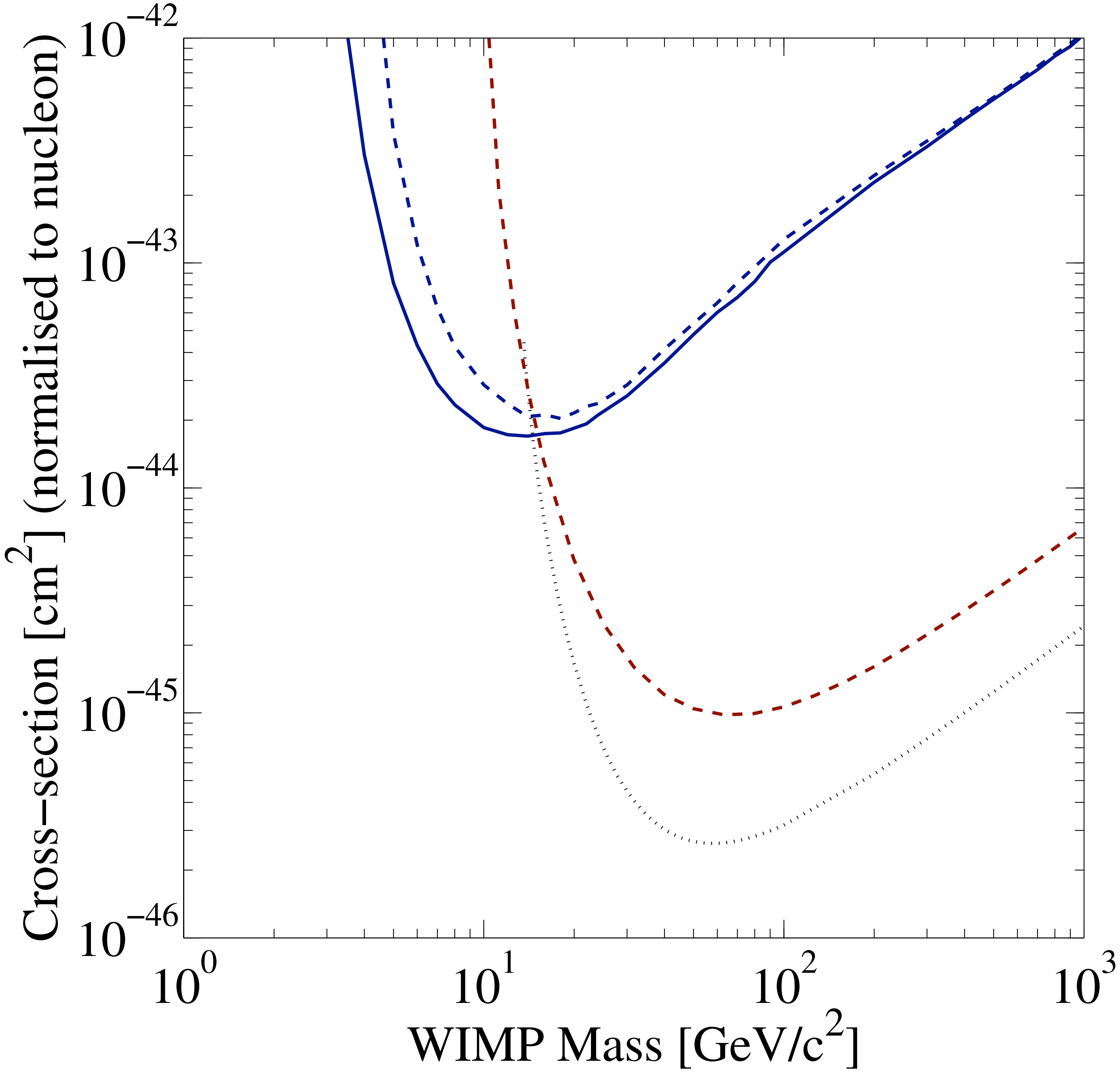

Mike Marino
PhD. Thesis, 2010

Figure 5.7: MAJORANA DEMONSTRATOR sensitivity to a WIMP signal (blue solid, 0.3 keV threshold; blue dashed, 0.5 keV threshold), comparing to SuperCDMS Phase A [96](red dashed) and LUX 300 [97] (black dotted). Plot generated with DMTools [86], lines are 90% CL exclusions.

Photon attenuation

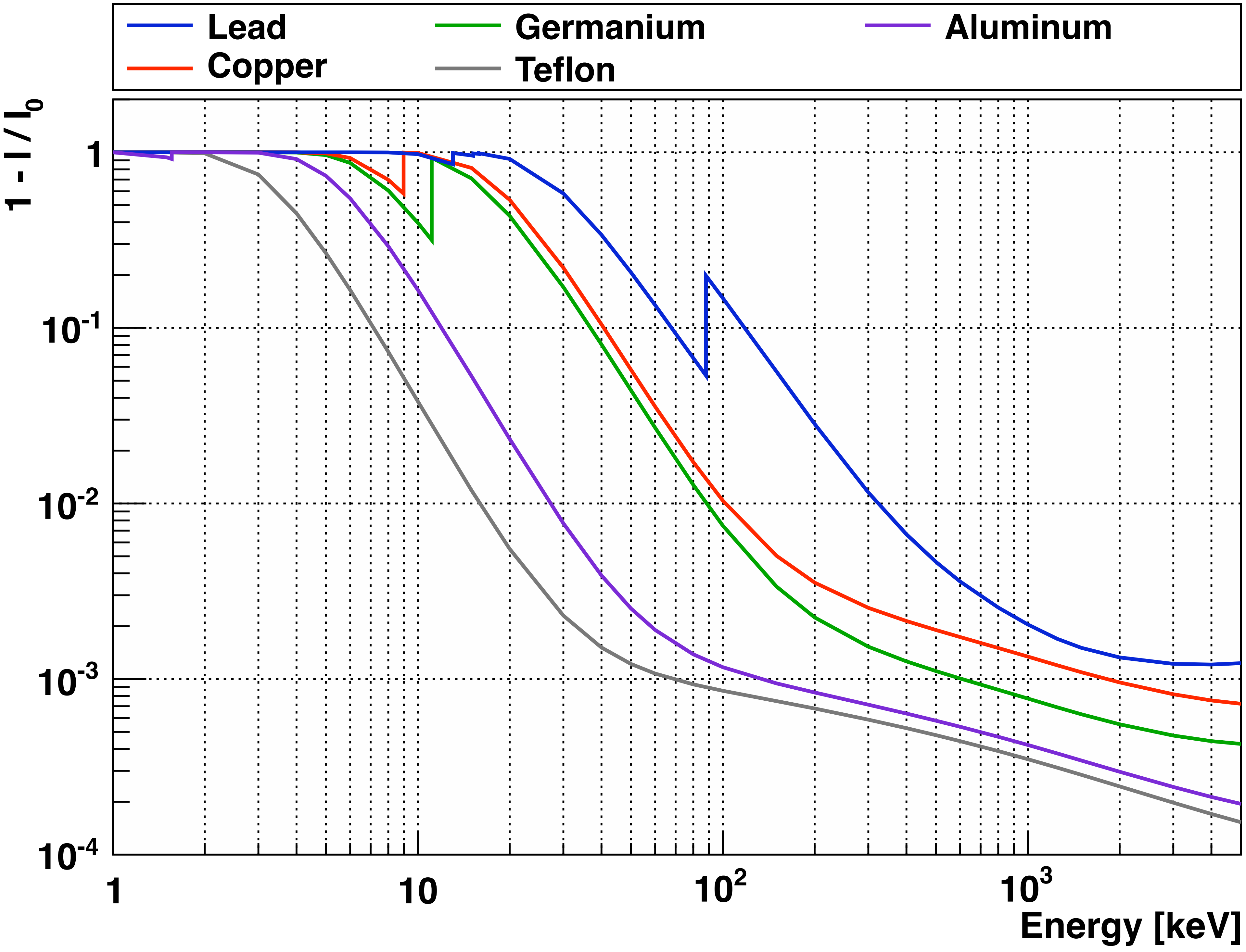

EXO 0νββ limit

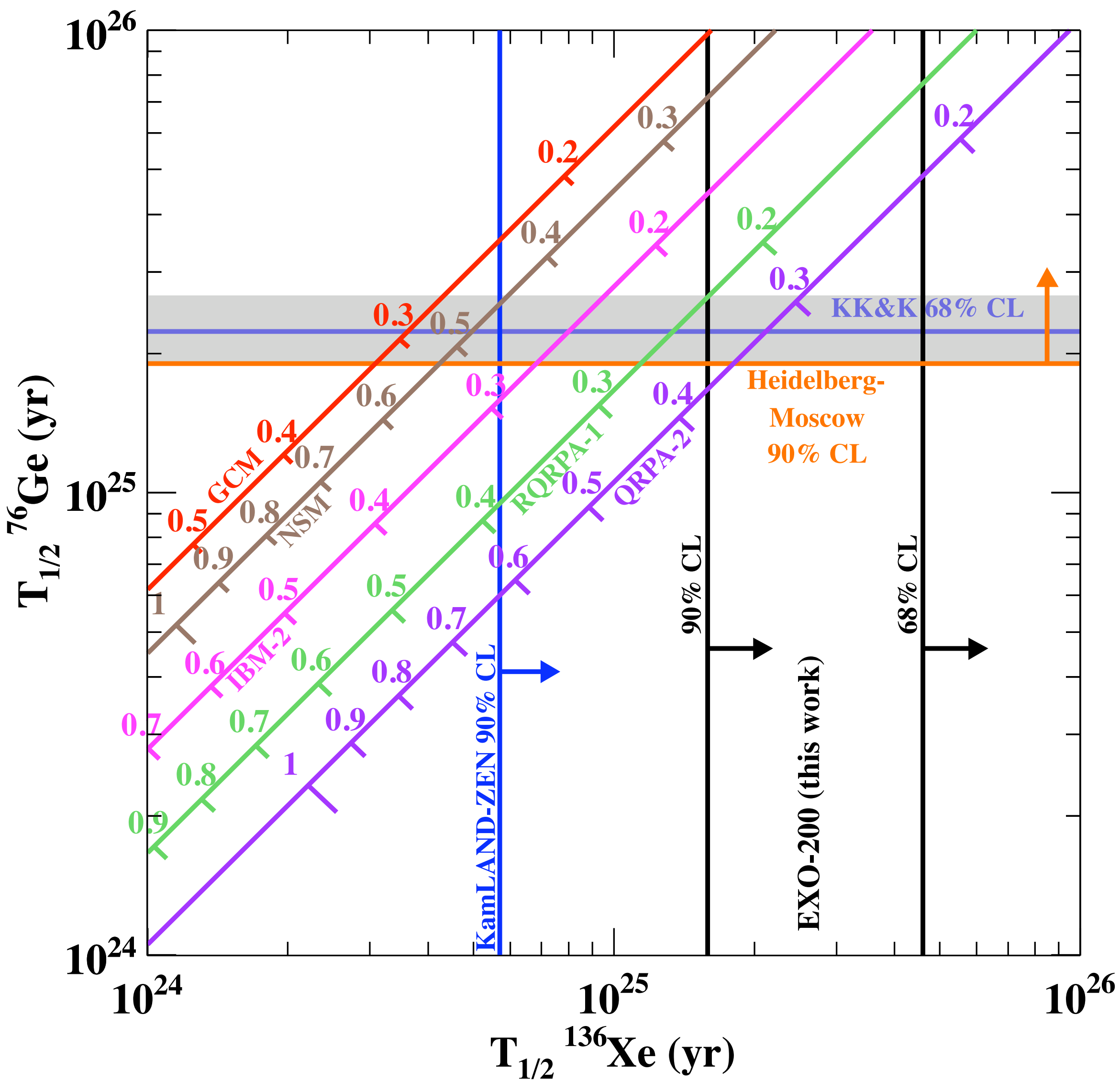

IG. 6: Relation between the $T_{1/2}^{0\nu\beta\beta}$ in ^{76}Ge and ^{136}Xe for ifferent matrix element calculations (GCM [20], NSM [21], 3M-2 [22], RQRPA-1 [23] and QRPA-2 [5]). For each matrix .ement $\langle m\rangle_{\beta\beta}$ is also shown (eV). The claim [4] is represented y the grey band, along with the best limit for ^{76}Ge [19]. The esult reported here is shown along with that from [7].

EXO-200: Phys. Rev. Lett. 109 (2012) 032505

Slow energy-degraded pulses from the MALBEK transition dead layer

Total dead layer measurement

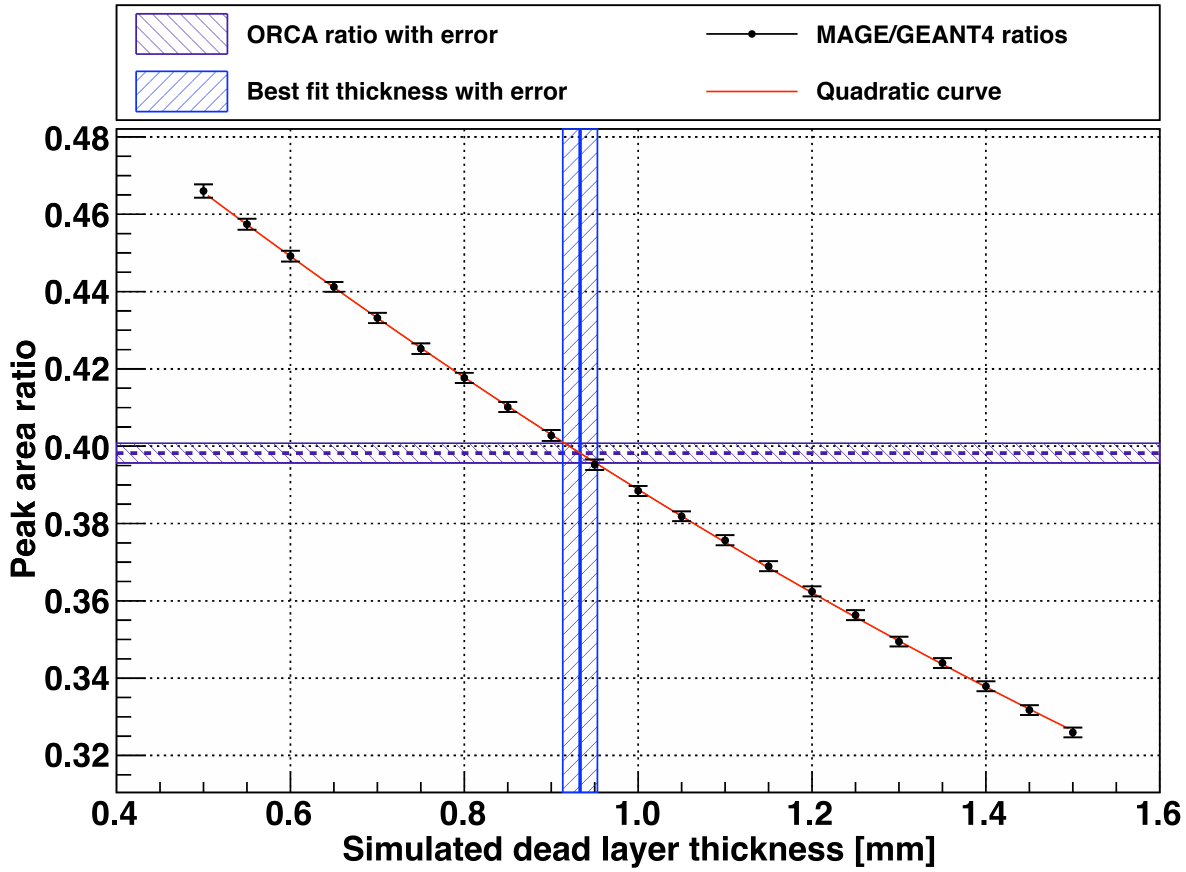

Fractional charge collection vs. depth

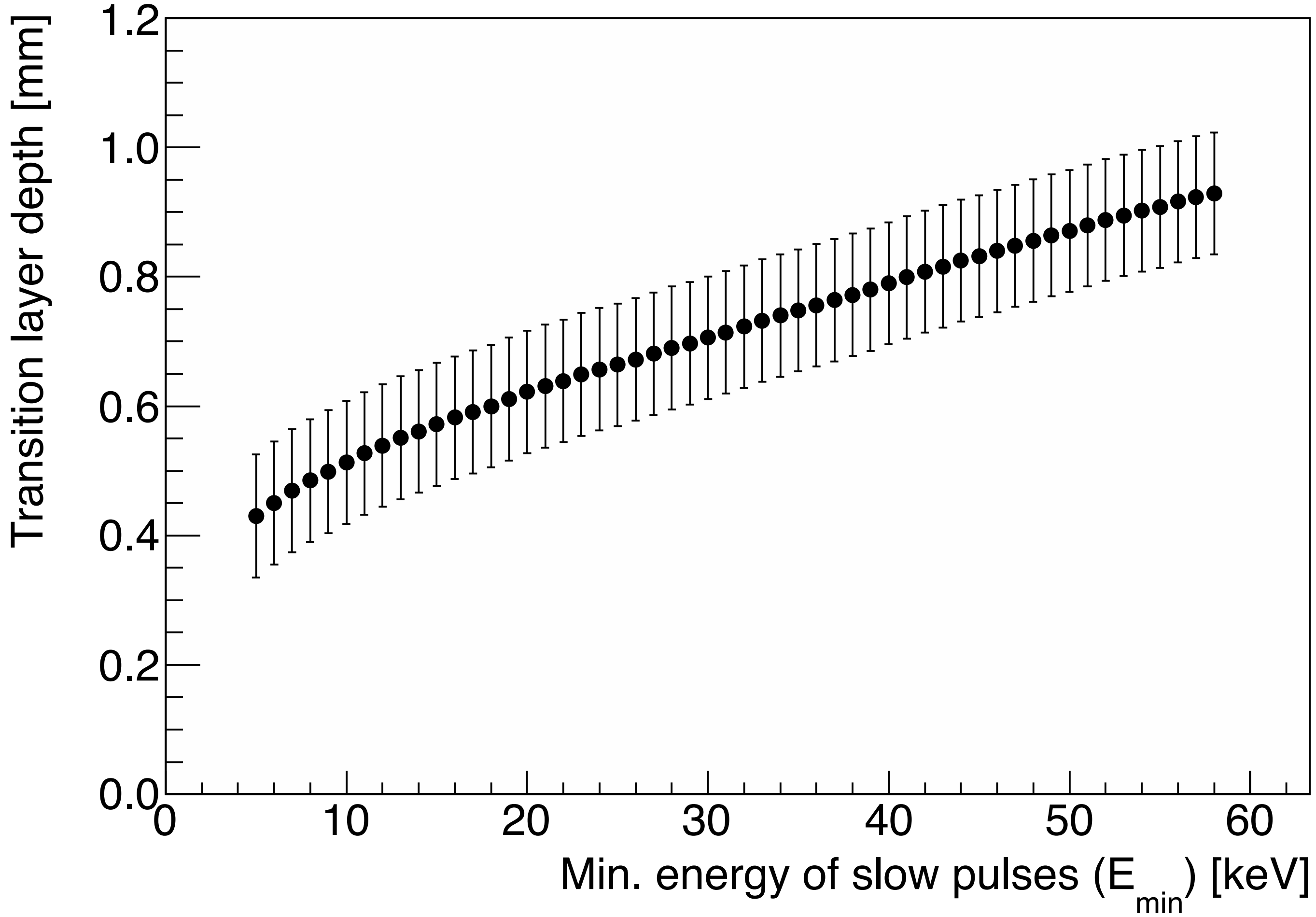

E. Agauayo et al, submitted to NIM A
arXiv:1207.6716

Pulsed-reset preamp

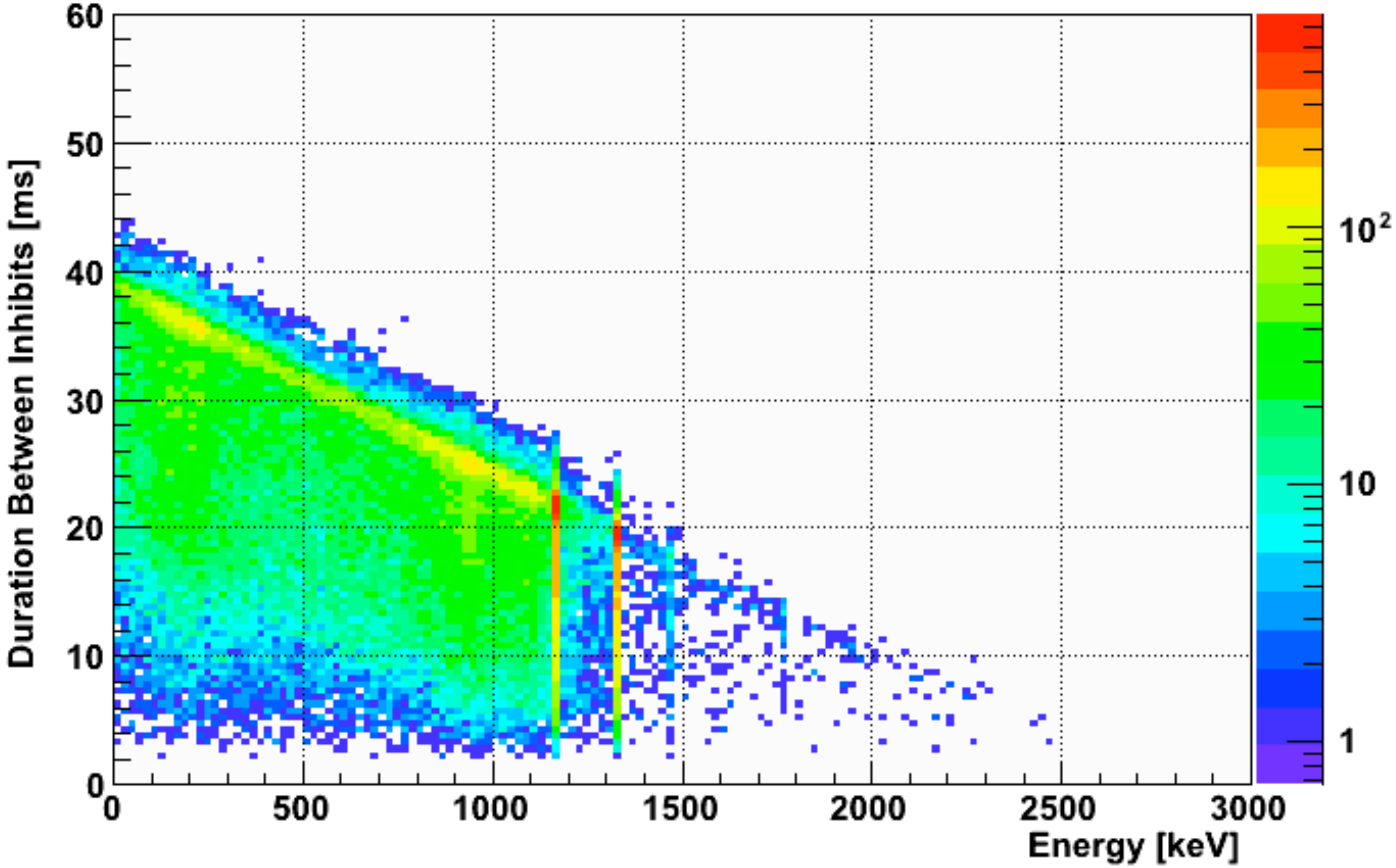

Pulsed-reset preamp

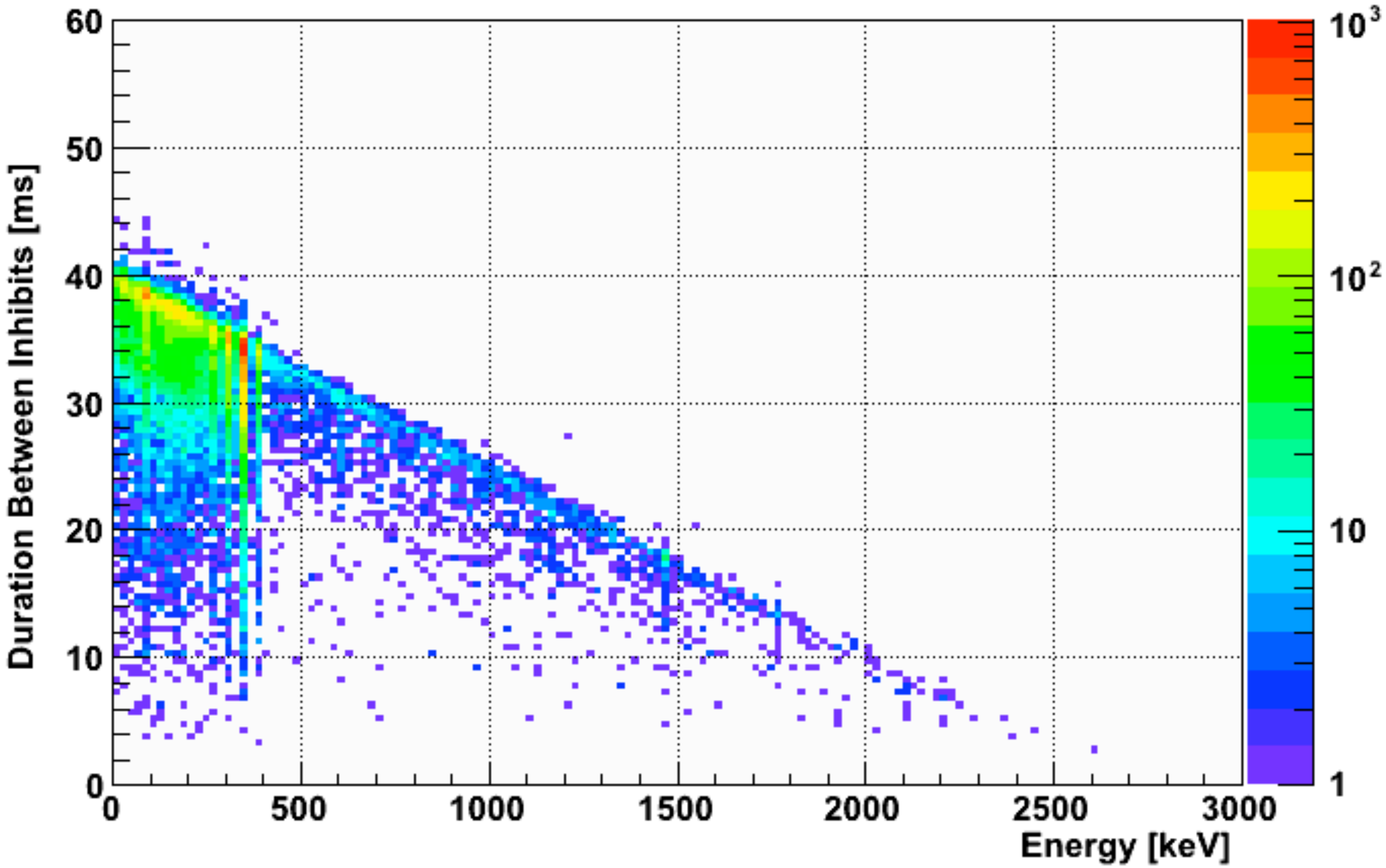

DEMONSTRATOR background model

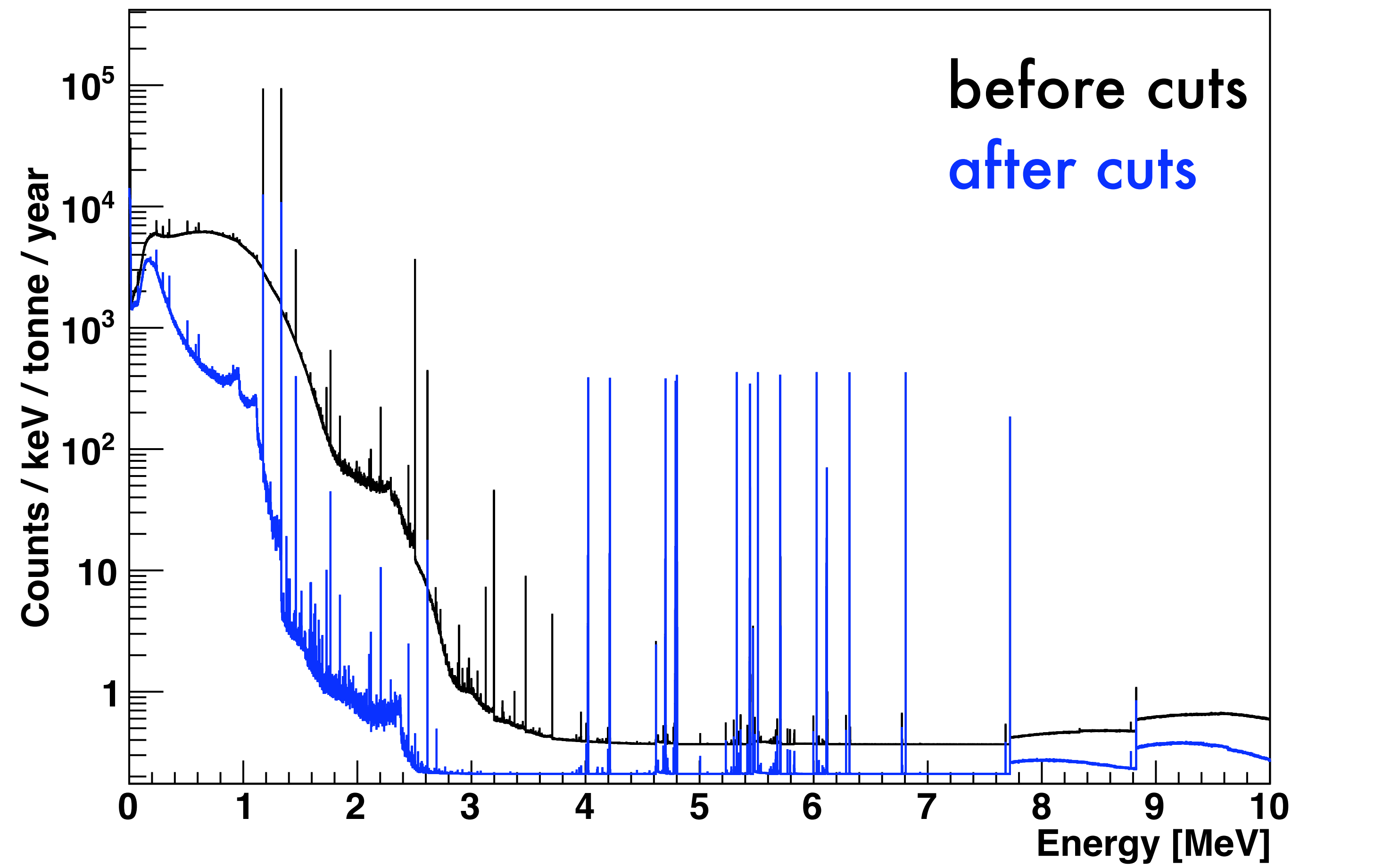

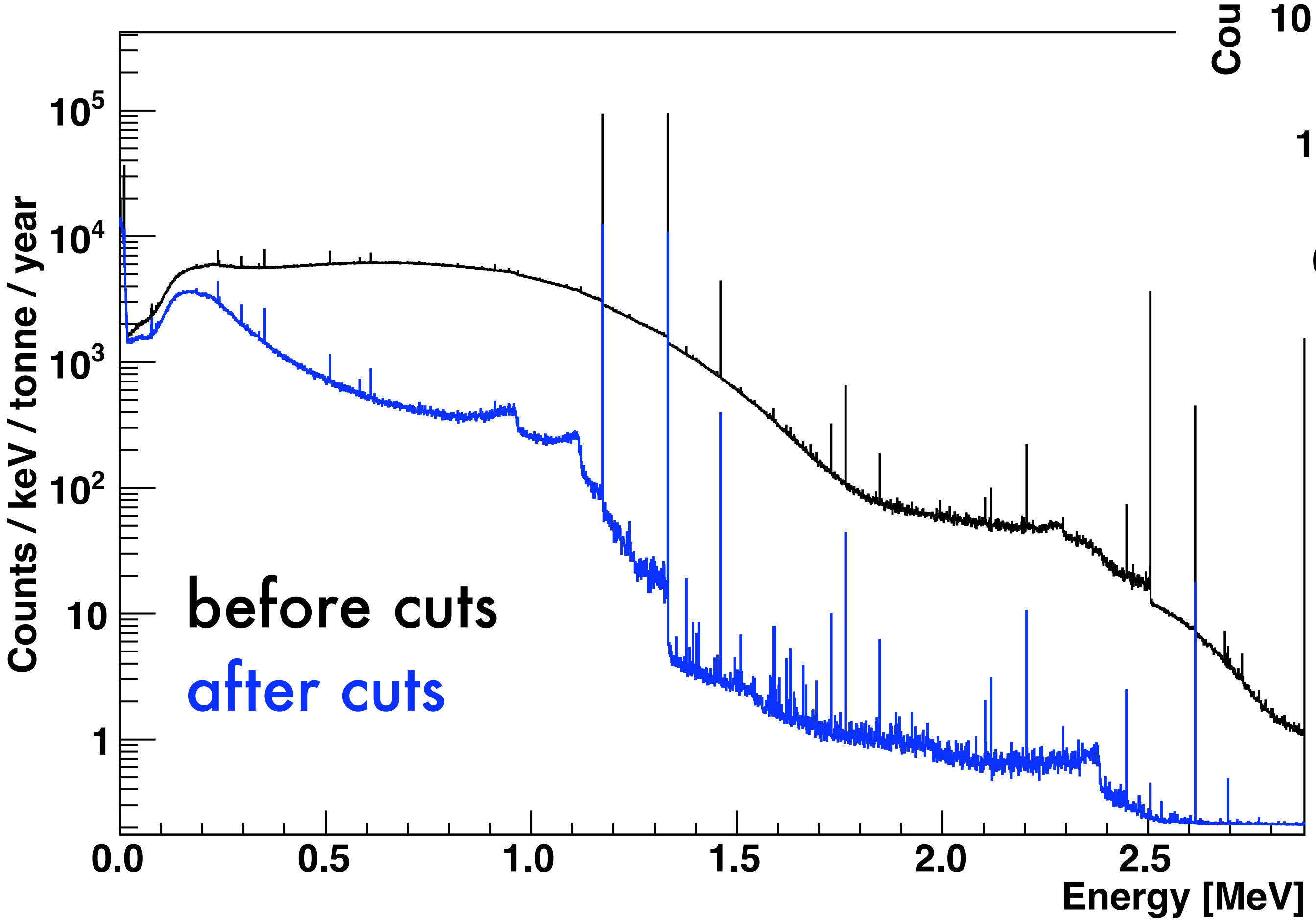

questions

- GERDA: P1=18kg enr-Ge, P2 = 20kg enr-Ge?
- Cu purity: limits or measurements?
- PPC technology
- enr. Ge
- add DM/PPC slide
- add assay achievements/
- put status bullets on pics

Make sure slide # is visible on every slide!